Collective Dynamics of Polarizable Particles and Electromagnetic Radiation

Dissertation

zur Erlangung des akademischen Grades

Doctor of Philosophy

eingereicht an der
Fakultät für Mathematik, Informatik und Physik
der Universität Innsbruck

von

Mag. Tobias Grießer

Betreuung der Dissertation:

Univ.-Prof. Dr. Helmut Ritsch,
Institut für Theoretische Physik,
Universität Innsbruck

und

Univ.-Prof. Dr. Andreas Läuchli,
Institut für Theoretische Physik,
Universität Innsbruck

Innsbruck, June 3, 2014

Contents

1 Danksagung

Ich möchte mich hier bei allen Menschen bedanken, die mich während des Studiums unterstützt haben und die dadurch das Zustandekommen dieser Dissertation erst ermöglicht haben. Zuvorderst gebührt meinem Betreuer Prof. Helmut Ritsch außerordentlicher Dank für seine nie enden wollende Geduld und stetige Ermutigung und nicht zuletzt auch dafür, dass ich durch ihn nie am Hungertuch nagen musste. All meinen Studienkollegen, besonders Wolfgang Niedenzu, Matthias Sonnleitner und Sebastian Krämer, welchen das (Un)glück zuteil wurde mit mir ein Zimmer teilen zu müssen und die meine sich ständig ändernden–jedoch lautstark und mit missionarischem Eifer zum Ausdruck gebrachten–Weltanschauungen mit stoischer Gelassenheit hingenommen haben, sei gedankt (obgleich eine Entschuldigung wohl eher angebracht erschiene). Meinen Schwestern Eva und Kathrin danke ich dafür, dass sie immer für mich da waren und dass sie so wunderbare Geschöpfe in die Welt gesetzt haben, die mich mit Stolz erfüllen Onkel zu sein. Meinem Schwager und Freund Dimo danke ich für die zahllosen, abendelangen philosophischen Diskurse, die für mich sehr wertvoll waren. Der größte Dank jedoch gebührt meinen Eltern, ohne die ich nichts zustande gebracht hätte.

2 Introduction and Outline

2.1 Introduction

It is an old idea that light can exert forces on inert matter. No lesser than Johannes Kepler proposed, in his work *De Cometis* from 1619, the theory that it is the sun's radiation, which causes the tail of a comet to point away from the latter. As a consequence of Maxwell-Lorentz theory of electrodynamics, light, conceived of as an electromagnetic wave, exerts a force–the so-called Lorentz force–on charged particles of matter. In terms of the charge q and the electric and magnetic fields $\mathbf{E}, \mathbf{B}$ it is given by

$$\mathbf{F} = q[\mathbf{E}(\mathbf{r}, t) + \dot{\mathbf{r}} \times \mathbf{B}(\mathbf{r}, t)]. \tag{2.1}$$

In this equation, the velocity $\dot{\mathbf{r}}$ of the charge was to be understood to be relative to some material medium, the luminiferous aether, in which electromagnetic waves exist and which was thought to provide an absolute system of coordinates, but with the advent of Einstein's Special Theory of Relativity (STR), it was interpreted as the velocity of the charge with respect to some arbitrary inertial observer. As atoms and molecules are known to be overall electrically neutral aggregates of charged particles such as electrons and protons, they too–within the framework of Maxwell-Lorentz electrodynamics– couple to an electromagnetic wave through higher order moments of their charge distribution. Furthermore, even if a molecule or atom is supposed not to possess permanent multipole moments, the Lorentz force caused by an electromagnetic wave accelerates the oppositely charged constituents differently and thus gives rise to induced moments. It is in this way that the phenomenon of electromagnetic forces on neutral pieces of matter (henceforth called light forces) received a classical theoretical explanation. The theory of Maxwell and Lorentz was soon confronted with serious difficulties, because the stipulated material medium in which electromagnetic fields were supposed to propagate refused to be detected by experiments, most notably the Michelson-Morley interferometer experiments, only some twenty-five years after the publication of Maxwell's equations in 1861-62. This unpleasant situation was remedied by STR by abolishing the Newtonian notion of absolute time and space and a radical reformulation also of the laws of mechanics. However, it was precisely the attempt to explain the very existence and stability of atoms and molecules as dynamical systems of point-like charges interacting via forces mediated by the electromagnetic field, which met insurmountable difficulties, even when the Maxwell-Lorentz theory was supplemented by STR. The reason is that if a point-charge executes accelerated motion (again, relative to some inertial system of coordinates), Maxwell's equations or, more precisely, Lorentz' retarded solution to

Maxwell's electromagnetic field equations, predict that this charge irreversibly radiates electromagnetic energy. Hence, in order to upkeep the principle of conservation of energy the particle must experience a force–sometimes called radiation-reaction force[1]–such that the work done by the latter accounts for the loss of energy by radiation. Due to such considerations it became generally accepted that the classical Maxwell-Lorentz theory would have electrons orbiting a nucleus continually loose energy and finally collapse into the core, hence making stable atoms impossible. The discovery of sharp spectral lines of light absorbed by atomic gases and the famous photoelectric effect revealed further deficiencies of the classical theory of electromagnetism, the latter prompting Einstein to introduce the notion of quanta of electromagnetic energy (nowadays commonly called photons), thus lending credence to Planck's "desperate" step a few years earlier of assuming a quantization of electromagnetic energy in order to explain the observed spectral energy density of thermal radiation emanating from cavities. The further course, which physics took is well-known, and by the work of some of the greatest minds the world saw the birth of the marvelous mathematical edifice, which together with a plethora of so-called correspondence rules is known as Quantum Theory. It cannot be doubted that this theory was and still is outstandingly successful in predicting and reproducing observable phenomena with unrivaled quantitative precision. In the context of electromagnetism and more specifically within the subfield of Quantum Optics, with which also this thesis is concerned, the theoretical description of the Laser and its subsequent realization is an achievement, which cannot be overestimated. The advent of this device opened up the road to the controlled manipulation of atoms and other small particles by the forces of light, which has since become an indispensable and routinely used experimental tool. One of the most fruitful application of light forces consists in the trapping of atoms and cooling of their motional degrees of freedom. The quantum mechanical account of the light force exerted on an atom is, in a manner analogous to the classical theory, attributed to the interaction of the induced atomic dipole with the quantized radiation field. Its analysis leads to the distinction of two separate components of this force. The first is called the radiation pressure force and is due to the recoil a particle suffers if it absorbs a photon from the field and thereby undergoes a transition to an excited state. It is this force which is used to great effect in the well-known laser-cooling schemes. The second component is called the dipole force and is connected to the appearance of a spatially varying optical potential caused by the dynamic Stark shift of atomic energy levels. Unlike the radiation pressure force, the dipole force can be substantial also for light which is not in resonance with any atomic transition and, as it does not involve absorption, can be used to create conservative spatially periodic potentials to trap

[1]This force cannot, however, be given by (2.1), because the fields created by a point-particle are divergent at its location, rendering the expression for the Lorentz force meaningless and is but one of many infinities, which appear in modern physical theories making them needful of so-called "renormalizations". The problem of combining the notion of *point*-charges and fields mathematically soundly is an issue, which has–according to the opinion of the author–not yet received a satisfactory solution and it seems doubtful that such a solution even exists.

atoms by counter-propagating laser beams. Such light induced dipole potentials are known as optical lattices [1] and play, in combination with cold atoms, an important rôle in the experimental study of certain related aspects of more complex and less controllable solid-state systems. Thus far we have only considered the influence of "external" electromagnetic fields on particles. However, as radiation impinges on a particle, it will be partly absorbed (giving rise to the radiation pressure force) and re-radiated as well as scattered (accompanied by the dipole force). If a particle is placed between the mirrors of a cavity, this scattered and re-radiated light is reflected back and forth and can therefore interact again with the particle, leading to a dynamical coupling between the atomic and electromagnetic degrees of freedom. A particularly interesting consequence of this coupling is the possibility to achieve a continual extraction of kinetic energy from the particle due to the work done by the dipole force, which arises from that part of the field, which having been previously scattered off the laser by the particle is being back-reflected by the mirrors. This new method of cooling an atom was first published by Horak *et al.* in 1997 [2] and has since received considerable attention in subsequent publications [3]. The main reason, why this scheme is of interest, can be understood if it is compared to standard laser cooling: being based on the dipole force it does not require closed spontaneous emission-repumping cycles and in principle is applicable to any sufficiently polarizable type of particle, such as, for example, a molecule. New phenomena appear if not a single particle, but a whole ensemble of particles is allowed to simultaneously interact with one or several selected modes of an optical cavity. Among the most noteworthy is the so-called selforganization of a laser illuminated cold gas, which is placed between the mirrors of an optical resonator, allowing for a collective coupling of the particles through the light scattered off the laser beam and into a mode of the cavity. This effect, first predicted by Domokos and Ritsch in 2002 [4] and confirmed experimentally shortly afterwards in 2003 [5], is akin to a phase transition. A cold gas, which is originally spatially homogeneous on a scale of the wavelength of a selected near-resonant (w.r.t. the illuminating laser) cavity mode and therefore scatters only a negligible amount of light into the resonator, spontaneously, upon crossing a specific threshold of the intensity of the illuminating laser, reorders into a periodic pattern, whereby the amount of light scattered into the cavity mode is greatly enhanced. In the final state, the forces, which hold the particles in place, are caused precisely by the dipole force due to the enhanced scattering. This self-consistency is the reason why the transition has been called *self*organization. In general, the collective nature of the dynamical interaction of polarizable particles with radiation gives rise to interesting dynamical effects, of which some aspects will be studied in the present thesis.

2.2 Outline of the Thesis

2.2.1 Content of the second Chapter

A cold gas of polarizable particles moving in the optical potential of a standing wave high finesse optical resonator acts as a dynamic refractive index. For a sufficiently strong cavity pump the optical forces generated by the intra cavity field perturb the particles' phase space distribution, which shifts the optical resonance frequency and induces a nonlinear optical response. By help of mean field theory, we predict that beyond the known phenomenon of optical bistability one finds regions in parameter space, where no stable stationary solution exists. The atom-field dynamics there exhibits oscillatory solutions converging to stable limit cycles of the system. Applied to a zero-temperature Bose condensate or a thermal gas one finds a strikingly similar behavior, if one simply replaces the recoil frequency by an appropriately chosen thermal frequency. The content of this chapter is largely based on a publication by the author [6].

2.2.2 Content of the third Chapter

In this chapter we study the spatial selforganization and cooling of a dilute cold gas of laser-illuminated polarizable particles inside an optical resonator. Deriving a non-linear Fokker–Planck equation for the particles' phase-space density allows us to treat arbitrarily large ensembles in the dispersive limit and explicitly calculate friction, diffusion and the selfconsistent statistical equilibrium states. In addition, we determine the selforganization threshold and thereby find the equilibrium phase boundary in closed form. The equilibrium velocity distribution of a gas in the unordered phase is found to be a q-Gaussian with a steady-state temperature determined by the cavity linewidth and detuning. The phase space distribution for a gas deeply within the selfordered phase turns out to be thermal and we give the corresponding temperature. Numerical simulations using large ensembles of particles confirm the analytical threshold condition for the appearance of an ordered equilibrium state, where the particles are trapped in a periodic pattern and can have energies close to a single vibrational excitation. The material presented is an adaptation and extension of [7] co-authored by me. All the calculations where performed individually by each author for the case of the unordered phase. The remaining calculations, extending the theory to selforganized ensembles is due to the present writer. Almost all the numerical simulations where done exclusively by Wolfgang Niedenzu.

2.2.3 Content of the fourth Chapter

In this chapter we generalize the kinetic theory derived in chapter 3 to the quantum mechanical regime. We find important corrections to the semi-classical results treating both Bosons and Fermions. The work presented here has not been published.

2.2.4 Content of the fifth Chapter

Here we study the dynamics of a multispecies mixture of laser-illuminated polarizable particles moving inside an optical resonator. Above a certain pump threshold the collective enhanced scattering of laser light into the cavity induces a phase transition from a homogeneous spatial distribution to a common crystalline order. We analytically show that adding particles of any mass and temperature always strictly lowers the minimum pump power required for selfordering and trapping. This allows to capture and trap new species of atoms, molecules or even polarizable nanoparticles in combination with proven examples, for which a high phase-space density is readily available. Cooperative light scattering mediates effective energy exchange and thus sympathetic cooling between different species without the need of direct collisional interaction. The predicted ordering thresholds and cooling timescales are in range of current technology for particles with a wide range of mass, polarizability and initial temperature. The content of this chapter can basically be found in [8]. The primary contribution of the author to this work consisted in the analytical calculations. The numerical implementation and analysis is due to Wolfgang Niedenzu.

2.2.5 Content of the sixth Chapter

Collective off resonant scattering of coherent light by a cold gas induces long-range interactions via interference of light scattered by different particles. In a 1D configuration these interactions grow particularly strong by coupling the particles via an optical nanofiber. Above a threshold pump laser intensity we predict a phase transition from a homogeneous density to a self-sustained crystalline order. In the dispersive regime we determine the critical condition for the onset of order as well as the forms of gas density and electric field patterns above threshold. Surprisingly, there can co-exist multiple stationary states with distinct density profiles. This chapter is a slightly extended version of the journal article [9] by the writer of this thesis.

3 Nonlinear Atom-Field Dynamics in high-Q Cavities: from a BEC to a Thermal Gas

3.1 Introduction

Based on the surprisingly fast progress in the experimental technology of laser cooling and manipulation of dilute atomic gases as well as optical resonator and laser stabilization technology, it is now experimentally possible to confine larger and larger numbers of colder and colder atoms within the mode volume of stabilized very high finesse resonators[10, 11]. For slow enough particles the optical dipole force induced by the intracavity field significantly influences the atomic motion even in the dispersive limit at very large detunings, where absorption and spontaneous emission only play a minor role. In this limit the dispersive scattering of the particles simply acts as a dynamic refractive index changing the intracavity field evolution[12, 2, 13]. The resulting complex coupled atom-field dynamics leads to a wealth of interesting physical phenomena and applications[14, 15], which can be analysed theoretically using a wide range of models of very different complexity.

In previous work we have developed a new approach based on a classical phase space density description of the particles involving a corresponding Vlasov equation together with classical equations for the field mode amplitudes[16]. This approach is particularly suitable to describe very large particle numbers dispersively coupled to a single or a few driven cavity modes, when spontaneous emission and direct interparticle interaction play only a minor role. Related approaches to cold atom dynamics have put forward also by other groups[17, 18].

It has been known theoretically and experimentally for some time now, that the particles in this case act as a nonlinear optical medium through their motional response to the field, even though they are only weakly excited in the regime of linear polarizability at this frequency and intensity [19, 20]. Even for the conceptually most simple case of a single-mode standing wave resonator, the coupled atom-field system can exhibit optical bistability. For a BEC in such a cavity self pulsing solutions were experimentally found[21]. They can be qualitatively well described via a fairly simple two-mode expansion for the atomic mean field dynamics as a nonlinearly coupled oscillator model[22]. This model was shown to be mathematically equivalent to a typical optomechanical setup of a high finesse resonator with a single field mode and a movable mirror at one end. Here we study the appearance of a very similar behavior for a general thermal gas in resonator and show that we can treat both

limits of very low and high temperatures in a unified mean field model.

3.2 Model and Basic Equations

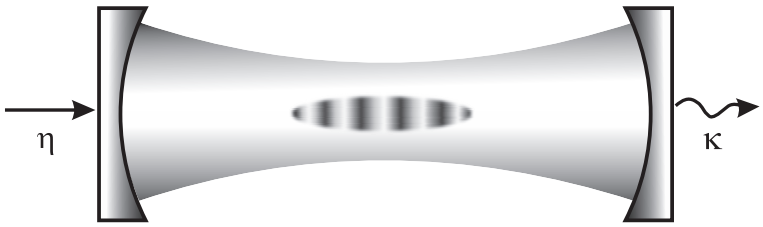

Figure 3.1 Schematic drawing of the physical system.

We consider a large number $N \gg 1$ polarizable (point-)particles of mass m inside a standing wave cavity and coupled to a single mode at wavelength λ thereof. In the dispersive regime, where the frequency of the electromagnetic field is far from any atomic resonance, the cavity photons induce dipole forces on the particles and the distribution of particles in turn shifts the cavity resonance through their dipole moments, thus giving rise to a nonlinearly coupled system. The dynamical quantities of the mean field type model we are about to examine in this chapter are the phase space (quasi-)distribution $f(x, v, t)$, which is the Wigner transform of the reduced one-body density matrix $\rho_{p,1}(x, x', t)$,

$$f(x, v, t) = \frac{m}{2\pi\hbar} \int e^{-izmv/\hbar} \rho_{p,1} \left(x + \frac{z}{2}, x - \frac{z}{2}, t \right) dz, \tag{3.1}$$

and the complex cavity field amplitude, the average of the annihilation operator: $\alpha(t) = \langle \hat{a}(t) \rangle$. The arguments of the Wigner distribution, $f(x, v, t)$, refer to the coordinate along the resonator axis, x, the particle velocity in that direction, v, and time t. The particular zeroth moments of this distribution with respect to velocity and position represent the spatial number density of particles and the distribution of velocity respectively. That is to say

$$n(x, t)\mathrm{d}x := \mathrm{d}x \int f(x, v, t)\mathrm{d}v \tag{3.2a}$$

is equal to the expected fraction of particles within an interval of size $\mathrm{d}x$ around x, whereas

$$F(v, t)\mathrm{d}v := \mathrm{d}v \int f(x, v, t)\mathrm{d}x \tag{3.2b}$$

represents the expected fraction of particles having a velocity within an interval of size $\mathrm{d}v$ around v. As detailed in the appendix, in the limit of large particle numbers, the phase space density obeys Wigner's equation:

$$\frac{\partial f}{\partial t} + v\frac{\partial f}{\partial x} - \frac{1}{m}\frac{\partial \Phi}{\partial x}\frac{f(x, v + v_R) - f(x, v - v_R)}{2v_R} = 0, \tag{3.3a}$$

where $v_R := \frac{\hbar k}{m}$ denotes the so-called recoil velocity and we have introduced the optical potential

$$\Phi := \hbar U_0 |\alpha|^2 \cos^2(kx). \tag{3.3b}$$

The cavity mode amplitude satisfies

$$\dot{\alpha} = [-\kappa + i(\Delta_c - NU_0/2)]\alpha - i\frac{NU_0}{2}\alpha \int_{-\infty}^{\infty} dv \int_0^{\lambda} f(x,v,t)\cos(2kx)dx + \eta. \tag{3.3c}$$

Note that we can, in the last equation, without loss of generality restrict the spatial integration to the interval $[0, \lambda]$ and impose periodic boundary conditions on the (quasi-) distribution

$$f(x + \lambda, v, t) = f(x, v, t) \tag{3.4}$$

due to the periodicity of the optical potential. The coupling constant U_0 can take on positive as well as negative values depending on whether the particles in question are weak- or strong field seekers respectively. It can bee interpreted as measuring the optical potential per photon. The constant Δ_c denotes the detuning between the pump laser frequency and the resonance frequency of the selected cavity mode. As can be seen, only the effective detuning $\delta := \Delta_c - NU_0/2$ enters the equations of motion, which corrects the bare detuning by the shift coming from the spatially homogeneous part of the gas density. Finally, κ denotes the decay rate of the resonator mode and η the pump strength related to the external driving laser.

The coupled system of time-dependent equations (3.3) is evidently highly nonlinear. This circumstance, however, does not exhaust the difficulties associated with it. Even the more modest endeavor of investigating stationary states is troubled by the fact that Wigner's equation allows for an infinite number of possible forms of equilibrium distributions for a given cavity mode amplitude. The reason is found in the mean-field nature of the present model, which lacks an entropy production mechanism. Hence, within the context of the chosen model, any hypothetical stationary state depends on the entire history of the dynamics resulting in its realization.

Before we present a way to cope with the above issues in a more or less satisfactory manner, let us give but one concrete example of a possible form of steady-state distributions allowed by (3.3). An obvious choice is given by the class of separable equilibrium phase-space densities, that is such distributions, which can be written in the form of a product

$$f(x, v) = n(x)F(v). \tag{3.5}$$

A density of this kind may be justifiably said to represent a classical state of the gas, since by the properties of $n(x)$ and $F(v)$ as stated in (3.2), it has to be positive throughout all of phase space and can thus be interpreted as a conventional probability distribution thereon. Substituting the ansatz (3.5) into the first of equations (3.3), it is not at all difficult to show that the sought for densities are given by

$$n(x) = n_0 \exp\big(-\frac{\Phi(x)}{2aE_R}\big), \tag{3.6a}$$

$$F(v) = e^{-a}\left[I_0(a)\delta(v) + \sum_{n=1}^{\infty} I_n(a)\big(\delta(v+nv_R) + \delta(v-nv_R)\big)\right], \tag{3.6b}$$

where $E_R := \hbar^2 k^2/2m$ denotes the recoil energy, I_n the modified Bessel functions of the first kind, n_0 a normalization constant and $a > 0$ represents a dimensionless, real-valued constant of separation, making the separable equilibria a one-parameter family of solutions. The spatial probability density (3.6a) is reminiscent of the classical Maxwell-Boltzmann distribution with $2aE_R$ playing the rôle of the thermal energy $k_{\mathrm{B}}T$. The distribution of velocities as given by (3.6b), however, clearly reflects the quantized nature of the interaction of the polarizable gas with the cavity photons. It is entirely localized on integer multiples of the recoil velocity v_R, which is the incremental velocity imparted on a particle upon scattering a photon. The particular form of the velocity distribution implies furthermore that a phase space density belonging to this class may be reached from some initial condition representing a gas forming a Bose-Einstein condensate.

Returning to our previous train of thought we repeat that even though (3.6) represents an exact class of stationary Wigner distributions, there is nothing to recommend the investigation of this particular family of solutions otherwise. We can, however, circumvent both the issue of non-Markovian time evolution and the intractable degree of nonlinearity by restricting ourselves to examining some of the consequences of (3.3) in the limit of a shallow optical potential. Since in this case the spatial inhomogeneity of the particle (quasi-) distribution will be small, we may write

$$f(x,v,t) = f_0(v) + \delta f(x,v,t), \tag{3.7}$$

where $f_0(v)$ denotes an assumed homogeneous bulk distribution and δf designates a small deviation therefrom. The above assumption implies that δf approximately satisfies the linearized Wigner equation

$$\left(\frac{\partial}{\partial t} + v\frac{\partial}{\partial x}\right)\delta f = -\frac{U_0|\alpha|^2}{2}\sin(2kx)\Big(f_0(v+v_R) - f_0(v-v_R)\Big). \tag{3.8}$$

Note however, that due to the large number of particles present, even a small spatial modulation of the gas density may nevertheless be accompanied by a considerable shift in the cavity resonance, giving rise to great variations in the magnitude of the cavity mode amplitude. Thus a similar, linear approximation regarding the equation of motion for α is thereby precluded. A closer inspection of the resulting simplified equations reveals that the only spatial Fourier mode of the deviation δf, which is actually coupled the cavity mode amplitude α is the one having a periodicity of $\lambda/2$. Hence, defining

$$\phi(v,t) := \int_0^{\lambda} \delta f(x,v,t) e^{-2ikx}\mathrm{d}x \tag{3.9}$$

and the velocity distribution of the unperturbed background, $F_0(v) := \lambda f_0(v)$, we are left with

$$\frac{\partial\phi}{\partial t} + 2ikv\phi = \frac{iU_0|\alpha|^2}{4}\Big(F_0(v+v_R) - F_0(v-v_R)\Big) \tag{3.10a}$$

$$\dot{\alpha} = (-\kappa + i\delta)\alpha - i\frac{NU_0}{2}\alpha \int_{-\infty}^{\infty} \mathrm{Re}\left\{\phi(v,t)\right\} \mathrm{d}v + \eta \tag{3.10b}$$

Note, that the velocity variable enters only parametrically and that for every fixed velocity class v, $\phi(v,.)$ satisfies the differential equation of a driven harmonic oscillator with a natural frequency given by $2k|v|$.

3.3 Stationary States

Let's turn to the determination of the steady states (ϕ_0, α_0) of (3.10a)-(3.10b). From (3.10a) one easily finds that every stationary particle mode $\phi_0(v)$ is related to the steady-state photon number $I_0 := |\alpha_0|^2$ via

$$\phi_0(v) = \frac{v_R U_0 I_0}{4} \frac{1}{kv} \frac{\Delta F_0}{\Delta v}, \tag{3.11}$$

where we have defined the difference quotient $\frac{\Delta F_0}{\Delta v}$ via

$$\frac{\Delta F_0}{\Delta v} := \frac{F_0(v + v_R) - F_0(v - v_R)}{2v_R}. \tag{3.12}$$

Substituting this expression into the steady-state version of (3.10b) we get

$$0 = (-\kappa + i\delta)\alpha_0 - i\frac{v_R N U_0^2}{8k} I_0 \alpha_0 \int_{-\infty}^{\infty} \frac{1}{v} \frac{\Delta F_0}{\Delta v} \mathrm{d}v + \eta. \tag{3.13}$$

Whenever the temperature of the bulk is nonzero, we can define a scalar function F and a thermal velocity v_T such that

$$F_0(v) = v_T^{-1} F(v/v_T). \tag{3.14}$$

To shorten the notation, let us furthermore introduce the factor

$$J(v_R/v_T) := \frac{1}{2} \int_{-\infty}^{\infty} \frac{1}{u} \frac{F(u + v_R/v_T) - F(u - v_R/v_T)}{v_R/v_T} \, \mathrm{d}u. \tag{3.15}$$

From (3.13) one obtains the steady-state condition for the photon number I_0 in form of a cubic equation

$$I_0 \left[\kappa^2 + \left(\delta - I_0 \frac{\omega_R N U_0^2 J}{4\omega_T^2}\right)^2\right] = \eta^2. \tag{3.16}$$

Here, we have in addition introduced the recoil frequency $\omega_R := \hbar k^2/2m$ and the thermal frequency $\omega_T = kv_T$. Clearly, equation (3.16) can have up to three distinct real solutions. A typical response curve is depicted in figure 3.2. In the interval of effective detuning designated by the letter A the system allows for several possible steady states at once. Which one of these (if any) can be attained? Needless to say,

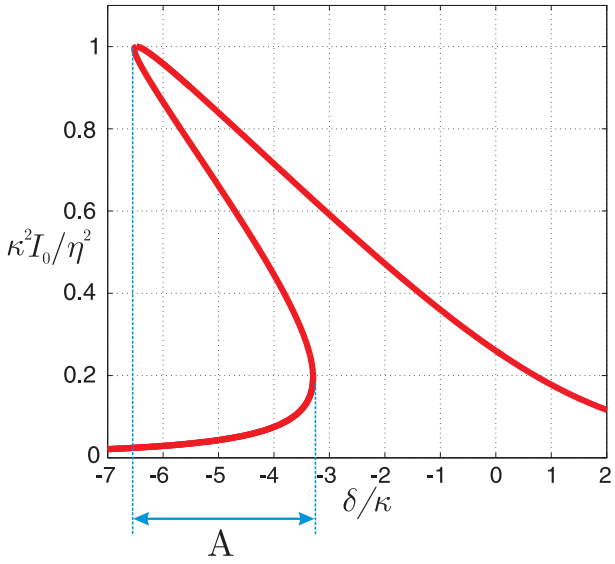

Figure 3.2 Normalized steady state photon number versus effective detuning δ/κ for $N = 10^5$, $U_0 = 0.04\kappa$, $\eta = 18\kappa$, $\omega_T = \kappa$, $\omega_R = 0.5 \cdot 10^{-3}\kappa$ and a Gaussian velocity distribution.

an indispensable condition for any steady solution (ϕ_0, I_0) to actually represent a physical state of the system, is the requirement that a small but otherwise arbitrary deviation from equilibrium does not entail a growth in time of this deviation. A general investigation of the linear stability properties of steady states defined by (3.13) will therefore shed some light on the above posed question. Let us therefore proceed to establish the necessary and sufficient conditions for a given steady state solution to be stable or unstable.

3.4 Stability Analysis

3.4.1 Analysis of the Linearized Equations

The starting point of our analysis will be equations (3.10a)-(3.10b), linearized around a steady state solution. Hence, let us write

$$\phi(v,t) = \phi_0(v) + \delta\phi(v,t), \tag{3.17}$$

$$\alpha(t) = \alpha_0 + \delta\alpha(t) \tag{3.18}$$

and substitute these decompositions into the equations of motion. By keeping only terms that are linear in the deviations $\delta\phi$ and $\delta\alpha$, we obtain

$$\frac{\partial\delta\phi}{\partial t} + 2ikv\delta\phi = \frac{iv_R U_0}{2}\left(\alpha_0\delta\alpha^* + \alpha_0^*\delta\alpha\right)\frac{\Delta F_0}{\Delta v} \tag{3.19}$$

$$\delta\dot{\alpha} = (-\kappa + i\Delta)\delta\alpha - i\frac{NU_0}{2}\alpha_0\int_{-\infty}^{\infty}\mathrm{Re}\left\{\delta\phi(v,t)\right\}\mathrm{d}v, \tag{3.20}$$

where we have set $\Delta := \delta - I_0 \frac{\omega_R N U_0^2 J}{4\omega_T^2}$, which represents the effective detuning pertaining to the given equilibrium. It is advantageous to introduce the Laplace transforms with respect to time of $\delta\phi$, $\delta\phi^*$, $\delta\alpha$ and $\delta\alpha^*$. To keep the notation to a minimum, we will not introduce new symbols for the transformed quantities. Introducing the susceptibility

$$\chi(s) := \frac{N U_0^2 v_R}{8} \int_{-\infty}^{\infty} \left(\frac{\Delta F_0/\Delta v}{s + 2ikv} - \frac{\Delta F_0/\Delta v}{s - 2ikv} \right) \mathrm{d}v, \tag{3.21}$$

where s denotes the complex frequency on which the Laplace transformed quantities depend, we obtain the following linear system of equations:

$$\begin{pmatrix} s + \kappa - i\Delta - I_0\chi(s) & \alpha_0^2\chi(s) \\ \alpha_0^{*2}\chi(s) & s + \kappa + i\Delta + I_0\chi(s) \end{pmatrix} \cdot \begin{pmatrix} \delta\alpha \\ \delta\alpha^* \end{pmatrix} = \begin{pmatrix} I_1 \\ I_2 \end{pmatrix}, \tag{3.22}$$

where (I_1, I_2) denotes an initial value contribution. Let $D(s)$ designate the determinant of the matrix on the left hand side of this last equation, i.e.

$$D(s) = (\kappa + s)^2 + \Delta^2 - 2i\Delta I_0 \chi(s). \tag{3.23}$$

We will henceforth call the function $D(s)$ dispersion relation. As explained at length e.g. in [16], instability of the given steady state is equivalent to the existence of zeros of the dispersion relation with a positive real part. On the other hand, absence of such zeros implies linear stability.

3.4.2 Limit of a Gas at Zero Temperature-BEC

Before we direct our attention to the limiting case of a classical gas at finite temperature, let us briefly take a closer look at the opposite limit, namely that of bosons at zero temperature forming a condensate (BEC). In that case, the velocity distribution of the bulk is given by

$$F_0(v) = \delta(v), \tag{3.24}$$

implying that all particles are at rest. Any steady state photon number can be calculated from (3.16) with the replacements: $J \to -1$ and $\omega_T \to 2\omega_R$. In order to make contact with the method of analysis used in other works, we decompose the solution of equation (3.10a) according to

$$\phi(v,t) = \phi_+(t)\delta(v - v_R) + \phi_-(t)\delta(v + v_R) + \phi_0(v,t), \tag{3.25}$$

where ϕ_0 is a solution of the homogeneous equation. This last contribution can be neglected for sufficiently smooth initial conditions due to rapid "phase mixing", i.e.

$$\int_{-\infty}^{\infty} \phi_0(v,0) e^{-2ikvt} \mathrm{d}v \to 0 \ , \quad \text{as} \quad t \to \infty \tag{3.26}$$

by the Riemann-Lebesgue Lemma. The delta functions appearing in (3.25) imply that the interaction of the condensate with the cavity field creates only particles with

velocities given by $\pm v_R$, which corresponds to the scattering of exactly one resonator photon and makes the meaning of the adopted approximation rather transparent in the present case. Defining the position-like variable

$$x(t) := \mathrm{Re}\left\{\phi_+(t) + \phi_-(t)\right\}, \tag{3.27}$$

one easily verifies that equations (3.10) are mapped onto

$$\ddot{x} + (4\omega_R)^2 x = -\omega_R U_0 |\alpha|^2 \tag{3.28a}$$

$$\dot{\alpha} = (-\kappa + i\delta)\alpha - i\frac{NU_0}{2}\alpha x + \eta, \tag{3.28b}$$

which are precisely the equations used to study the dynamics of a weakly excited BEC inside a standing wave cavity obtained by a Gross-Pitaevskii equation approach[23]. Thus it is seen that the present formalism includes the latter as a special case. The stability of steady states is governed by (6.23), in which the susceptibility takes on the simple form

$$\chi(s) = \frac{i\omega_R N U_0^2}{2}\frac{1}{s^2 + (4\omega_R)^2}. \tag{3.29}$$

As this special case has already been treated, we limit ourselves to the remark that no steady state with $\Delta = \delta + \frac{NU_0^2 I_0}{32\omega_R} > 0$ is stable. This also means that a positive effective detuning, $\delta > 0$, automatically implies instability. We will see in the next section that such a situation does not prevail for a gas at finite temperature.

3.4.3 Thermal Gas - Classical limit

Let us now investigate the dispersion relation for a gas at nonzero temperature in more detail. Note, that as it stands, (6.23) together with (3.42) are defined only for $\mathrm{Re}(s) > 0$. To find the boundary in parameter space, which separates unstable from stable equilibrium states, we need to find the limiting form of the dispersion relation as $\mathrm{Re}(s) \to 0^+$. To this end we recall the Plemjel formula

$$\lim_{\epsilon\to 0^+}\frac{1}{x - y \pm i\epsilon} = \frac{\mathrm{P}}{x-y} \mp i\pi\delta(x-y). \tag{3.30}$$

Here and elsewhere, P denotes the cauchy principal value. Setting $s = \gamma + i\omega$ and writing sloppily $\chi(\omega) = \lim_{\gamma\to 0^+}\chi(s)$, we find

$$\chi(\omega) = -\frac{NU_0^2 v_R}{8k}\left[\frac{1}{i}\mathrm{P}\int_{-\infty}^{\infty}\frac{v\Delta F_0/\Delta v}{(\omega/2k)^2 - v^2}dv + \frac{\pi}{2}\left(\frac{\Delta F_0}{\Delta v}\Big|_{\frac{\omega}{2k}} - \frac{\Delta F_0}{\Delta v}\Big|_{\frac{-\omega}{2k}}\right)\right]. \tag{3.31}$$

It does not make much sense to try to extract general (i.e. true for arbitrary F_0) consequences of (6.23) and (3.31), for even if the stability boundary could be found analytically in terms of a function $I_0^{\mathrm{crit}} = I_0^{\mathrm{crit}}(\delta, N, U_0, \ldots)$, we would still have to

find the intersection of this curve with the one specifying the actually possible combinations $(I_0, \delta, \ldots)$ (defined by (3.16)), and this is obviously a hopelessly complicated task. We will therefore concentrate on the physically most relevant velocity distribution, namely on the thermal distribution. Well above the condensation threshold, it is given by the classical Maxwell-Boltzmann distribution, which reads

$$F_0(v) = \frac{1}{v_T\sqrt{\pi}} e^{-(v/v_T)^2}. \tag{3.32}$$

In this regime, the thermal velocity by far exceeds the recoil velocity, $v_T \gg v_R$, such that we may replace the difference quotient by a derivative

$$\frac{\Delta F_0}{\Delta v} \to \frac{dF_0(v)}{dv} \tag{3.33}$$

in all relevant equations, including (3.10a). This enables the evaluation of the integral in (3.15) with the result $J = -2$. Finally, we should state the condition, that the deviation of the actual particle (quasi-) distribution from the homogeneous background be small, namely

$$\hbar U_0 |\alpha|^2 \ll \frac{m v_T^2}{2}, \quad \text{or} \quad 4\frac{\eta^2}{\kappa^2}\frac{U_0\omega_R}{\omega_T^2} \ll 1, \tag{3.34}$$

which simply means, that the potential energy per particle must be much smaller than the corresponding kinetic energy. We will not try to solve the stability problem fully analytically (which is impossible), but use graphical and numerical methods where necessary instead. Using (3.31) and writing $\lim_{\gamma\to 0^+} D(s) = D_r(\omega) + iD_i(\omega)$, we find

$$D_r(\omega) = \kappa^2 + \Delta^2 - \omega^2 + \frac{NU_0^2\Delta I_0\omega_R}{\omega_T^2}\left(1 - \frac{\omega}{\omega_T}\mathrm{Da}\left(\frac{\omega}{2\omega_T}\right)\right) \tag{3.35}$$

$$D_i(\omega) = 2\kappa\omega - \sqrt{\pi}\frac{NU_0^2\Delta I_0\omega_R}{2\omega_T^2}\frac{\omega}{\omega_T}e^{-\left(\frac{\omega}{2\omega_T}\right)^2} \tag{3.36}$$

Here, $\mathrm{Da}(x)$ denotes Dawson's integral which is defined as

$$\mathrm{Da}(x) = e^{-x^2}\int_0^x e^{t^2}dt \tag{3.37}$$

Note, that the dispersion relation belonging to a thermal velocity distribution can now be seen (upon substituting $\Delta \to \delta$ and $U_0^2 I_0 \to 4\eta^2$) as being identical to the one considered in [16]. Therefore all the results exactly carry over to the present case: A given steady state I_0 is unstable if and only if we have

$$D_r(\omega_0) > 0 \tag{3.38a}$$

for all ω_0 such that

$$D_i(\omega_0) = 0. \tag{3.38b}$$

3.4.4 Graphical Solution of the Stability Problem

In order to extract the information included in the general criterion (3.38), we will resort to graphical means. In order to do so, we note, that the two conditions $D_i = 0, \quad D_r = 0$ define a function

$$I_0 = I_0^{\text{crit}}(\Delta) \tag{3.39}$$

(the dependence on the other parameters is understood implicitly), with the property, that a steady state I_0 is unstable if and only if $I_0 > I_0^{\text{crit}}$. Hence $(\Delta, I_0^{\text{crit}}(\Delta))$ defines the stability boundary in the parameter-space spanned by (Δ, I_0). However, the detuning Δ depends on the given equilibrium photon number and is thus not a freely variable quantity. Using, that

$$\delta = \Delta - \frac{NU_0^2\omega_R}{2\omega_T^2} I_0 \tag{3.40}$$

we can nonetheless parametrically plot the stability boundary, i.e. the mapping

$$\Delta \mapsto \left(\Delta - \frac{NU_0^2\omega_R}{2\omega_T^2} I_0^{\text{crit}}(\Delta), I_0^{\text{crit}}(\Delta) \right) \tag{3.41}$$

in the space of interest, namely the one spanned by (δ, I_0). Together with the response curve defined by (3.16), this allows to analyze the stability properties of the system. Consider again the set of parameters used to plot figure 3.2. Figure 3.3 depicts the response curve and regions of instability defined by (3.16) and (3.39) for two different values of the pump parameter. Clearly, there exists an interval of effective detunings, wherein two distinct steady photon numbers are both linearly stable. Such a state of affairs is known as bistability. Perhaps more surprising however is the existence of an interval, where there can be no stable steady state at all (fig 3.3b)! To summarize the possible behavior of the system when varying the pump strength, we can state that below a certain value, the response curve is single-valued and lies entirely in the stable domain. Above that value, we find multi-valuedness and a region of bistability (fig 3.3a). Only upon crossing a second threshold does the completely unstable interval appear (fig 3.3b).

3.5 Long Time Behavior

3.5.1 Classification

Whenever a (or two) stable steady state(s) is (are) available, we expect the system to relax to it (or one of them) starting from arbitrary initial conditions. How does the system behave for parameters that allow for no stable steady state? To answer this question and to see whether the first guess is correct, we discretized and solved (3.10a)-(3.10b) numerically. Figure 3.4a depicts the time averaged photon number (divided by the maximally possible) for different effective detunings for the usual set of parameters. It is clearly visible, that this averaged photon number deviates from

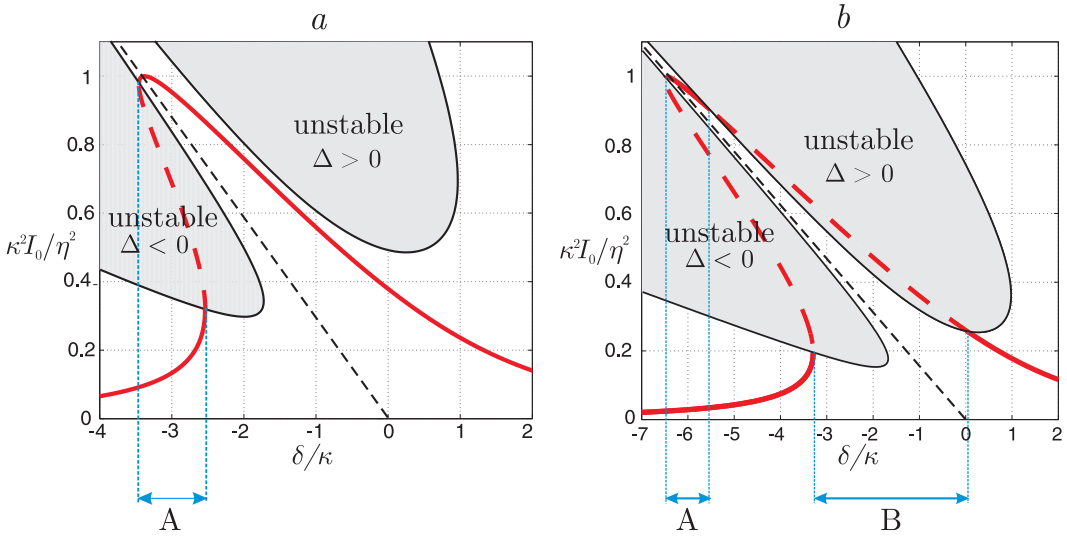

Figure 3.3 Response curve (red) and regions of instability (shaded) for $\eta = 13\kappa$ (a) and $\eta = 18\kappa$ (b). Those parts of the response curve, that lie inside the unstable region (red dashed), correspond to linearly unstable steady states. The black dashed line separates the parameter space into positive and negative values of the equilibrium detuning Δ. The intervals designated A correspond to bistability, the interval designated B supports *no* stable steady state at all. All other parameters as in figure 3.2.

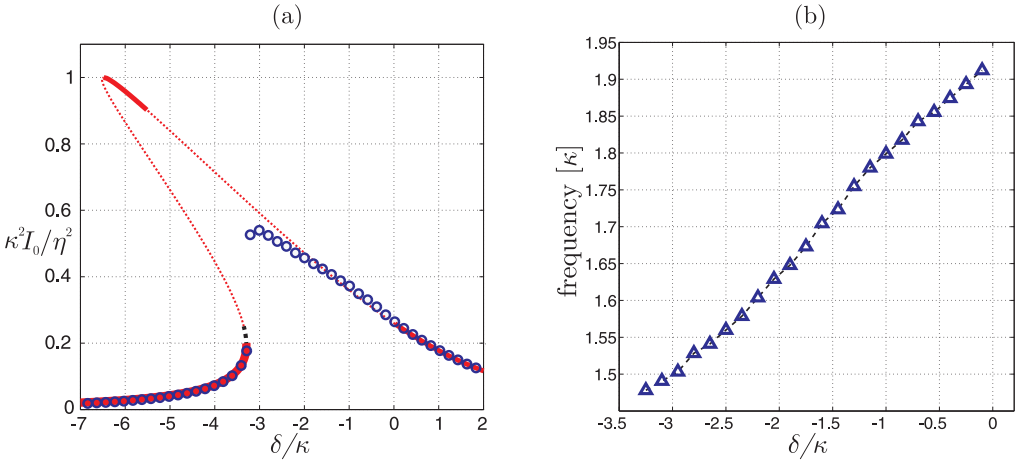

Figure 3.4 a: Response curve (stable parts solid red, unstable parts dotted) and time averaged normalized photon number (blue circles) versus effective detuning. A deviation from the response curve occurs only inside the unstable interval $[-3.3, 0]$, where the system exhibits limit cycle oscillations. b: Limit cycle frequency versus detuning. Parameters as usual.

the steady state photon number only for detunings within the unstable interval, confirming our calculations. To our surprise and for generic sets of parameters, the

system exhibits **limit cycle oscillations** within the completely unstable interval. Unlike in the case of a collisionless BEC, where oscillatory solutions depend on the initial conditions, these are true limit cycles independent of the initial conditions. This difference may be attributed to the phenomenon of "phase mixing" of the infinite number of oscillators in the classical case, which mimics dissipation. The "observed" frequencies of the latter versus detuning are shown in figure 3.4b. For the chosen parameters, these frequencies are of the order of the thermal frequency. If the underlying steady state is weakly unstable, the corresponding limit cycle oscillation is almost monochromatic. Figure 3.5 depicts these oscillations of the photon number for two different detunings inside the unstable interval. As visible, the photon number varies almost harmonically with time. Associated to these oscillations is a standing density wave formed by the particles.

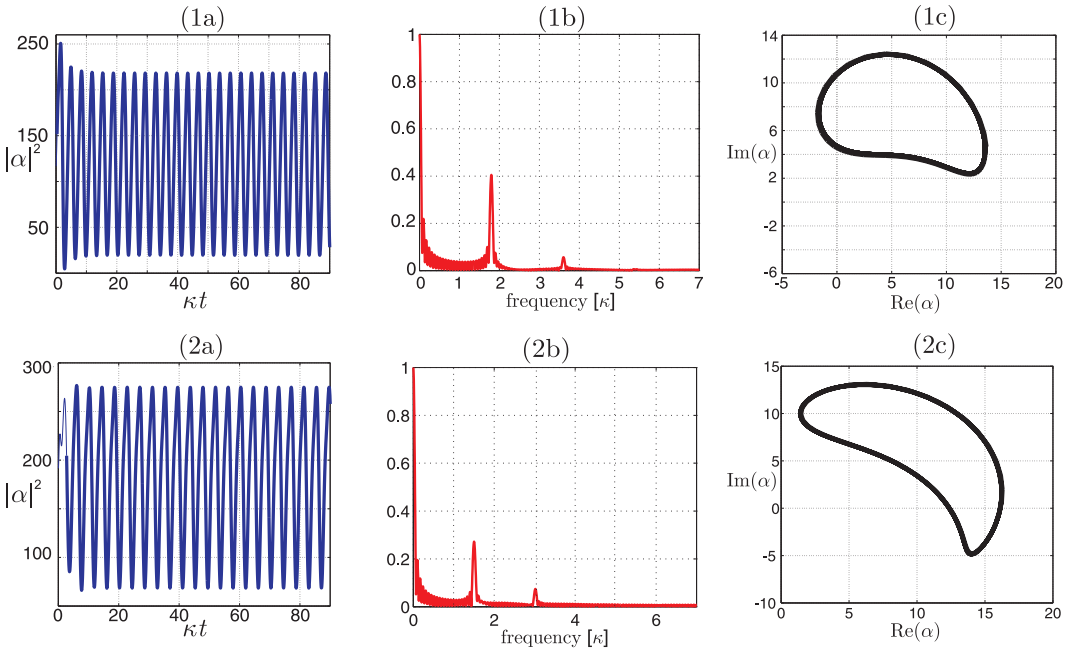

Figure 3.5 (a) Photon number as a function of time for $\delta = -\kappa$ (upper row) and $\delta = -3\kappa$ (lower row) and (b) normalized power spectrum. (c) Shape of the limit cycle. All additional parameters as in fig 4.37.

In figure 3.6 we compare the numerical solution of the reduced model with the solution of Vlasov's equation (3.76) for the same parameters as in figure 3.5. The agreement between the two models is excellent, confirming the validity of the approximations we introduced.

3.5.2 Limit Cycle Frequency Close to Threshold

As mentioned, one finds numerically, that for parameters such that the steady state with $\Delta > 0$ is *weakly* unstable, in its place there exists a periodic oscillation (limit

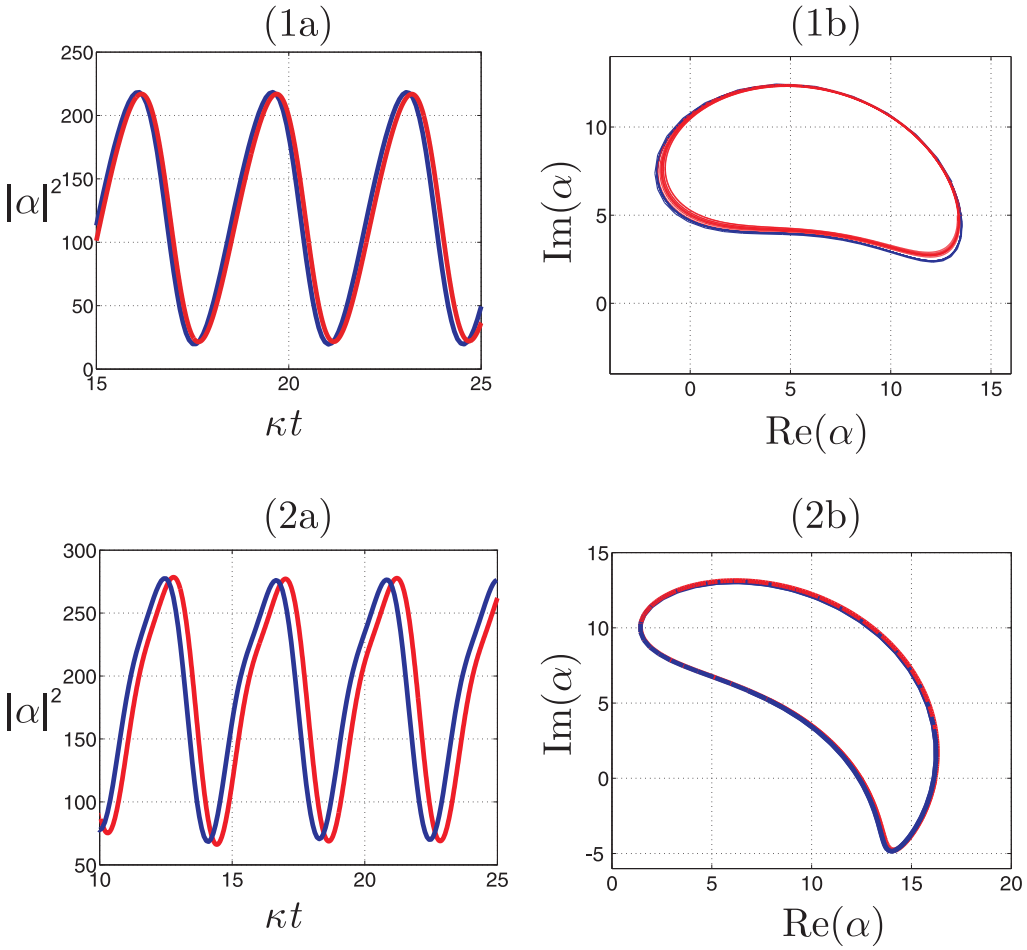

Figure 3.6 Comparison between the reduced (3.10)(blue) and the Vlasov model (3.76) (red). Apart from a phase shift, the results are almost identical. All parameters as in fig 4.37 and fig 3.5.

cycle), which is almost monochromatic. This enables us to construct these cycles in a perturbative manner. Without loss of generality, we may assume, that the sought for solution satisfies

$$\chi(t) := \int_{-\infty}^{\infty} \mathrm{Re}\left\{\phi(v,t)\right\} dv \sim \chi_0 + \chi_1 \cos(\omega t) \tag{3.42}$$

and

$$|\alpha(t)|^2 =: I(t) = \sum_n I_n \, e^{in\omega t} \tag{3.43}$$

with real coefficients χ_0 and χ_1 and $I_n = I_{-n}^* \in \mathbb{C}$. Of course, ω denotes the sought for limit cycle frequency. Substituting (3.42) into (3.10b) and using

$$e^{ix\cos(\varphi)} = \sum_n J_n(x) e^{in\varphi}, \tag{3.44}$$

we obtain the Fourier coefficients of the photon number in terms of ω, χ_0, χ_1 as

$$I_n(\chi_0, \chi_1) = \eta^2 \sum_{m=-\infty}^{\infty} \frac{J_m\left(\frac{NU_0\chi_1}{2\omega}\right) J_{m-n}\left(\frac{NU_0\chi_1}{2\omega}\right)}{[-\kappa + i\Delta - im\omega]\,[-\kappa - i\Delta - i(n-m)\omega]}, \tag{3.45}$$

where $\Delta = \delta + \frac{NU_0\chi_0}{2}$. In order to link χ_0, χ_1 to the photon number coefficients I_n self-consistently, we must evaluate the response of the particles to an applied intensity varying like $\sum_n I_n e^{in\omega t}$ in the form $\phi = \sum_n \phi_n(v) e^{in\omega t}$, i.e. we have to solve

$$(\omega + 2kv)\phi_n = \frac{v_R U_0 I_n}{2} \frac{\partial F_0}{\partial v}. \tag{3.46}$$

Note carefully, that we cannot simply divide this equation by $n\omega + 2kv$ to obtain the solution because of the singularity at $v = -\omega/2k$. Instead, we have to regard $\phi_n(v)$ as a generalized function to obtain

$$\phi_n(v) = \frac{v_R U_0 I_n}{2} \left(\frac{\partial F_0(v)}{\partial v} \frac{\mathrm{P}}{n\omega + 2kv} + h_n(v)\delta\left(n\omega + 2kv\right) \right), \tag{3.47}$$

where P denotes the Cauchy principal value and $h_n(v)$ is arbitrary. As a remedy to this uniqueness problem, one may introduce collisions characterized by a collision frequency and let this frequency go to zero in the end. Alternatively, one may replace

$$e^{in\omega t} \to \lim_{\gamma \to 0^+} e^{(in\omega + \gamma)t}, \tag{3.48}$$

which means to consider the intensity as turned on infinitely slowly from the infinitely remote past. In either case the arbitrariness is lifted and we get

$$h_n(v) = i\pi \frac{\partial F_0(v)}{\partial v}. \tag{3.49}$$

From this solution we find

$$\chi_0 = \frac{v_R U_0 I_0}{2k} \int_{-\infty}^{\infty} \frac{1}{v} \frac{\partial F_0(v)}{\partial v} dv = \frac{U_0 \omega_R J}{2\omega_T^2} I_0 \tag{3.50}$$

and

$$\chi_1 = \frac{U_0 v_R}{4k} \left(I_a \int_{-\infty}^{\infty} \frac{\frac{\partial F_0(v)}{\partial v} dv}{\omega/2k + v} - I_b \pi \frac{\partial F_0}{\partial v}(\omega/2k) \right), \tag{3.51}$$

where $I_a = I_1 + I_1^*$ and $I_b = i(I_1 - I_1^*)$.
As we have chosen $\int_0^{2\pi/\omega} \chi(t) \sin(\omega t) dt = 0$, we have additionally

$$I_b \int_{-\infty}^{\infty} \frac{\frac{\partial F_0(v)}{\partial v} dv}{\omega/2k + v} = -\pi I_a \frac{\partial F_0}{\partial v}(\omega/2k). \tag{3.52}$$

By means of (3.45), equations (3.50), (3.51) and (3.52) constitute three equations for the three unknowns ω, χ_0, χ_1 characterizing the limit cycle solution we wish to find. To simplify the problem at hand, let us assume, that the cycle be such, that

$$\left| \frac{NU_0\chi_1}{2\omega} \right| \ll 1. \tag{3.53}$$

Then we may use, that for $n \geq 0$: $J_n(x) \approx \frac{1}{n!}\left(\frac{x}{2}\right)^n$, if $|x| \ll \sqrt{1+n}$ and $J_{-n} = (-1)^n J_n$ and we have the expansion

$$\chi_0 = \chi_0^{(0)} + \chi_0^{(2)}(\omega)\left(\frac{NU_0\chi_1}{4\omega}\right)^2 + \ldots, \tag{3.54}$$

where $\chi_0^{(0)}$ solves

$$\chi_0^{(0)} = \frac{U_0\omega_R J}{2\omega_T^2}\frac{\eta^2}{\kappa^2+\Delta_0^2}, \tag{3.55}$$

with $\Delta_0 = \delta + NU_0\chi_0^{(0)}/2$. This last equation of course implies, that to lowest order the time averaged shift of the cavity resonance frequency in the cycle is the same as the one corresponding to the unstable steady state. With these results, one may write

$$I_1 = I_1^{(1)}(\omega, \chi_0^{(0)})\frac{NU_0\chi_1}{4\omega} + I_1^{(3)}(\omega, \chi_0^{(0)})\left(\frac{NU_0\chi_1}{4\omega}\right)^3 + \ldots, \tag{3.56}$$

where

$$I_1^{(1)}(\omega, \chi_0^{(0)}) = \frac{2\eta^2\omega\Delta_0}{(\kappa^2+\Delta_0^2)(\kappa^2+\Delta_0^2-\omega^2+2i\kappa\omega)} \tag{3.57}$$

Now, to get the cycle frequency ω, we solve (3.52) with (3.56) to lowest order in the small quantity. This yields the dispersion relation for limit cycles just above threshold as

$$2\kappa\omega\int_{-\infty}^{\infty}\frac{\frac{\partial F_0(v)}{\partial v}dv}{\omega/2k+v} = (\kappa^2+\Delta_0^2-\omega^2)\pi\frac{\partial F_0}{\partial v}(\omega/2k), \tag{3.58}$$

which, for a thermal distribution, is the equation determining the frequency of oscillations of perturbations of the unstable steady state. Unfortunately, the transcendent equation (3.58) cannot be solved in closed form. But in the special case that $\omega \ll \omega_T \equiv kv_T$ we find

$$\omega = \sqrt{\kappa^2+\Delta_0^2+\frac{4\kappa\omega_T}{\sqrt{\pi}}}. \tag{3.59}$$

Note, that as Δ_0 (if positive) is monotonously increasing with increasing effective detuning δ, so is the limit cycle frequency. In figure 3.7 we compare the prediction of (3.58) to the numerically determined limit cycle frequency for parameters such that the equilibrium state is weakly unstable throughout most of the interval of detunings supporting limit cycle oscillations. Note the good agreement as well as the confirmation of the result that the time averaged photon number equals the corresponding steady state value.

3.6 Conclusions and Outlook

The nonlinear dynamical response of a high-Q optical cavity filled with a cold gas of polarizable particles can be treated by an effective Vlasov type mean field approach over a surprisingly large range of temperatures from close to zero (BEC)

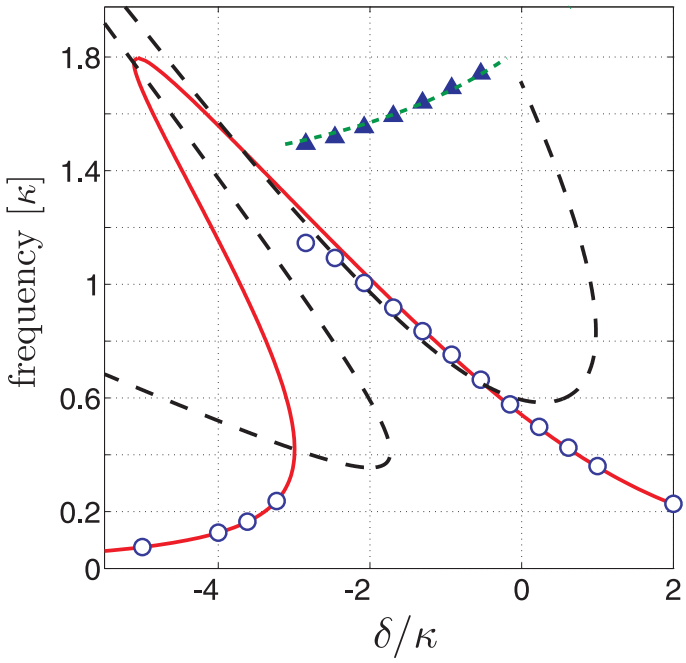

Figure 3.7 Response curve and numerically determined limit cycle frequency (blue triangles) vs. theoretical frequency from (3.58) (green dashed). The blue circles show the time averaged photon number. Parameters: $N = 10^5$, $\omega_T = \kappa$, $\omega_R = 10^{-3}\kappa$ and $U_0 = 0.05\kappa$.

to a thermal gas. In both cases density waves of the medium are strongly coupled to the intracavity field dynamics. Besides the well-known optical bistability effect concurrent with a hysteresis effect, we can clearly identify the regions in parameter space, where no stable stationary solutions exists and time evolution converges to a periodic limit cycle. Its frequency is characteristic for the temperature and gas properties and can be explicitly calculated in the BEC limit or close to threshold for a thermal gas. In both cases such oscillations have been reported experimentally and thoroughly studied[21, 24, 25]. The observations agree well with our model. Interestingly, the effect is predicted to persist at much higher temperatures creating a nonlinear response in a linearly polarizable medium. As to its practical observability a few critical remarks are in order. All of our calculations concerning the long-term fate of the system are based on a reduced model of the dynamics, in which the overall distribution of velocities remains invariant, amounting to a neglect of any change in kinetic energy of the gas. However, a coherent oscillation at some frequency ω as predicted in this work will inescapably lead, on a classical level, to a strong acceleration of such particles as possess resonant velocities $v \sim \pm\omega/2k$. Therefore, one might reasonably expect the cycle frequency to drift in time. This in turn would

continuously increase the number of particles affected resonantly and lead to an irreversible heating of the gas, thereby pushing it towards temperatures, where a stable steady state becomes again available and the oscillation ceases. Alternatively, it is also thinkable that the field-gas dynamics becomes chaotic through the acceleration of resonant particles. By this line of reasoning we are lead to conclude that, in the absence of a collisional redistribution of energy or thermostatting, the predicted limit cycle oscillations could very well turn out to be a transient phenomenon. Nevertheless, a gas with a non-negligible rate of collisions could show a qualitatively similar but stable behavior.

In the long run the system thus represents a well controllable and experimentally implementable toy system to study generic nonlinear dynamics in the transition range from classical to quantum mechanics. Adding extra modes or atomic species will allow to extend its scope and complexity in many directions.

3.7 Appendix: Quantum and Classical Mean Field Limit

Here we show, how the mean field Wigner equation and its classical counterpart, namely Vlasov's equation, can be obtained from the quantum mechanical equations for $N \to \infty$ polarizable particles coupled to one or more resonator modes. When spontaneous emission is neglected, the Heisenberg equation of motion for the particle field operator $\hat{\psi}(x,t)$ in the strong trapping approximation reads

$$\frac{\partial}{\partial t}\hat{\psi} = \frac{i\hbar}{2m}\frac{\partial^2}{\partial x^2}\hat{\psi} + \frac{1}{i\hbar}\hat{\Phi}\hat{\psi}, \tag{3.60}$$

wherein $\hat{\Phi} = \hat{\Phi}(x, \hat{a}_1, \ldots, \hat{a}_M) = \hat{\Phi}^\dagger$ is the potential at the location x created by the photons of the $M \geq 1$ modes. Let us introduce the phase space density operator

$$\hat{f}(x,p) = \frac{1}{2\pi\hbar}\int e^{-izp/\hbar}\ \hat{\psi}^\dagger\left(x - \frac{z}{2}\right)\hat{\psi}\left(x + \frac{z}{2}\right)dz, \tag{3.61}$$

where $p = mv$ is the momentum. Taking its expectation value it may be noted that

$$\langle\hat{f}(x,p)\rangle = \frac{1}{2\pi\hbar}\int e^{-izp/\hbar}\rho_{p,1}\left(x + \frac{z}{2}, x - \frac{z}{2}\right)dz. \tag{3.62}$$

Hence, $\langle\hat{f}(x,p)\rangle$ is the Wigner transform of the one-body reduced density matrix $\rho_{p,1}(x,x') = \langle\hat{\psi}^\dagger(x')\hat{\psi}(x)\rangle$ and therefore equal to the phase space quasi-distribution $f(x,p)$ considered in this chapter, expressed in terms of the momentum instead velocity. To derive the equation of motion for the phase space density operator, let us write for the sake of brevity

$$\hat{\psi}_\pm = \hat{\psi}(x \pm z/2), \quad \hat{\Phi}_\pm = \hat{\Phi}(x \pm z/2). \tag{3.63}$$

Then it follows from equation (3.60) that

$$\frac{\partial \hat{f}}{\partial t} = \frac{1}{2\pi\hbar}\int dz e^{-ipz/\hbar}\Big[\frac{2i\hbar}{m}\left(\hat{\psi}_-^\dagger \frac{\partial^2}{\partial z^2}\hat{\psi}_+ - \frac{\partial^2}{\partial z^2}\left(\hat{\psi}_-^\dagger\right)\hat{\psi}_+\right) + \\ + \frac{1}{i\hbar}\hat{\psi}_-^\dagger\hat{\psi}_+\left(\hat{\Phi}_+ - \hat{\Phi}_-\right)\Big]. \quad (3.64)$$

Here, we have used that the potential and the field operator commute. The first of these two terms may be written as

$$\begin{aligned}\frac{2i\hbar}{m}\frac{1}{2\pi\hbar}\int dz e^{-ipz/\hbar}&\left(\hat{\psi}_-^\dagger\frac{\partial^2}{\partial z^2}\hat{\psi}_+ - \frac{\partial^2}{\partial z^2}\left(\hat{\psi}_-^\dagger\right)\hat{\psi}_+\right) = \\ &= \frac{2i\hbar}{m}\frac{1}{2\pi\hbar}\int dz e^{-ipz/\hbar}\frac{\partial}{\partial z}\left(\hat{\psi}_-^\dagger\frac{\partial}{\partial z}\hat{\psi}_+ - \frac{\partial}{\partial z}\left(\hat{\psi}_-^\dagger\right)\hat{\psi}_+\right) = \\ &= -\frac{2p}{m}\frac{1}{2\pi\hbar}\int dz e^{-ipz/\hbar}\left(\hat{\psi}_-^\dagger\frac{\partial}{\partial z}\hat{\psi}_+ - \frac{\partial}{\partial z}\left(\hat{\psi}_-^\dagger\right)\hat{\psi}_+\right) = \\ &= -\frac{p}{m}\frac{1}{2\pi\hbar}\int dz e^{-ipz/\hbar}\left(\hat{\psi}_-^\dagger\frac{\partial}{\partial x}\hat{\psi}_+ + \frac{\partial}{\partial x}\left(\hat{\psi}_-^\dagger\right)\hat{\psi}_+\right) = \\ &= -\frac{p}{m}\frac{\partial}{\partial x}\hat{f}(x,p). \quad (3.65)\end{aligned}$$

To handle the second, define

$$\hat{U}(x,q) := \frac{i}{2\pi\hbar}\int dz\left(\hat{\Phi}(x+z/2) - \hat{\Phi}(x-z/2)\right)e^{-iqz}. \quad (3.66)$$

Then one obtains

$$\frac{1}{2\pi\hbar}\frac{1}{i\hbar}\int dz e^{-ipz/\hbar}\hat{\psi}^\dagger\hat{\psi}\left(\hat{\Phi}_+ - \hat{\Phi}_-\right) = -\int \hat{U}(x,q)\hat{f}(x,p-\hbar q)dq. \quad (3.67)$$

Thus the equation of motion for the phase space operator reads

$$\frac{\partial \hat{f}}{\partial t} + \frac{p}{m}\frac{\partial \hat{f}}{\partial x} + \int \hat{U}(x,q)\hat{f}(x,p-\hbar q)dq = 0. \quad (3.68)$$

In case of a single standing wave resonator mode, the optical potential is given by

$$\hat{\Phi}(x,\hat{a}) = \hbar U_0 \hat{a}^\dagger\hat{a}\,\cos^2(kx). \quad (3.69)$$

In this case one can easily evaluate (3.66) and finds

$$\hat{U}(x,q) = \frac{U_0}{2}\hat{a}^\dagger\hat{a}\sin(2kx)\left[\delta(k+q) - \delta(k-q)\right]. \quad (3.70)$$

The equation for the phase space density operator thus reads:

$$\frac{\partial \hat{f}}{\partial t} + \frac{p}{m}\frac{\partial \hat{f}}{\partial x} + \frac{U_0}{2}\hat{a}^\dagger\hat{a}\sin(2kx)\left[\hat{f}(x,p+\hbar k) - \hat{f}(x,p-\hbar k)\right] = 0. \quad (3.71)$$

To arrive at a self-contained model this equation is to be supplemented by the Heisenberg-Langevin equation for the annihilation operator $\hat{a}$ of the cavity mode:

$$\dot{\hat{a}} = (-\kappa + i\Delta_c)\hat{a} - iU_0\hat{a}\int \mathrm{d}x \int \hat{f}(x,p)\cos(2kx)\mathrm{d}p + \eta + \hat{a}_{in}, \tag{3.72}$$

where $\hat{a}_{in}$ represents the quantum noise caused by the loss of photons through the mirrors. The mean-field limit $N \to \infty$ can be found by decomposing both the cavity mode annihilation operator $\hat{a} = \alpha + \delta\hat{a}$ and the phase space operator $\hat{f} = f + \delta\hat{f}$ into their expectation values and fluctuations, with $\langle\delta\hat{a}\rangle = \langle\delta\hat{f}\rangle = 0$, then taking the expectation value of (3.71) and (3.72) and neglecting all correlations. This procedure leads to Wigner's equation (sometimes called the Quantum Vlasov equation) for the expectation value of $\hat{f}(x,p)$

$$\frac{\partial f}{\partial t} + \frac{p}{m}\frac{\partial f}{\partial x} + \frac{U_0}{2}|\alpha|^2\sin(2kx)\left[f(x,p+\hbar k) - f(x,p-\hbar k)\right] = 0 \tag{3.73}$$

and similarly

$$\dot{\alpha} = (-\kappa + i\Delta_c)\alpha - iU_0\frac{\alpha}{2}\int \mathrm{d}x \int f(x,p)\cos(2kx)\mathrm{d}p + \eta. \tag{3.74}$$

These are the basic equations employed in this chapter. The question naturally arises, under which conditions the neglect of correlations constitutes a valid approximation. Note also that at the given level of sophistication, there exists no difference between bosonic and fermionic particles. We will have to say more about these issues in the next chapter. If we further assume that the typical particle momentum is much larger than the recoil momentum $\hbar k$, we can expand

$$f(x,p\pm\hbar k) \approx f(x,p) \pm \hbar k\frac{\partial f}{\partial p}(x,p) + \frac{\hbar^2k^2}{2}\frac{\partial^2 f}{\partial p^2}(x,p). \tag{3.75}$$

Then (3.73) becomes

$$\frac{\partial f}{\partial t} + \frac{p}{m}\frac{\partial f}{\partial x} + \hbar k U_0|\alpha|^2\sin(2kx)\frac{\partial f}{\partial p} = 0, \tag{3.76}$$

which is Vlasov's equation. Hence, the classical model employed for example in [16] and also in this work can be recovered as a limiting case of Wigner's mean field equation and is expected to be accurate if $k_B T \gg \hbar^2k^2/2m$, i.e. if the thermal energy (or kinetic energy per particle) of the gas is much higher than the recoil energy.

4 Kinetic Theory of Cavity Cooling and Selforganisation – Classical

4.1 Introduction

A dilute cold gas of polarisable particles can be manipulated in a controlled way using the light forces induced by a sufficiently strong laser far off any internal optical resonance [26]. For a free-space laser setup this force generates a conservative optical potential for the particles with a depth proportional to the local light intensity. As the forces are generated via photon redistribution among different spatial directions, the particles in turn alter the field distribution and act essentially as a spatially varying refractive index. While this backaction can safely be ignored in standard optical traps [27], it was shown to have a significant effect if the light fields are confined within an optical resonator enhancing the effective particle-light interaction [3].

For transverse illumination a threshold pump intensity where this coupled particle-field dynamics can lead to spatial selfordering of the particles into a regular pattern—resembling very closely a phase transition—was theoretically predicted and experimentally confirmed [4, 5, 28]. Due to cavity losses this dynamics is dissipative and thus can constitute a new cooling mechanism for a very general class of polarisable objects [29, 30]. Extensive simulations using fairly large numbers of particles with large detunings predict that already with current molecular sources and cavity technology a useful phase-space compression could be achieved [31]. However, particle-based simulations cannot be applied to sufficiently large particle numbers and laser powers for the whole parameter range of interest. As an alternative, a mean-field approach based on (Wigner's or) Vlasov's equation [16] for the particles' phase-space distribution provides a description for arbitrarily large ensembles. This theory has proven capable of determining the conditions necessary for the spatial selfordering of a gas to occur and to describe various dynamical aspects of gas-cavity systems (as shown for example in the previous chapter), but due to its inherent neglect of dynamical correlations the basis for both the cavity cooling mechanism and uniquely defined equilibrium states has been lost. We have already remarked on the lack of an entropy production mechanism of mean-field models in the last chapter and the difficulties associated with the resulting non-Markovian dynamics. The present chapter attempts to provide a remedy for this problem exemplified in the case of a transversally illuminated gas of polarisable particles interacting with a single mode of an optical resonator. Focusing on a semi-classical model, we adopt methods from plasma kinetic theory to extend the Vlasov kinetic theory to include correlations, leading to a non-linear Fokker–Planck equation for the statistically av-

eraged microscopic phase-space distribution, which includes friction and diffusion and allows to predict cooling time scales and the unique steady-state distribution. In the next chapter we extend the theory to the quantum domain.

4.2 Semiclassical equations of motion

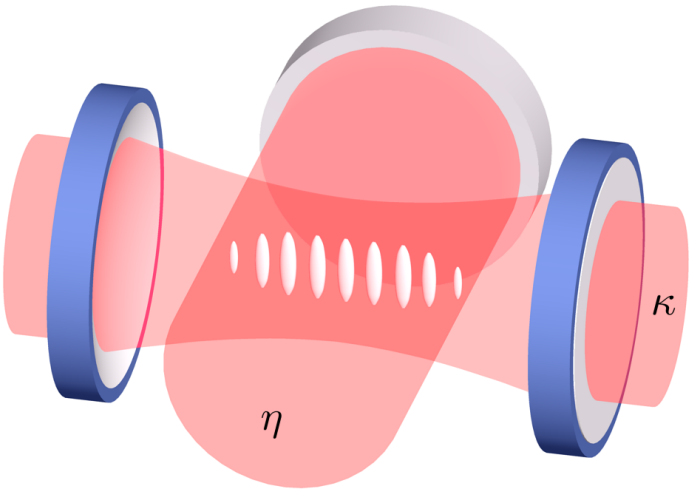

Figure 4.1 An ensemble of particles is illuminated by a transverse standing-wave laser and scatters light into the resonator (effective pump strength η). Above a threshold pump intensity the particles selforganise in a periodic pattern. Cavity losses are characterised by the decay rate κ.

We consider N polarisable particles moving along the axis of a lossy standing-wave resonator assuming strong transversal confinement. The particles are off-resonantly illuminated by a transverse standing-wave pump laser and scatter light, whose phase is determined by the particle positions, into the cavity. The quantum master equation describing this system can be transformed into a partial differential equation for the Wigner function [13]. Truncating this equation at second-order derivatives (semiclassical limit) yields a Fokker–Planck equation, which for positive Wigner functions—excluding all non-classical states [32]—is equivalent to the Itō stochastic

differential equation (SDE) system

$$\mathrm{d}x_j = v_j \,\mathrm{d}t \tag{4.1a}$$

$$\mathrm{d}v_j = -\frac{1}{m}\frac{\partial \Phi(x_j,\alpha)}{\partial x_j}\,\mathrm{d}t \tag{4.1b}$$

$$\begin{aligned}\mathrm{d}a = &\left[i\left(\Delta_\mathrm{c} - U_0\sum_{j=1}^{N}\sin^2(kx_j)\right) - \kappa\right] a\,\mathrm{d}t - \\ &- i\eta\sum_{j=1}^{N}\sin(kx_j)\,\mathrm{d}t + \sqrt{\frac{\kappa}{2}}\left(\mathrm{d}W_1 + i\,\mathrm{d}W_2\right),\end{aligned} \tag{4.1c}$$

with the single-particle optical potential

$$\Phi(x,a) = \hbar U_0 |a|^2 \sin^2(kx) + \hbar\eta(a+a^*)\sin(kx). \tag{4.2}$$

Each particle has the mass m; x_j and v_j denote the centre-of-mass position and velocity of the jth particle, respectively. U_0 is the light shift per photon and κ the cavity decay rate; the associated input noise is taken into account by the two Wiener processes $\mathrm{d}W_1$ and $\mathrm{d}W_2$. Here we have neglected momentum diffusion caused by spontaneous emission, which is valid for large ensembles and large detunings [30]. The transverse laser standing wave gives an effective position-dependent pump of magnitude η of the field mode a with wave number k. This laser is detuned by $\Delta_\mathrm{c} = \omega_\mathrm{L} - \omega_\mathrm{c}$ from the bare cavity resonance frequency. We will focus on the weak-coupling limit $N|U_0| \ll |\Delta_\mathrm{c}|$ throughout much of this chapter. Refer to fig. 4.1 for a schematic view of the system.

We used the scheme proposed in [33, 34] for the direct numerical integration of the SDE system (4.1). However, for analytical predictions and the description of very large ensembles, a continuous phase-space description as described below proves far more suitable.

4.3 Derivation of the Classical Kinetic Theory

Now that the stage has been set and the model sufficiently elucidated, we will develop the formalism for the announced extension of the previous mean-field Vlasov kinetic theory, which permits the investigation of the long-term dynamics and equilibrium of polarizable particles inside a standing-wave cavity. This section is unavoidably rather technical and lengthy, but the reader may skip it without danger and jump directly to section 4.4, as the main concepts will be reiterated there.

The semi-classical equations of motion as stated in equations (4.1) can be reformulated in an equivalent way by introducing the microscopic (or Klimontovich) phase space density $f_\mathrm{K}(x,p,t)$. This object is defined in terms of the Newtonian

trajectories of the particles $\{x_j(t), p_j(t)\}$ as

$$f_{\mathrm{K}}(x,p,t) := \sum_{j=1}^{N} \delta(x - x_j(t))\delta(p - p_j(t)), \tag{4.3}$$

where we have used the momentum $p = mv$ rather than the velocity variable and note that

$$\iint f_{\mathrm{K}}(x,p,t)\mathrm{d}x\mathrm{d}p = N. \tag{4.4}$$

Apart from this section we use the above mircroscopic distribution function but multiplied by N^{-1}, which however should not cause to great a confusion. The designation "microscopic" phase space density is well-deserved, because $f_{\mathrm{K}}(x,p,t)\mathrm{d}x\mathrm{d}p$ is equal to the actual number of particles located around the phase space point $(x,p) =: z$ at the particular instant of time. With its help the equations of motions can be recast in the form

$$\frac{\partial f_{\mathrm{K}}}{\partial t} + \{f_{\mathrm{K}}, h\} = 0, \tag{4.5a}$$

$$\dot{a} = (-\kappa + i\Delta_c)a - \frac{i}{\hbar}\int f_{\mathrm{K}} \frac{\partial h}{\partial a^*}\mathrm{d}z + \sqrt{\kappa}\xi, \tag{4.5b}$$

where $h := p^2/2m + \Phi$ denotes the one-body Hamiltonian and $\{\,,\,\}$ the ordinary Poisson bracket

$$\{f,g\} := \frac{\partial f}{\partial x}\frac{\partial g}{\partial p} - \frac{\partial f}{\partial p}\frac{\partial g}{\partial x}. \tag{4.6}$$

As they stand, equations (4.5) represent nothing but a peculiar way of describing the dynamics of the system and offer no advantage over the original formulation in terms of computational effort. Being interested in the behavior of the system when the number of particles is large, we do not care about the details of a single realization, which is determined by the set of initial positions and momenta, the particular realization of the noise process and the initial value of the cavity mode amplitude. Rather, we aim at a statistically averaged description of the gas-cavity system under the assumption of similar initial conditions. In many cases of many-body problems, where one is interested mainly in studying equilibrium situations, Gibbs' statistical mechanics provides an ideal tool. In the present case, however, the openness of the system, that is the loss of light through the mirrors, prevents us from utilizing the latter. Therefore, we seek inspiration from the discipline known as kinetic theory. What follows is in essence an adaption and application of methods used in this field to the present model system. Let us decompose the microscopic phase space densities and the mode amplitude according to

$$f_{\mathrm{K}}(x,p,t) = f(x,p,t) + \delta f(x,p,t) \tag{4.7a}$$

$$a(t) = \alpha(t) + \delta\alpha(t), \tag{4.7b}$$

where $f(x,p,t) := \langle f_{\mathrm{K}}(x,p,t)\rangle$ and $\alpha(t) := \langle a(t)\rangle$ denote the statistical average over an ensemble of suitable (i.e. similar) initial conditions

$x_j(0), p_j(0), a(0)$ and realizations of the white noise process ξ. Accordingly, we may split the optical potential $\Phi = \langle\Phi\rangle + \delta\Phi$, such that

$$h = \frac{p^2}{2m} + \langle\Phi\rangle + \delta\Phi =: H + \delta\Phi. \tag{4.8}$$

Let it be noted that we will always approximate

$$\langle\Phi(x, a, a^*)\rangle \simeq \Phi(x, \alpha, \alpha^*), \tag{4.9}$$

that is, we will neglect terms stemming from mode-mode correlations. Then, by taking the average of (4.5a), we have

$$\frac{\partial f}{\partial t} + \{f, H\} = -\langle\{\delta f, \delta\Phi\}\rangle\,. \tag{4.10}$$

If we neglect the correlation on the r.h.s., we recover the mean-field Vlasov equation,

$$\frac{\partial f}{\partial t} + \frac{p}{m}\frac{\partial f}{\partial x} - \frac{\partial\Phi}{\partial x}\frac{\partial f}{\partial p} = 0, \tag{4.11}$$

which is a valid approximation to the system for short enough times. The meaning of "short enough times" or initial stage of the time evolution essentially depends on the number of particles N. The crucial assumption, which allows to go beyond Vlasov's theory, is that this initial stage is terminated by a mean-field steady-state and that the system will afterwards, driven by particle-field correlations, "slowly" (the meaning of which will be made clearer later on) relax to it's true equilibrium state by passing through a sequence of mean-field steady states. As we will see later, numerical simulations of the N-body equations (4.1) confirm the validity of this assumption. In this context, it is helpful to note that an arbitrary averaged distribution function $f(x, p)$, which corresponds to an equilibrium solution of Vlasov's equation, necessarily depends on the phase space coordinates (x, p) only through the one-body Hamiltonian $H(x, p)$ as defined in (4.8). This fact, known as Jeans' theorem, is an immediate consequence of the steady-state equation $\{f, H\} = 0$, which in the present one-dimensional setting implies $f = f(H)$.

To repeat, we shall henceforth postulate that after the lapse of some initial mean-field stage described by Vlasov's equation (4.11), the averaged distribution depends only on the instantaneous Hamiltonian and preserves this form during the course of its further evolution in time, i.e.

$$f(x, p, t) \simeq f(H, t). \tag{4.12}$$

Note that we say instantaneous, because in fact we have
$H = H(x, p, \alpha(t), \alpha^*(t))$, that is, the Hamiltonian depends on time through the average value of the mode amplitude. Hence, in order to effectively implement the assumptions about the long-term dynamics just outlined, a change in variables from

(x, p) to some new pair containing as one of its variables the Hamiltonian or some function thereof suggests itself naturally. An obvious choice of transformation, which fulfills this and furthermore, being canonical, preserves the Poisson bracket, is given by $(x, p) \to (I, \theta)$, the latter denoting instantaneous action-angle variables corresponding to the Hamiltonian H. Here we need to make a few remarks on the scope and limitation of the endeavor we are about to embark on. The introduction of action-angle variables is, in the most general case, not entirely trivial. The averaged optical potential may possess up to three distinct minima inside the interval $[0, \lambda]$, thereby dividing the single-particle phase into up to four different regions: three or less regions of trapped particle orbits and an additional region of passing particle orbits. The action-angle variables will have to be defined in all of these regions separately for a given value of the averaged mode amplitude α. The problem enters when we bear in mind that particles can cross from one region to another and that regions can even appear and disappear multiple times in the course of time. The theory we are about to develop does not attempt to deal with these issues. Instead, it will allow us to identify the processes which drive the evolution of the system for a given division of phase space and, in certain simple cases, will enable us to find equilibrium states.

Now, upon changing variables we find

$$\frac{\partial f}{\partial t} + \frac{\partial I}{\partial t}\frac{\partial f}{\partial I} + \frac{\partial \theta}{\partial t}\frac{\partial f}{\partial \theta} + \omega\frac{\partial f}{\partial \theta} = \frac{\partial}{\partial I}\left\langle \delta f \frac{\partial \delta\Phi}{\partial \theta}\right\rangle - \frac{\partial}{\partial \theta}\left\langle \delta f \frac{\partial \delta\Phi}{\partial I}\right\rangle, \tag{4.13}$$

wherein

$$\omega(I) := \frac{\partial H}{\partial I} \tag{4.14}$$

denotes the nonlinear orbital frequency. In the new variables, the assumption that the system passes sequentially through mean-field equilibrium states can be conveniently stated in the form

$$f(I, \theta, t) \simeq f(I, t), \tag{4.15}$$

because the action variable I depends on (x, p) only through the Hamiltonian H. Using the approximation (4.15) in (4.13) we obtain after averaging over the angle variable θ, denoted by an over line,

$$\frac{\partial f}{\partial t} = \frac{\partial}{\partial I}\overline{\left\langle \delta f \frac{\partial \delta\Phi}{\partial \theta}\right\rangle}. \tag{4.16}$$

Here we have used that $\overline{\partial_t I} = 0$ as can easily be shown. Meanwhile, the averaged mode amplitude α is, in keeping with the assumption of a "slow" relaxation, to be calculated self-consistently from the equilibrium equation

$$\alpha = -\frac{i\eta}{\kappa - i\delta}\int f \sin(kx)\mathrm{d}x\mathrm{d}p, \tag{4.17}$$

where we have defined the effective detuning

$$\delta := \Delta_c - U_0 \int f \sin^2(kx)\mathrm{d}x\mathrm{d}p. \tag{4.18}$$

If the description of the system in terms of averaged quantities (f, α) is to be meaningful, the deviations from the mean values $(\delta f, \delta\alpha)$ ought to be small in some sense. This second major assumption will be quantified by using a linearized form of the equations of motion for the fluctuations, with the result

$$\frac{\partial \delta f}{\partial t} + \omega \frac{\partial \delta f}{\partial \theta} = \frac{\partial \delta \Phi}{\partial \theta} \frac{\partial f}{\partial I}, \tag{4.19a}$$

$$\delta\dot{\alpha} = (-\kappa + i\delta)\delta\alpha - i \int \delta f \left(\eta \sin(kx) + \alpha U_0 \sin^2(kx)\right) dz + \sqrt{\kappa}\xi, \tag{4.19b}$$

where we have neglected terms of the order of $\partial_t I \delta f$ and $\partial_t \theta \delta f$, with the justification that they are products of the time variation of a "slow" quantity with a "small" quantity and are thus of higher order. Now we need to express everything in terms of the action-angle variables. Using that all functions are 2π-periodic in the angle variable, we can write

$$\delta\Phi = \sum_{n=-\infty}^{\infty} \hbar \left(B_n(I)\delta\alpha + A_n(I)\delta\alpha^*\right) e^{in\theta} =: \sum_n \Phi_n e^{in\theta}, \tag{4.20}$$

wherein the orbit-averaged amplitudes

$$A_n(I) := \frac{1}{2\pi} \int_0^{2\pi} \left(\eta \sin(kx) + U_0 \alpha \sin^2(kx)\right) e^{-in\theta} \mathrm{d}\theta, \tag{4.21a}$$

$$B_n(I) := \frac{1}{2\pi} \int_0^{2\pi} \left(\eta \sin(kx) + U_0 \alpha^* \sin^2(kx)\right) e^{-in\theta} \mathrm{d}\theta \tag{4.21b}$$

appear. Expanding also the fluctuations of the microscopic distribution function

$$\delta f(I, \theta, t) = \sum_n f_n(I, t) e^{in\theta}, \tag{4.22}$$

we finally arrive at

$$\frac{\partial f}{\partial t} = -2 \frac{\partial}{\partial I} \sum_{n>0} n \mathrm{Im} \left\{\langle f_n^* \Phi_n \rangle\right\}, \tag{4.23a}$$

$$\frac{\partial f_n}{\partial t} + in\omega f_n = in\Phi_n \frac{\partial f}{\partial I}, \tag{4.23b}$$

$$\delta\dot{\alpha} = (-\kappa + i\delta)\delta\alpha - 2\pi i N \sum_n \int f_n^* A_n \mathrm{d}I + \sqrt{\kappa}\xi, \tag{4.23c}$$

$$\delta\dot{\alpha}^* = (-\kappa - i\delta)\delta\alpha^* + 2\pi i N \sum_n \int f_n^* B_n \mathrm{d}I + \sqrt{\kappa}\xi^*, \tag{4.23d}$$

The solution of this set of coupled equations is obviously a formidable task and the reader is forgiven if he begins to loose patience and wonders, where all of this should lead to. Therefore, we will now outline the route taken in this work as clearly as possible. Let us suppose, that there exists a separation of time scales characterizing

the evolution of the averaged distribution function f on the one hand and the relevant dynamical correlations

$$C_n(I,t) := \mathrm{Im}\,\{\langle f_n^* \Phi_n \rangle\} \tag{4.24}$$

on the other hand. By this we mean the following: Let us fix some instant of time $t > 0$ and introduce a new, "fast", time variable τ. Then we set $f_n(I,t,\tau) := f_n(I,t+\tau)$ and likewise for all other dynamical quantities as well. Now, assume there is some time $T(t)$, such that approximately $f(I,t+\tau) \simeq f(I,t)$ for all $t < \tau < T(t)$. Furthermore, assume that there exists also a "damping time" $\tau_d(t) \ll T(t)$, such that the correlations $C_n(I,t,\tau)$, calculated from the equations of motion for the fluctuations (4.23b)-(4.23d) together with the approximation $f(I,t,\tau) \approx f(I,t)$, have reached a unique limiting form, if $T \gg \tau \gg \tau_d$, depending on t only via $f(I,t)$, i.e.

$$C_n(I,t,\tau) \to \mathcal{C}_n(I; f(t)), \quad \tau \gg \tau_d. \tag{4.25}$$

With these presuppositions the notion of a "slow" relaxation employed up to now has been given a more precise meaning. Under such conditions, it is obvious that we can approximate the equation of motion for the averaged distribution (4.23a) by

$$\frac{\partial f}{\partial t} = \frac{\partial}{\partial I} \mathcal{J}(I; f(t)), \tag{4.26}$$

where the probability current is given by

$$\mathcal{J}(I; f(t)) := -2 \sum_{n>0} n\, \mathcal{C}_n(I; f(t)). \tag{4.27}$$

Equation (4.26), in which the correlations have been "adiabatically" eliminated and which therefore involves only the averaged distribution at the given instant of time itself, will constitute the sought for Markovian kinetic theory. That the above assumptions do in fact hold (at least far from the selforganisation threshold) will become more plausible by the considerations of the following subsection. The reason for this essentially lies in the fact that the dynamical equations (4.23b)-(4.23d) are identical to the linearized Vlasov equation and the corresponding equation for the mode amplitude. This allows to draw the conclusion, that if the averaged distribution function is linearly mean-field stable, any sufficiently smooth "initial" fluctuation will decay in time τ at a rate characteristic of $f(I,t)$, which will be seen to provide the stipulated damping time scale τ_d. The decay of fluctuations is also responsible for the existence of a unique functional $\mathcal{C}_n(I; f(t))$.

4.3.1 Calculation of the Correlation Functional

Let us now see how this is done by performing the necessary calculations, which are tedious but otherwise quite straight-forward. To this end, we take the Laplace transform w.r.t. the fast time τ of the conjugate of (4.23b) to obtain

$$f_n^*(I,t,\Omega) = \frac{f_n^*(I,t,\tau=0)}{\Omega - in\omega} - in\hbar \frac{\partial f/\partial I}{\Omega - in\omega} \left(A_n^* \delta\alpha + B_n^* \delta\alpha^*\right), \tag{4.28}$$

where Ω denotes the complex frequency on which the Laplace transformed variables depend. Here, the "initial" value of the fluctuation appears. Bearing in mind that $\delta f = f_{\mathrm{K}} - f$ and

$$f_{\mathrm{K}}(I,\theta,t) = \frac{1}{N}\sum_{j=1}^{N}\delta(I - I_j(t))\delta(\theta - \theta_j(t)), \tag{4.29}$$

we have for $n \neq 0$

$$f_n^*(I,t,\tau=0) = \frac{1}{2\pi N}\sum_{j=1}^{N}\delta(I - I_j(t))e^{in\theta_j(t)} \tag{4.30}$$

and $f_{n=0}^*(I,t,\tau=0) = 0$. Henceforth we shall suppress the slow time variable t. Substituting (4.28) into the Laplace transformed equations (4.23c) and (4.23d) we obtain the linear system of equations

$$\mathbb{D}(\Omega)\cdot\begin{pmatrix}\delta\alpha\\ \delta\alpha^*\end{pmatrix} = \begin{pmatrix}J_1\\ J_2\end{pmatrix} + \sqrt{\kappa}\begin{pmatrix}\xi\\ \xi^*\end{pmatrix}, \tag{4.31}$$

where

$$\mathbb{D}(\Omega) := \begin{pmatrix}\Omega + \kappa - i\delta + \chi_1(\Omega) & \chi_2(\Omega)\\ -\chi_3(\Omega) & \Omega + \kappa + i\delta - \chi_4(\Omega)\end{pmatrix}, \tag{4.32}$$

$$\begin{pmatrix}J_1\\ J_2\end{pmatrix} := 2\pi i\sum_n\int\frac{f_n^*(I,0)}{\Omega - in\omega}\begin{pmatrix}-A_n\\ B_n\end{pmatrix}\mathrm{d}I \tag{4.33}$$

and

$$\begin{pmatrix}\chi_1\\ \chi_2\\ \chi_3\\ \chi_4\end{pmatrix} := 2\pi\hbar\sum_n n\int\frac{\partial f/\partial I}{\Omega - in\omega}\begin{pmatrix}|A_n|^2\\ A_nB_n^*\\ A_n^*B_n\\ |B_n|^2\end{pmatrix}\mathrm{d}I. \tag{4.34}$$

The above system of equations is easily inverted to yield

$$\begin{pmatrix}\delta\alpha\\ \delta\alpha^*\end{pmatrix} = \mathbb{D}^{-1}(\Omega)\cdot\left[\begin{pmatrix}J_1\\ J_2\end{pmatrix} + \sqrt{\kappa}\begin{pmatrix}\xi\\ \xi^*\end{pmatrix}\right], \tag{4.35}$$

with the inverse matrix

$$\mathbb{D}^{-1}(\Omega) = \frac{1}{D(\Omega)}\begin{pmatrix}\Omega + \kappa + i\delta - \chi_4 & -\chi_2\\ \chi_3 & \Omega + \kappa - i\delta + \chi_1\end{pmatrix}, \tag{4.36}$$

The very important linear response function (also called dispersion relation in this work) $D(\Omega)$ is defined as the determinant of $\mathbb{D}(\Omega)$ and is given by

$$D(\Omega) = (\Omega+\kappa)^2 + \delta^2 + (\Omega + \kappa + i\delta)\chi_1 - (\Omega + \kappa - i\delta)\chi_4 + \chi_2\chi_3 - \chi_1\chi_4. \tag{4.37}$$

Splitting the components of the fluctuating optical potential $\Phi_n(I,\Omega) = \Phi_n^P(I,\Omega) + \Phi_n^N(I,\Omega)$ into particle- and noise- contributions, we immediately find

$$\Phi_n^P(I,\Omega) = 2\pi i\hbar \sum_m \int \frac{f_m^*(I',0)}{\Omega - im\omega} U_{nm}(I,I',\Omega^*)\mathrm{d}I', \tag{4.38a}$$

$$\Phi_n^N(I,\Omega) = \hbar\sqrt{\kappa}\int_{-\infty}^{\infty} \frac{\mathrm{d}u}{\Omega - iu} \begin{pmatrix} B_n(I) \\ A_n(I) \end{pmatrix} \mathbb{H}(\Omega) \begin{pmatrix} \xi(u) \\ \xi^*(u) \end{pmatrix}, \tag{4.38b}$$

$$f_n^{*P}(I,\Omega) = \frac{f_s^*(I,0)}{\Omega - in\omega} - in\frac{\partial f/\partial I}{\Omega - in\omega}[\Phi_n^P(I,\Omega^*)]^*, \tag{4.38c}$$

$$f_n^{*N}(I,\Omega) = -in\frac{\partial f/\partial I}{\Omega - in\omega}[\Phi_n^N(I,\Omega^*)]^*, \tag{4.38d}$$

wherein

$$U_{nm}(I,I',\Omega^*) := \begin{pmatrix} B_n(I) \\ A_n(I) \end{pmatrix} \mathbb{H}(\Omega) \begin{pmatrix} -A_m(I') \\ B_m(I') \end{pmatrix}, \tag{4.39}$$

with $\mathbb{H}(\Omega) := \mathbb{D}^{-1}(\Omega)$ and we have made use of the fact that $\phi_n^*(I,\Omega) = [\phi_n(I,\Omega^*)]^*$. Furthermore we have Fourier analyzed the white noise according to

$$\xi(\tau) = \int_{-\infty}^{\infty} \xi(u) e^{iu\tau}\mathrm{d}u \tag{4.40a}$$

$$\xi^*(\tau) = \int_{-\infty}^{\infty} \xi^*(u) e^{iu\tau}\mathrm{d}u, \tag{4.40b}$$

with the nonvanishing correlations given by

$$2\pi \left\langle \xi(u)\xi^*(u') \right\rangle = \delta(u+u'). \tag{4.41}$$

From (4.38) we must proceed to calculate the correlations $C_n(I,\Omega,\tilde{\Omega}) := \left\langle f_n^*(I,\Omega)\Phi_n(I,\tilde{\Omega}) \right\rangle$. To this end we note that

$$\left\langle f_n(I,0) f_{n'}^*(I',0) \right\rangle = \frac{1}{2\pi}\delta_{nn'} f(I,t)\delta(I-I') + \mathcal{R}_{nn'}(I,I',t) \tag{4.42a}$$

$$\left\langle f_n^*(I,0) f_{n'}^*(I',0) \right\rangle = \frac{1}{2\pi}\delta_{n',-n} f(I,t)\delta(I-I') + \mathcal{R}_{-n,n'}(I,I',t). \tag{4.42b}$$

The first contributions stem from the uncorrelated part of the N-body probability distribution

$$P_{\mathrm{uc}}(I_1,\theta_1,\ldots,I_N,\theta_N,t) = \prod_{j=1}^{N} \frac{f(I_j,t)}{N}, \tag{4.43}$$

while the second contributions arise from particle-particle correlations present at time t. It is evidently impossible to know the latter without having already solved

the whole problem of time evolution. However, a detailed knowledge of those contributions will turn out to be unnecessary, if only we assume them to be smooth functions of the actions (I, I'). The $\mathcal{O}(U)$ contribution to the correlations $C_n(I, \Omega, \tilde{\Omega})$, denoted $C_n^{(1)}(I, \Omega, \tilde{\Omega})$, is given by

$$C_n^{(1)} = i\hbar f(I) \frac{U_{n,-n}(I, I, \tilde{\Omega}^*)}{(\Omega - in\omega)(\tilde{\Omega} + in\omega)} + C_{\mathcal{R}}^{(1)}, \tag{4.44a}$$

where $C_{\mathcal{R}}^{(1)}$ denotes the contribution due to $\{\mathcal{R}_{nn'}\}$. The $\mathcal{O}(U^2)$ contribution to the same correlations, denoted $C_n^{(2)}(I, \Omega, \tilde{\Omega})$, is given by

$$\begin{aligned} C_n^{(2)} = \\ = -2\pi i\hbar^2 \frac{\partial f}{\partial I} \sum_m n \int f(I') \frac{U_{nm}(I, I', \tilde{\Omega}^*)[U_{nm}(I, I', \Omega)]^*}{(\Omega - in\omega(I))(\Omega + im\omega(I'))(\tilde{\Omega} - im\omega(I'))} \mathrm{d}I' + \\ + C_{\mathcal{R}}^{(2)}, \end{aligned} \tag{4.44b}$$

with an analogous meaning of $C_{\mathcal{R}}^{(2)}$. Finally the noise-induced part of the correlations are given by

$$C_n^N(I, \Omega, \tilde{\Omega}) = -in \frac{\hbar^2 \kappa}{2\pi} \frac{\partial f}{\partial I} \int_{-\infty}^{\infty} \mathrm{d}u \frac{N_n(I, \Omega)^* \cdot N_n(I, \tilde{\Omega}^*)}{(\Omega + iu)(\Omega - in\omega(I))(\tilde{\Omega} - iu),} \tag{4.44c}$$

wherein we have defined the vector

$$N_n(I, \Omega^*) := \mathbb{H}^T(\Omega) \begin{pmatrix} B_n(I) \\ A_n(I) \end{pmatrix} \tag{4.45}$$

and the dot denotes the ordinary (real) scalar product. It remains to perform the inverse Laplace transformation

$$C_n(I, \tau) = \left(\frac{1}{2\pi i}\right)^2 \int_{\gamma - i\infty}^{\gamma + i\infty} d\Omega\, e^{\Omega\tau} \int_{\tilde{\gamma} - i\infty}^{\tilde{\gamma} + i\infty} d\tilde{\Omega}\, e^{\tilde{\Omega}\tau} C_n(I, \Omega, \tilde{\Omega}). \tag{4.46}$$

Obviously we cannot perform the inversion exactly. However, let $g(\Omega)$ be the Laplace transform of some function $g(\tau)$, such that

$$g(\tau) = \frac{1}{2\pi i} \int_{\gamma - i\infty}^{\gamma + i\infty} \mathrm{d}\Omega\, e^{\Omega\tau} g(\Omega) \tag{4.47}$$

and $\gamma > 0$ is greater than the largest real part of any singularity of $g(\Omega)$. Assume that $g(\Omega)$ can, up to a finite number of poles $\Omega = \Omega_k$, be analytically continued into the entire complex plane. Then, by deforming the contour, we can write

$$g(\tau) = \frac{1}{2\pi} e^{-\Gamma\tau} \int_{-\infty}^{\infty} g(-\Gamma + i\omega) e^{-i\omega\tau} \mathrm{d}\omega + \sum_k \mathrm{Res}_{\Omega = \Omega_k} \left\{ g(\Omega) e^{\Omega\tau} \right\}, \tag{4.48}$$

where $\Gamma > 0$ arbitrary and $\mathrm{Res}_{\Omega=\Omega_k}$ denotes the residuum at the pole $\Omega = \Omega_k$. Here it is important to realize that asymptotically, for $\tau \to \infty$, the first term vanishes due to the Riemann-Lebesgue Lemma, such that

$$g(\tau) \sim \sum_k \mathrm{Res}_{\Omega=\Omega_k} \left\{ g(\Omega) e^{\Omega\tau} \right\}, \quad \tau \to \infty. \tag{4.49}$$

The time needed for the first term in (4.48), the "transient", to be negligible depends on the regularity of $g(\Omega)$, but in what follows, we will assume that this time defines the shortest scale. It is evident from equations (4.44) that the poles of the functions of which we have to take the Laplace inverse are either purely imaginary, or originate from the zeros of the analytically continued linear response function $D(\Omega)$. Therefore, we must presuppose, in order to obtain a definite limiting form of C_n, that all the zeros of the response function have a negative real part, i.e. $f(I,t)$ is linearly Vlasov-stable. The inverse of the smallest of these real parts can thus serve to define the "damping time" τ_d spoken about previously. With these things said, we can perform the inverse transformation using the asymptotic formula (4.49) to obtain

$$C_n^{(1)} = i\hbar f(I) U_{n,-n}(I, I, in\omega), \tag{4.50a}$$

$$C_n^{(2)} = -2\pi^2 i\hbar^2 \frac{\partial f}{\partial I} \sum_m n \int f(I') |U_{nm}(I, I', in\omega)|^2 \delta(n\omega + m\omega') \mathrm{d}I' + \text{ real}, \tag{4.50b}$$

$$C_n^N = -in \frac{\hbar^2 \kappa}{2} \frac{\partial f}{\partial I} |N_n(I, in\omega)|^2 + \text{ real}, \tag{4.50c}$$

where we have made use of the fact that asymptotically

$$\frac{e^{ix\tau}}{x} \sim i\pi\delta(x), \quad \tau \to \infty \tag{4.51}$$

and $\omega' := \omega(I')$ as well as $\omega = \omega(I)$. Note that the "initial" correlations $C_{\mathcal{R}}^{(1,2)}$ vanish as $\tau \to \infty$ on the transient time scale, because we assume $\mathcal{R}_{nn'}(I, I', t)$ to be a smooth function of (I, I'), as mentioned before. Hence, under the condition of a linearly Vlasov-stable distribution function, a unique limiting form of $C_n(I, \tau)$ indeed exists and is given by

$$\mathcal{C}_n(I; f(t)) = \hbar f(I) \mathrm{Re}\left\{ U_{n,-n}(I, I, in\omega) \right\} - \tag{4.52}$$

$$- 2\pi^2 \hbar^2 \frac{\partial f}{\partial I} \sum_m n \int f(I') |U_{nm}(I, I', in\omega)|^2 \delta(n\omega + m\omega') \mathrm{d}I' - \tag{4.53}$$

$$- n \frac{\hbar^2 \kappa}{2} \frac{\partial f}{\partial I} |N_n(I, in\omega)|^2. \tag{4.54}$$

4.3.2 General Form of the Kinetic Equation

Collecting the results of the previous subsection we can write the equation of the kinetic theory (4.26) in the form of a nonlinear Fokker-Planck equation

$$\frac{\partial f}{\partial t} = \frac{\partial}{\partial I} \left(\mathcal{F} f + \mathcal{D} \frac{\partial f}{\partial I} \right), \tag{4.55}$$

with the "drift" coefficient

$$\mathcal{F}(I;f(t)) := -2\sum_{n>0} n\mathrm{Re}\left\{U_{n,-n}(I,I,in\omega)\right\} \tag{4.56}$$

and the "diffusion" coefficient

$$\mathcal{D}(I;f(t)) := 4\pi^2\hbar^2 \sum_{n>0,m} n^2 \int f(I')|U_{nm}(I,I',in\omega)|^2\delta(n\omega+m\omega')\mathrm{d}I' + \\ + \hbar^2\kappa\sum_{n>0} n|N_n(I,in\omega)|^2, \tag{4.57}$$

both of which depend on the distribution function in a functional manner. The reason, why we have put the terms "drift" and "diffusion" in quotation marks is that if (4.55) is brought to the standard form of a Fokker-Planck equation, it actually reads

$$\frac{\partial f}{\partial t} + \frac{\partial}{\partial I}\left(F(I;f)f\right) = \frac{1}{2}\frac{\partial^2}{\partial I^2}\left(D(I;f)f\right), \tag{4.58}$$

where the proper drift is given by

$$F = -\mathcal{F} + \frac{\partial \mathcal{D}}{\partial I} \tag{4.59}$$

and the proper diffusion by

$$D = 2\mathcal{D}. \tag{4.60}$$

This equation will form the basis for the investigations following in the next sections. In closing this derivation we wish to point out that it would be a mistake to think of the kinetic theory just developed as superseding the mean-field description represented by Vlasov's equation. Rather, both theories are to be viewed as complementing each other. Indeed, Vlasov's equation provides a satisfactory description of the initial phase of the systems time evolution, whereas the Fokker-Planck equation models the later stages thereof. The factor, which determines when the former stage ends and the latter begins is given by the number of particles.

4.4 Mean-field description, instability threshold

For those readers, who have spared themselves the pain to read through the previous section, we will briefly recall the main concepts necessary to understand the present section. The semiclassical SDEs (4.1) are equivalent to the Klimontovich's equation [35]

$$\frac{\partial f_\mathrm{K}}{\partial t} + v\frac{\partial f_\mathrm{K}}{\partial x} - \frac{1}{m}\frac{\partial \Phi}{\partial x}\frac{\partial f_\mathrm{K}}{\partial v} = 0 \tag{4.61}$$

together with an evolution equation for the field mode amplitude a obtained replacing the sums in eq. (4.1c) by the integrals $N\iint \bullet f_\mathrm{K}(x,v,t)\mathrm{d}x\mathrm{d}v$. $f_\mathrm{K}(x,v,t)$ is

the so-called Klimontovich or microscopic distribution function. Its initial condition reads

$$f_{\mathrm{K}}(x,v,0) = \frac{1}{N}\sum_{j=1}^{N}\delta(x - x_j(0))\delta(v - v_j(0)). \tag{4.62}$$

As this function is highly irregular, the above reformulation has no computational merit by itself, but provides an ideal starting point for a statistical treatment. To this end we decompose every quantity (f_{K}, a and Φ) into its smooth mean value and fluctuations,

$$f_{\mathrm{K}}(x,v,t) =: f(x,v,t) + \delta f(x,v,t), \tag{4.63a}$$

$$a(t) = \alpha(t) + \delta\alpha(t), \tag{4.63b}$$

with $\langle \delta f(x,v,t)\rangle = \langle \delta\alpha(t)\rangle = 0$. The statistical average $\langle \bullet \rangle$ is over an ensemble of similar initial conditions $\{(x_j(0), v_j(0))\}$ and $a(0)$, as well as over the realisations of the white noise process mimicking the input noise for the cavity field.

We can distinguish two basic phases the system can be found in: Whenever there is, on average, no cavity field, $\alpha = 0$, we shall speak of the system as being in the unordered phase. Conversely, if a mean cavity field is present, we shall say that the system is in the ordered phase.

For the smooth ensemble-averaged Klimontovich distribution, called *one-particle distribution function*, we find upon substituting the decomposition (4.63a) into (4.61) the following equation of motion

$$\frac{\partial f}{\partial t} + v\frac{\partial f}{\partial x} - \frac{1}{m}\frac{\partial \langle\Phi\rangle}{\partial x}\frac{\partial f}{\partial v} = \left\langle \frac{\partial \delta\Phi}{\partial x}\frac{\partial \delta f}{\partial v}\right\rangle. \tag{4.64}$$

Neglecting all correlations in eq. (4.64) leads to Vlasov's equation (see (4.11)), which becomes exact in the limit $N \to \infty$ [16].

In the context of this mean-field description, the unordered phase characterized by $\alpha = 0$ is infinitely degenerate. Every spatially homogeneous phase space distribution, $f(x,v) = f(v)$, is a stationary solution of Vlasov's equation. With this simple observation however, the conclusions obtainable from mean-field theory are not yet exhausted. Because for some stationary distribution to represent a physical state of the system it has to be insensitive to perturbations and not all solutions $f(x,v) = f(v)$ with $\alpha = 0$ are necessarily stable. Indeed, for any (dimensionless) symmetric velocity distribution defined by $g(v/v_{\mathrm{T}}) := \lambda v_{\mathrm{T}} f(v)$ and a negative effective detuning $\delta := \Delta_{\mathrm{c}} - NU_0/2 < 0$ we find, that if the inequality

$$\frac{N\eta^2}{k_{\mathrm{B}}T}\mathrm{P}\int_{-\infty}^{\infty}\frac{g'(\xi)}{-2\xi}\mathrm{d}\xi > \frac{\delta^2 + \kappa^2}{\hbar|\delta|}, \tag{4.65}$$

holds, any small perturbation of the homogeneous equilibrium triggers a self-organisation process. Here, P denotes the Cauchy principal value and we have defined the thermal velocity $v_{\mathrm{T}}^2 := 2k_{\mathrm{B}}T/m$. For a Gaussian distribution, corresponding to a gas

at thermal equilibrium the integral evaluates to one. The relation (4.65) has been derived by methods presented in [16]. There it was shown that the threshold can be computed from the zeros of the dispersion relation ($\mathrm{Re}(\Omega) > 0$)

$$D(\Omega) = (\Omega + \kappa)^2 + \delta^2 - \\ - i\hbar k\delta \frac{N\lambda\eta^2}{2m} \int_{-\infty}^{\infty} \left(\frac{\partial_v f}{\Omega + ikv} - \frac{\partial_v f}{\Omega - ikv} \right) \mathrm{d}v. \quad (4.66)$$

Note that this dispersion relation is contained in the definition of the linear response function introduced in the previous section in equation (4.37) as a special case.

To sum up we can say that according to mean-field theory, the unordered phase is infinitely degenerate and consists of all spatially homogeneous phase space distributions, which are dynamically stable in accord with the criterion (4.65).

4.5 Kinetic equation for the unordered phase

The multiplicity of phase space distributions corresponding to the unordered phase within mean-field theory reflects the latter's incapability to correctly capture the behavior of the gas on longer time scales. It is thus inherently unsuited to determine the equilibrium of the system. Therefore, let us now return to eq. (4.64), which for weak spatial inhomogeneity—as expected in the unordered phase—approximately reads

$$\frac{\partial f}{\partial t} \approx \frac{\partial}{\partial v} \overline{\left\langle \delta f \frac{\partial \delta\Phi}{\partial x} \right\rangle}, \quad (4.67)$$

where the overbar denotes the spatial average. This last equation is really but a special case of the more general equation (4.16) of the last section for the case of a vanishing average mode amplitude $\alpha = 0$. The right-hand-side correlation function can be computed using established methods from plasma physics as in [35] (as detailed in the previous section) when the fluctuations evolve on a much faster time scale than the average values, which are considered "frozen". This is justified as long as the system remains far from instability. For symmetric distributions and $\alpha = 0$ the general non-linear Fokker–Planck equation (4.55) takes the simple form

$$\frac{\partial}{\partial t} F + \frac{\partial}{\partial v} \Big(A[F] F \Big) = \frac{\partial}{\partial v} \left(B[F] \frac{\partial}{\partial v} F \right) \quad (4.68)$$

for the velocity distribution $F(v,t) := \lambda f(v,t)$, with the coefficients given by

$$A[F] := \frac{2\hbar k\delta\kappa\eta^2}{m} \frac{kv}{|D(ikv)|^2} \quad (4.69a)$$

$$B[F] := \frac{\hbar^2 k^2 \eta^2 \kappa}{2m^2} \frac{\kappa^2 + \delta^2 + k^2 v^2}{|D(ikv)|^2}. \quad (4.69b)$$

Note that the coefficients functionally depend on the velocity distribution F through the dispersion relation $D(i\omega) := \lim_{\varepsilon \downarrow 0} D(\varepsilon + i\omega)$. A and B represent the deterministic part of the equations and the field noise, respectively. All cavity-mediated long-range particle interactions are encoded in the dispersion relation. Note that very far below instability threshold the full dispersion relation (4.66) reduces to $D(ikv) \simeq (ikv + \kappa)^2 + \delta^2$, which implies that collective effects are negligible.

4.6 Equilibrium distribution

As pointed out above, Vlasov's equation renders every spatially homogeneous phase space distribution stationary. This degeneracy is no longer present in the solution of the Fokker-Planck equation, as friction and diffusion will modify an initially stable but otherwise arbitrary homogeneous distribution. Therefore, let us inquire into the form of equilibrium predicted by (4.68).

Normalisable steady-state solutions of eq. (4.68) exist only for negative effective detuning $\delta < 0$, where light scattering is accompanied by an extraction of kinetic energy from the motion of the scattering particle. On the other hand, for positive effective detuning the gas is heated. Interestingly, the unique solution of the steady-state equation can be found in closed form and is given by the non-thermal q-Gaussian velocity distribution function (also known as Tsallis distribution and closely related to Student's t-distribution) [36, 37]. Defining the so-called q-exponential

$$\exp_q(x) = [1 + (1-q)x]^{\frac{1}{1-q}}\,, \tag{4.70}$$

we can write the equilibrium distribution in the suggestive form

$$F(v) \propto \exp_q\left(-\frac{mv^2}{2k_{\mathrm{B}}T}\right), \tag{4.71}$$

with

$$q := 1 + \frac{\omega_{\mathrm{R}}}{|\delta|} \tag{4.72}$$

and the recoil frequency $\omega_{\mathrm{R}} := \hbar k^2/2m$. We have defined an effective temperature-like parameter T via

$$k_{\mathrm{B}}T = \hbar\frac{\kappa^2 + \delta^2}{4|\delta|} = \frac{\hbar\kappa}{2}. \tag{4.73}$$

The latter minimum value of T appears for $\delta = -\kappa$ and is known as the cavity-cooling limit temperature.

The parameter q or equivalently the ratio $|\delta|/\omega_{\mathrm{R}}$ determines the shape of the distribution and gives rise to further restrictions. Normalisable solutions exist for $|\delta| > \omega_{\mathrm{R}}/2$, the second moment (kinetic energy) only for $|\delta| > 3\omega_{\mathrm{R}}/2$. The case $|\delta| = \omega_{\mathrm{R}}$ corresponds to a Lorentzian distribution. For $|\delta|/\omega_{\mathrm{R}} \to \infty$, i. e. $q \to 1$, the

distribution (4.71) converges to a Gaussian distribution with kinetic temperature $k_{\mathrm{B}}T_{\mathrm{kin}} := m\langle v^2\rangle$ given by the parameter $k_{\mathrm{B}}T$ defined in eq. (4.73), which justifies the usage of the designation of "temperature" above. In figure 4.2 one can see an example of a solution featuring a marked deviation from thermal equilibrium, i.e. a prominently q-Gaussian behaviour ($q = 1.4$). The main difference lies in the much longer tail of (4.71) as compared to a Gaussian distribution. Tsallis distributions have already been observed experimentally in dissipative optical lattices [38].

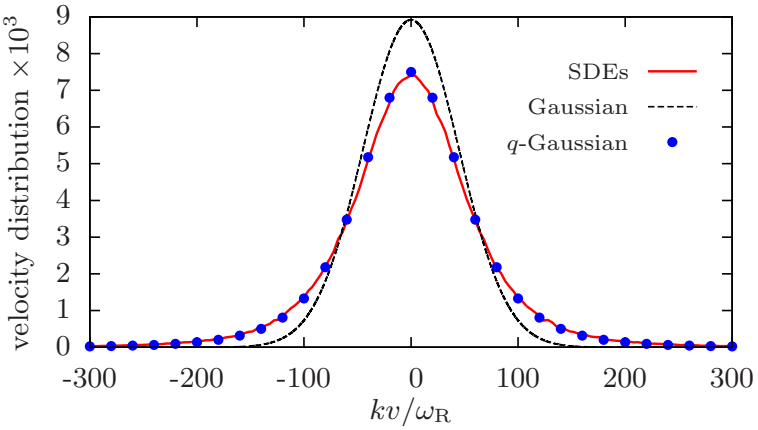

Figure 4.2 (Colour on-line) Normalised q-Gaussian velocity distribution for $\delta = -2.5\omega_{\mathrm{R}}$ obtained by integrating the semiclassical equations (4.1) up to $\omega_{\mathrm{R}}t = 5N$ (solid line) compared to the theoretically predicted q-Gaussian (4.71) (circles). The Gaussian (dashed line) is plotted for the temperature (4.73). The kinetic temperature differs considerably from eq. (4.73), $k_{\mathrm{B}}T_{\mathrm{kin}} = 2.5k_{\mathrm{B}}T$. Parameters: $N = 5000$, $NU_0 = -0.1\omega_{\mathrm{R}}$, $\sqrt{N}\eta = 1800\omega_{\mathrm{R}}$, $\kappa = 100\omega_{\mathrm{R}}$ and $\Delta_{\mathrm{c}} = -2.55\omega_{\mathrm{R}}$. Ensemble average over 25 initial conditions and 10 realisations of the white noise process.

Having found the unique equilibrium state corresponding to the unordered phase, we can use the stability criterion (4.65) to determine the phase boundary, that is the curve in parameter space, where the spatially homogeneous equilibrium (4.71) becomes dynamically unstable. By inserting the q-Gaussian into (4.65), we find that the unordered phase ceases to exist if

$$\sqrt{N}\eta > \sqrt{N}\eta_{\mathrm{c}} := \frac{\kappa^2+\delta^2}{2|\delta|}\sqrt{\frac{2}{3-q}} \overset{\delta=-\kappa}{=} \kappa\sqrt{\frac{2}{3-q}}, \tag{4.74}$$

For a Gaussian and $\delta = -\kappa$, which implies $\kappa \gg \omega_{\mathrm{R}}$, this criterion may be reformulated as

$$N|U_0|V_{\mathrm{opt}} > \hbar\kappa^2, \tag{4.75}$$

where V_{opt} is the optical potential depth created by the pump laser. If the condition (4.74) is satisfied, we conclude that there exists no spatially homogeneous,

stable equilibrium state at all and consequently we expect the system to eventually selforganize.

Based on these considerations we predict the occurrence of dissipation-induced self-organisation if the self-consistent relation (4.74) is fulfilled. That is, any initially stable, unorganised distribution will loose kinetic energy (by cavity-cooling) and eventually selforganise. Contrary to the self-organisation process of an initially unstable state (well described by Vlasov's equation), which is abrupt and accompanied by a strong increase of the gas' kinetic energy, dissipation-induced self-organisation is characterised by a much slower buildup of the photon number and monotonous cooling. The diagram shown in figure 4.3 visualizes the possible fates of an initially homogeneous gas.

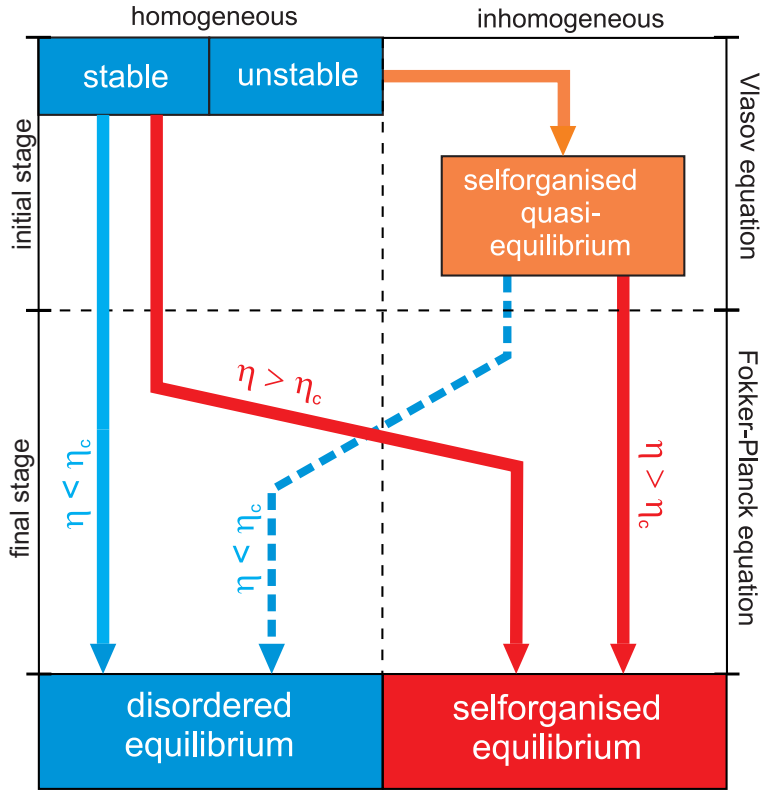

Figure 4.3 Evolution to equilibrium for an initially homogeneous gas. An initially unstable state evolves quickly towards a mean-field steady state. An initially stable state may nonetheless become selforganized in equilibrium due to dissipation.

4.7 Kinetic equation for the selforganised phase

Let us now direct our attention to the case of a non-vanishing average cavity mode amplitude, i.e. to a gas which has crossed the selforganisation threshold. Using action-angle variables [39, 40], we can also in this case derive a Fokker–Planck equation similar to eq. (4.68) [8]. The reader interested in the details is advised to study section 4.3.1. For convenience, we will briefly recap the main steps. We limit ourselves here to the discussion of the weak coupling limit

$$N|U_0| \ll |\Delta_c|, \tag{4.76}$$

in which the shift of the cavity resonance frequency caused by the gas can be neglected and we can use δ and Δ_c interchangeably. In this limit the mean optical potential can be approximated by

$$\Phi(x, \alpha, \alpha^*) \simeq \hbar\eta(\alpha + \alpha^*)\sin(kx). \tag{4.77}$$

Returning to (4.64), we perform a canonical transformation of variables $(x, p = mv) \to (I, \theta)$. Here, I denotes the one-body action based on the ensemble-averaged Hamiltonian function

$$H(x, p, \alpha, \alpha^*) := \frac{p^2}{2m} + \Phi(x, \alpha, \alpha^*), \tag{4.78}$$

and can be expressed as

$$I = \pm\frac{1}{2\pi}\oint \sqrt{2m\left[H - \Phi(x')\right]}\,\mathrm{d}x'. \tag{4.79}$$

θ denotes its canonically conjugate angle variable

$$\theta = \frac{\partial S}{\partial I}, \tag{4.80}$$

obtained from the generating function

$$S = \pm\int^x \sqrt{2m\left[H - \Phi(x')\right]}\,\mathrm{d}x'. \tag{4.81}$$

Although (4.78) is immediately recognized as the Hamiltonian function of the simple mathematical pendulum and the above well-known integrals can be written down in terms of elliptic functions, no particular insight is gained by this and hence we refrain from doing so. The reason for the above change of variables is found in the observation that at the end of the initial, mean-field governed dynamics, the one-particle distribution depends on the phase space coordinates (x, p) solely through the ensemble-averaged one-body Hamiltonian function $H(x, p)$ and thus on the action variable alone. From that point onwards, it is slowly modified by the dynamical correlations in such a way that the system evolves towards statistical equilibrium in a sequence of mean-field steady states [40]

$$f(x, p, t) \simeq f(I, t). \tag{4.82}$$

The general equation (4.55) for the distribution function takes on the following simplified form

$$\frac{\partial f}{\partial t} = \frac{\partial}{\partial I}\Big(Af + B\frac{\partial f}{\partial I} + C[f,f]\Big) \tag{4.83a}$$

and the quasi-stationary ensemble-averaged mode amplitude is determined by the implicit equation

$$\alpha = \frac{2\pi}{\Delta_c + i\kappa} N\eta \int f(I)\, g_0(I,\alpha)\, \mathrm{d}I, \tag{4.83b}$$

wherein

$$g_n(I,\alpha) := \frac{1}{2\pi}\int_0^{2\pi} \sin(kx)\, e^{-in\theta}\, \mathrm{d}\theta. \tag{4.84}$$

The r.h.s. of equation (4.83a), describing the redistribution of particles among the orbits characterized by different values of the action I, consists of two contributions originating from fluctuations and decay of the mode amplitude as in (4.68)

$$A[f] = -4\hbar\Delta_c\kappa\omega \sum_{n=-\infty}^{\infty} \frac{n^2\eta^2|g_n|^2}{|D(in\omega)|^2} \tag{4.85a}$$

$$B[f] = \hbar^2\kappa \sum_{n=-\infty}^{\infty} \frac{n^2\eta^2|g_n|^2}{|D(in\omega)|^2}\left(\kappa^2 + \Delta_c^2 + n^2\omega^2\right) \tag{4.85b}$$

and a generalized Balescu-Lenard operator [41, 42, 39]

$$C[f,f] = \sum_{n,m=-\infty}^{\infty} \int w_{nm}(I,I')\Big(n\frac{\partial f}{\partial I}f(I') - m\frac{\partial f}{\partial I'}f\Big)\mathrm{d}I', \tag{4.85c}$$

with the cross-section

$$w_{nm}(I,I') := 8\pi^2\hbar^2\Delta_c^2 N\, \frac{\eta^4|g_n(I)|^2|g_m(I')|^2}{|D(in\omega(I))||D(im\omega(I'))|}\, n\,\delta\left(n\omega(I) - m\omega(I')\right). \tag{4.85d}$$

Here, $\omega(I) = \partial H/\partial I$ denotes the nonlinear orbital frequency. The linear response function $D(i\omega)$, defined generally in (4.37), assumes the comparably simple form

$$D(i\omega) = (i\omega+\kappa)^2 + \Delta_c^2 - 4\pi\hbar N\eta^2\Delta_c \sum_{n=-\infty}^{\infty} \int \frac{\partial f}{\partial I}\frac{n|g_n|^2}{\omega + n\omega(I) - i0}\,\mathrm{d}I\,. \tag{4.86}$$

The appearance of the additional term (4.85c) as compared to (4.68) is rather intriguing, because it can be interpreted as describing a collision-like process between pairs of gas particles occupying resonant orbits (I, I'), as can be seen from the condition $n\omega(I) = m\omega(I')$ in the cross section (4.85d). We will have occasion to explore some of its consequences in the context of a multispecies gas examined in chapter 6.

4.8 Equilibrium distribution

Unfortunately, the general form of the equilibrium phase space distribution corresponding to the ordered phase cannot be obtained from (4.83a) due to its formidable complexity. If, however, we restrict attention to strongly organised equilibria, where a harmonic approximation for the potential becomes valid, the steady-state solution can be found and is given by a thermal distribution

$$f(x,p) \propto \exp\left(-\frac{H}{k_\mathrm{B}T_\mathrm{kin}}\right), \tag{4.87}$$

with a kinetic temperature depending on the linewidth κ, the detuning and the trap frequency $\omega_0 := \omega(I=0)$,

$$k_\mathrm{B}T_\mathrm{kin} = \hbar\frac{\kappa^2+\delta^2+4\omega_0^2}{4|\delta|}. \tag{4.88}$$

The trap frequency is related to the cavity mode amplitude via

$$\omega_0^2 = 4\eta\omega_\mathrm{R}\left\langle|\operatorname{Re}\alpha|\right\rangle \tag{4.89}$$

and can be approximated by

$$\omega_0^2 \simeq \sqrt{N}\eta\omega_\mathrm{R}\left(\frac{\eta}{\eta_\mathrm{c}}+\sqrt{\frac{\eta^2}{\eta_\mathrm{c}^2}-1}\right) \sim N \tag{4.90}$$

in the far-detuned regime where $|\delta| \gg \omega_\mathrm{R}$; η_c is the self-consistent critical value defined in eq. (4.74). As the temperature depends explicitly on the laser power, higher pump strengths result in deeper trapped ensembles with increased kinetic energy. Note that this system has the interesting property that the more particles we add, the deeper the optical potential gets as is the case for self-gravitating systems [43]. At this point we have to remark that an increased kinetic energy does not necessarily imply a "hotter" gas. Indeed, if we assume the case that the trap frequency is much larger than the cavity linewidth, $\omega_0 \gg \kappa$, the minimal value of the thermal energy is found to be

$$k_\mathrm{B}T_\mathrm{kin}\big|_\mathrm{min} = \hbar\omega_0 \tag{4.91}$$

and is attained for a detuning $\delta = -2\omega_0$. As $k_\mathrm{B}T_\mathrm{kin}$ is equal to the expected energy per particle in the mean optical potential, this implies that all particles are close to their ground state. The equilibrium trap frequency of course depends itself on the detuning as seen in (4.90), which gives rise to the criterion

$$\delta = -2\omega_0 = -2\sqrt[3]{2N\eta^2\omega_\mathrm{R}} \tag{4.92}$$

for such (near) ground state cooling.

The discussion of (strongly) selforganised equilibrium states would be incomplete

without stating their stability properties. Without going into the details, we note that an investigation of the linear response function (4.86) reveals that for negative detuning and $\frac{\partial f}{\partial I} \leq 0$ (as for (4.87)) an equilibrium is stable if and only if

$$N\eta^2 < \frac{\kappa^2+\delta^2}{4\pi\hbar|\delta|}\left|\sum_{n\neq 0}\int \frac{|g_n|^2}{\omega}\frac{\partial f}{\partial I}\mathrm{d}I\right|^{-1}. \tag{4.93}$$

Applying this criterion to (4.87), we find that such a strongly organised state is stable if

$$N\eta^2 > \frac{3-q}{3/2-q}\frac{N\eta_c^2}{4} \overset{q=1}{=} N\eta_c^2. \tag{4.94}$$

As one can show that the assumption of strong trapping requires $|\delta| \gg \omega_\mathrm{R}$ and hence $q \sim 1$, we conclude that the found solutions are dynamically stable as soon as the unordered phase ceases to be so. Therefore we can, for large enough detunings, exclude the possibility of a coexistence of the ordered and unordered phases.

4.9 Equilibrium phase diagram

The order parameter defined as

$$\Theta := \lim_{t\to\infty}\iint \sin(kx) f(x,v,t)\mathrm{d}x\mathrm{d}v \tag{4.95}$$

is an adequate measure of particle localisation in equilibrium as it is zero for a completely homogeneous distribution and plus/minus one for the perfectly selforganised phase (i. e. δ-peaks), the sign depends on whether the odd- or even wells are populated [28]. In fig 4.4 we depict its behaviour as a function of the pump strength. Initially, the particles were spatially homogeneously distributed with a (stable) Gaussian velocity distribution; self-organisation sets in because of the cavity cooling effect. Hence the branching point is given by the self-consistent threshold (4.74).

For the strongly organized phase, where the distribution function is a thermal state with temperature (4.88), the order parameter reads (in harmonic oscillator approximation)

$$\Theta = \pm\left(1 - \frac{k_\mathrm{B}T_\mathrm{kin}}{\hbar\omega_0^2}\omega_\mathrm{R}\right). \tag{4.96}$$

Its maximum value is limited by the detuning and the recoil frequency, $\Theta \to \pm(1-\omega_\mathrm{R}/|\delta|)$ for $\eta \to \infty$. This corresponds to a Gaussian spatial distribution with width $k^2(\Delta x)^2 = 2\omega_\mathrm{R}/|\delta|$. Let us also briefly investigate the opposite limit of pump strengths slightly above threshold. Solving the self-consistency equation

$$\mathrm{Re}\,\langle\alpha\rangle_\infty = \frac{-N\eta|\delta|}{\kappa^2+\delta^2}\Theta \tag{4.97}$$

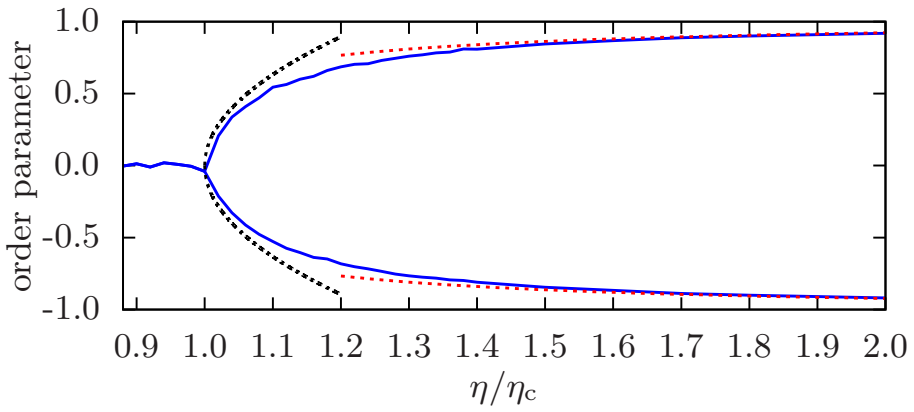

Figure 4.4 (Colour on-line) Order parameter (4.95) as function of the pump strength obtained from eqs. (4.1) in the long-time limit ($\omega_R t = 50N$). The red dashed line is given by eq. (4.96), the black dashed line around the critical point corresponds to eq. (4.98). Parameters: $N = 1000$, $NU_0 = -\omega_R$, $\kappa = 100\omega_R$, $\Delta_c = NU_0/2 - \kappa$ (i. e. $\delta = -\kappa$) and $k_B T_0 = 110 E_R$. Ensemble average of 20 (away of the critical point) and 60 (around the critical point) noise trajectories, respectively, for one initial condition.

perturbatively around the critical point for a thermal state yields

$$\Theta \simeq \pm 2\sqrt{\frac{\eta}{\eta_c} - 1} \tag{4.98}$$

and thus a critical exponent of 1/2, as already predicted in [28]. Let it be noted, however, that the present kinetic theory does not in fact predict a thermal state close to threshold, which could explain the rather poor agreement visible in figure 4.4. We have not found it worthwhile to solve (4.83a) in the limit of weak spatial inhomogeneity in order to improve upon (4.98).

Summarizing the findings of the present work, the equilibrium phase diagram is sketched in figure 4.5. For small $|\delta|/\omega_R$ the ensemble will always remain weakly organized (i. e. a small spatial modulation on top of a homogeneous background) above threshold as the necessary prerequisites for a strongly organized equilibrium—and hence the validity of equation (4.88)—cannot be fulfilled. We wish to point out once more that the phase diagram could not have been obtained by means of Gibbsian equilibrium statistical mechanics, due to the dissipative nature of the system.

4.10 Cooling time

Let us take a closer look at the cooling time τ. If one chooses to define the latter as the time characteristic for the kinetic-energy equilibrisation, the following picture presents itself.

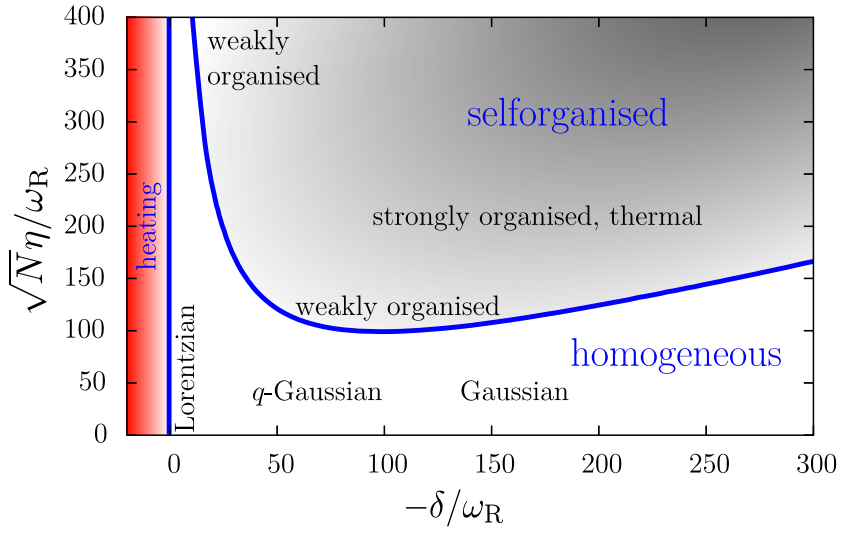

Figure 4.5 (Colour on-line) Schematic view of the phase diagram in the weak-coupling limit ($N|U_0| \ll |\Delta_c|$) for $\kappa = 100\omega_R$. Equilibrium solutions exist only for $\delta < -\omega_R/2$, the Lorentzian corresponds to the case $|\delta| = \omega_R$. For large values of the detuning $|\delta|$, strongly organized equilibria exist already for pump strengths slightly above the critical value, cf. also figure (4.4).

First we treat the case of a fixed ensemble size and variable pump strength. The drift term $A+\partial_v B$ in the non-linear Fokker–Planck equation (4.68)—scaling as $\sim \eta^2/\omega_R$—might suggest the conclusion that the larger the pump strength the shorter the cooling time. However, numerical simulations (cf. figure 4.6) prove this expectation to be somewhat misleading. The situation is worst for initially unstable ensembles. Hence, it seems a plausible requirement that selforganization has to be avoided to realize the optimal cooling time. Accordingly, as a rule of thumb we may state that the latter is achieved for a laser power which renders the desired gas temperature critical. Hence the optimal cooling time is estimated from equation (4.68) to be

$$\tau_{\text{opt}} \approx \frac{k v_{T_0}}{4\sqrt{\pi}\kappa^2} N \tag{4.99}$$

assuming a Gaussian and $\delta = -\kappa$ for simplicity. This estimate is valid for $k v_{T_0} \gg \kappa$, where T_0 is the initial temperature.

For a fixed η, all ensembles composed of $N < N_c$ particles experience in a good approximation the same cooling time $\tau \sim \omega_R/\eta^2$ for reaching the minimal temperature (4.73). N_c is the critical particle number rendering the given η critical. Note however, that this time scale is suboptimal for all ensemble sizes except $N = N_c$. Refer to figure 4.9. For initially stable ensembles the cooling rate is approximately the same until the instability point is reached.

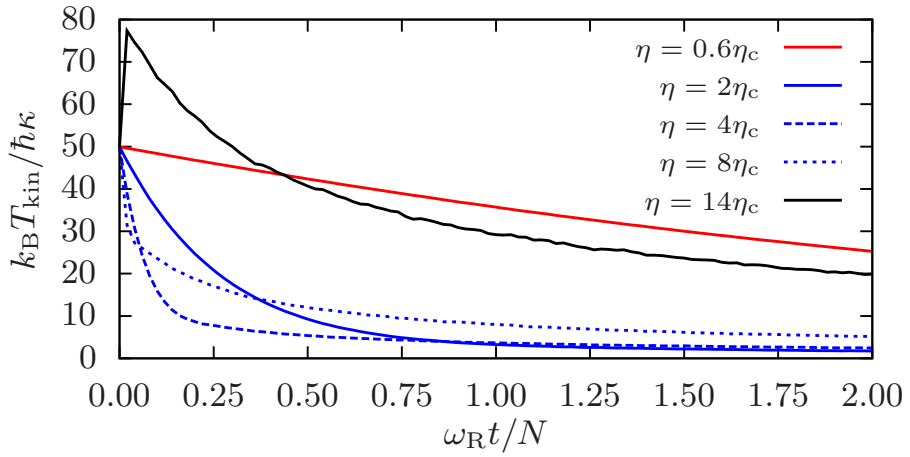

Figure 4.6 (Colour on-line) Kinetic temperature for $N = 500$ and different pump strengths. Parameters: $\kappa = 100\omega_R$ and $\delta = -\kappa$. The initial instability threshold is at $\eta = 10\eta_c$. Ensemble average over 5 initial conditions with 5 noise trajectories.

Let us point out that the above definition of cooling in terms of kinetic energy is inadequate for a gas in the organized phase, because it is *not* kinetic energy, which is dissipated, but rather *action* (or total energy). Nevertheless, kinetic energy as an observable does provide a numerically convenient means to monitor the system's approach to equilibrium. And regardless of the suitability of the employed definition of cooling, the results depicted in figures 4.6 and 4.9 seem to corroborate a deterioration of equilibrisation efficiency above threshold. This observation merits a more detailed analysis of the cooling rate for selforganized ensembles. If we neglect collective effects, the Fokker-Planck equation (4.83a) predicts a maximal cooling rate for a detuning $\Delta_c = -2\omega_0$, precisely the detuning for which also the lowest energy can be reached. Hence, at first sight it seems that the observed worsening of cooling efficiency above threshold is due only to off-resonant detuning. Surprisingly, this is not the whole story. To render the discussion more quantitative, let us define the cooling rate γ as

$$\gamma := -\frac{1}{\langle H\rangle}\frac{\mathrm{d}}{\mathrm{d}t}\langle H\rangle\,, \tag{4.100}$$

where

$$\langle H\rangle = 2\pi\int H(I)f(I)\mathrm{d}I \tag{4.101}$$

denotes the expected energy per particle in the averaged optical potential. To estimate the cooling rate, we will assume a strongly organized (non-equilibrium) thermal state

$$f(I) = \frac{\omega_0}{2\pi k_B T}e^{-\frac{\omega_0 I}{k_B T}} =: \frac{1}{2\pi}F(I), \tag{4.102}$$

with some temperature T, such that $\langle H\rangle = k_\mathrm{B}T \gg k_\mathrm{B}T_\mathrm{kin}$. Using (4.83a) we find

$$\gamma \approx \frac{\omega_0}{k_\mathrm{B}T}\int_0^\infty A[f]F(I)\mathrm{d}I, \tag{4.103}$$

because the Balescu-Lenard term vanishes for strongly organized states. For what follows it is very convenient to introduce the transmission function $S_r(\omega)$ for the energy stored in the real part of α, which can be computed from the linear response of the gas-cavity system to a weak time-harmonic driving at a frequency ω relative to the driving laser and is given by

$$S_r(\omega) = \frac{\kappa^2 + (\Delta_\mathrm{c} - \omega)^2}{4|D(i\omega)|^2}. \tag{4.104}$$

Ignoring collective effects amounts to the approximation $D(i\omega) \simeq (i\omega + \kappa)^2 + \Delta_\mathrm{c}^2$ in (4.104) and corresponds to the assumption of perfectly random phases $\theta_1, \ldots, \theta_N$ of the particles. With its help we can write the cooling rate as

$$\gamma = 16\eta^2\omega_0\frac{\hbar\kappa}{k_\mathrm{B}T}\int_0^\infty |g_2(I)|^2\left[S_r(2\omega) - S_r(-2\omega)\right]F(I)\mathrm{d}I, \tag{4.105}$$

where $\omega = \omega(I) \approx \omega_0\left(1 - \frac{k^2 I}{24m\omega_0}\right)$ denotes the orbital frequency and

$$|g_2(I)|^2 \approx \frac{1}{16}\left(\frac{k^2}{m\omega_0}\right)I^2 \tag{4.106}$$

is the (only relevant) coupling coefficient. It thus appears that the cooling rate is proportional to a weighted average of the difference of the transmission at the two frequencies $\omega_L \pm 2\omega(I)$. This has its origin in the fact that a given gas particle induces, due to its oscillatory motion inside the optical potential, a time-harmonic fluctuation in the real part of α at a frequency close to $\pm 2\omega_0$ relative to the driving laser (motional sidebands). Note that for $\Delta_\mathrm{c} < 0$, we have $S_r(\omega) > S_r(-\omega)$ for all frequencies and thus certainly $\gamma > 0$. In figure 4.7 we plot the cooling rate (4.105) with and without collective effects in units of κ as a function of detuning for fixed ratios η/η_c and T/T_kin. The resonance at $\Delta_\mathrm{c} = -2\omega_0$ is completely absent if back-action is taken into account. The deterioration of the cooling rate shown in this figure is typical for all parameters. It is interesting to look at the cooling rate for (near) ground state cooling, which requires $\Delta_\mathrm{c} = -2\omega_0$. Without collective effects we obtain the estimate

$$\gamma \sim \tau\frac{\omega_\mathrm{R}^{4/3}}{\kappa}\left(\frac{\eta}{N}\right)^{2/3}, \tag{4.107}$$

where $\tau := \frac{k_\mathrm{B}T}{\hbar\omega_0}$. Obviously, the cooling rate for a fixed pump strength gets worse for larger ensembles, but for a given number of particles it can be made arbitrarily large by increasing η. If we take the collective effects into account, we find that

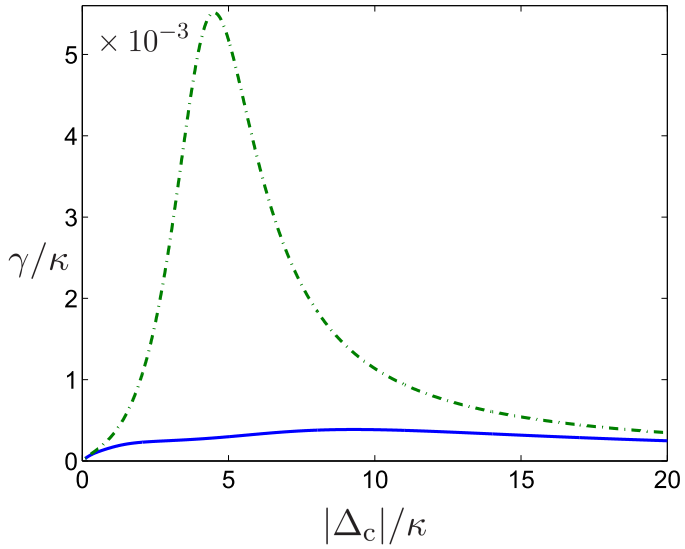

Figure 4.7 Cooling rate (4.105) versus detuning with (blue) and without (green) collective effects for a fixed ratios $\eta/\eta_c = 10$ and $T/T_{\rm kin} = 50$. The maximum at $\Delta_{\rm c} \approx -2\omega_0$ disappears due to collective back-action, causing the cooling rate to be much less than expected. Further parameters: $N = 100$, $\omega_{\rm R} = 0.01\kappa$.

for a *given* temperature relative to the final one, τ, there exists an optimal pump strength, which scales like $\eta_{\rm opt} \sim N^{-1/2}$, for which

$$\gamma \sim \frac{1}{N}. \tag{4.108}$$

Thus, it seems that collective effects seriously spoil the cooling efficiency for large ensembles and cannot be overcome by increasing the pump strength. In fact, increasing the pump strength indefinitely causes $\gamma \to 0$.

To see why this is so, it is instructive to have a look at the transmission function $S_r(\omega)$. Figure 4.8 depicts the transmission function with and without collective effects for a thermal phase space distribution and a detuning $\Delta_{\rm c} = -2\omega_0$. From the figure we see that at this detuning, particle induced fluctuations at $\omega_L + 2\omega_0$ are in resonance with the bare cavity and thus maximally amplified, which explains why this detuning leads to optimal cooling without collective effects. If the latter are taken into account, the picture is radically changed. Due to collective back-action, the motional sidebands are actually always strongly suppressed! The reason for this suppression lies in the fact that for strongly trapped ensembles, the orbital frequencies of all the particles are nearly equal and they are thus close to resonant, which leads to a partial anti-synchronization of their motions. In the singular limit of a perfectly harmonic mean potential, anti-synchronization is in full effect and the particles get trapped in a "dark state", where no light is scattered into the sidebands

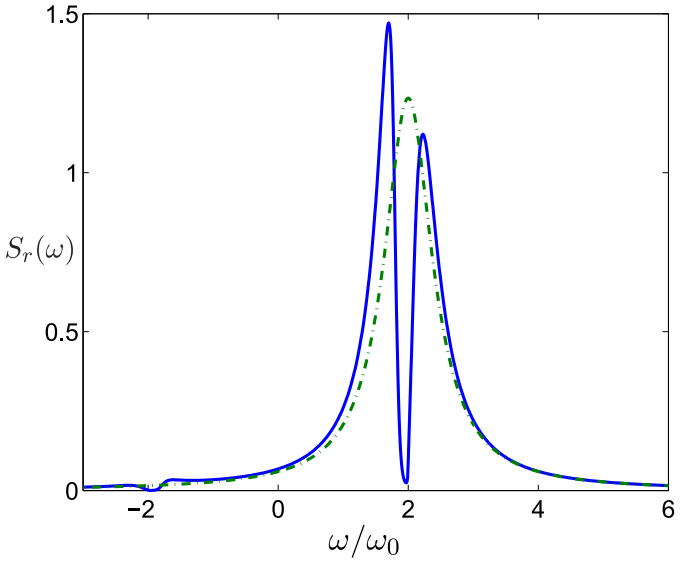

Figure 4.8 Transmission function (4.104) for a thermally selforganized gas out of equilibrium without (green) and with (blue) collective effects. In the latter case the motional sidebands, which have frequencies close to $\pm 2\omega_0$ relative to the pump laser are strongly suppressed. Parameters: $\Delta_c = -2\omega_0$, $\kappa = 0.45\omega_0$, $\eta = 10\eta_c$, $T = 50T_{\mathrm{kin}}$.

and no further dissipation of energy is possible.

Let us briefly mention another aspect of the scaling of the Fokker–Planck equation (4.68) particularly useful for numerical simulations. Fixing $\sqrt{N}\eta$ for different particle numbers yields a cooling time $\tau \sim N/\omega_{\mathrm{R}}$. Numerical simulations of the semiclassical equations (4.1) confirm this result, cf. figs. 4.10 and 4.11. There we have depicted the temperature evolution for the pump strength being a fixed fraction of the critical value η_{c} for two different particle numbers, i. e. $\sqrt{N_1}\eta_1 = \sqrt{N_2}\eta_2$. In fig. 4.11 the threshold (4.65) is surpassed during the time evolution.

In order to verify the Fokker–Planck equation (4.68), we consider the equation

$$\frac{\mathrm{d}}{\mathrm{d}t} k_{\mathrm{B}} T_{\mathrm{kin}} = -2m \int_{-\infty}^{\infty} v \left(-AF + B \frac{\partial F}{\partial v} \right) \mathrm{d}v. \tag{4.109}$$

for the kinetic temperature $k_{\mathrm{B}} T_{\mathrm{kin}} := m \langle v^2 \rangle$ and close it by assuming $F(v,t)$ to be a Gaussian velocity distribution with temperature $k_{\mathrm{B}} T_{\mathrm{kin}}$ for all times. This assumption is well justified for large detunings $|\delta| \gg \omega_{\mathrm{R}}$ and its predicted temperature reproduces the results obtained from the SDEs (4.1) quite well, cf. fig. 4.10. The main difference between the curves stems from the relatively small particle numbers in combination with pump values close to threshold, where the hypothesis of separated time scales used to derive eq. (4.68) is no longer valid due to long-lived

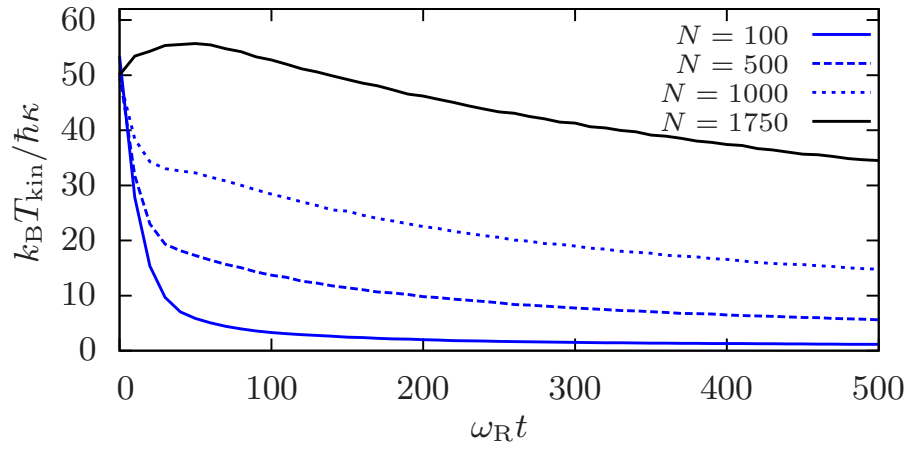

Figure 4.9 (Colour on-line) Kinetic temperature for fixed pump strength and $N = \{100, 500, 1000, 1750\}$, from bottom to top.. Parameters: $\eta = 28\omega_R$, $\kappa = 100\omega_R$ and $\delta = -\kappa$. The self-consistent threshold (4.74) is surpassed for all curves; the ensemble with $N = 1750$ is initially unstable. Ensemble average over 25 ($N = 100$) and 8 (higher particle numbers) initial conditions, respectively, and 5 noise trajectories.

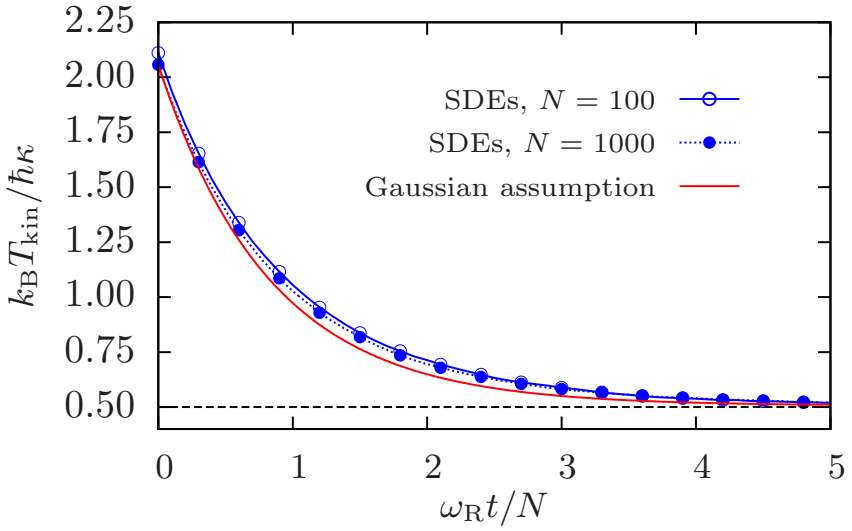

Figure 4.10 (Colour on-line) Comparison of the kinetic temperature obtained from the SDEs (4.1) and as solution of eq. (4.109) for two different particle numbers and constant $\sqrt{N}\eta$. As expected, both ensembles evolve on a time scale $\sim N/\omega_R$. Parameters: $NU_0 = -0.01\omega_R$, $\kappa = 100\omega_R$, $\Delta_c = NU_0/2 - \kappa$ (i. e. $\delta = -\kappa$) and $\sqrt{N}\eta = 80\omega_R \equiv 0.8\sqrt{N}\eta_c$. Ensemble average of 50 ($N = 100$) and 2 ($N = 1000$) initial conditions, respectively, and 50 realisations of the white noise process.

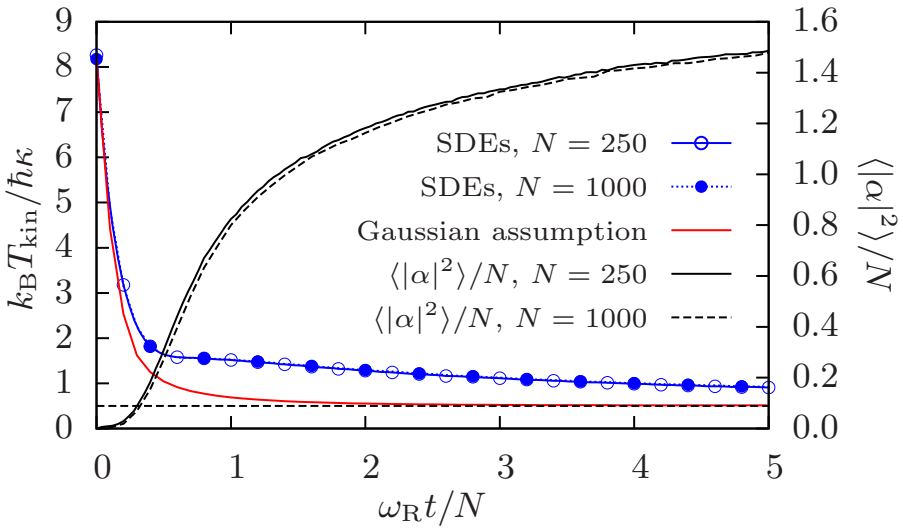

Figure 4.11 (Colour on-line) Temperature evolution above the self-consistent threshold (4.74). The homogeneous distribution is stable until the relation (4.65) is satisfied. This also limits the validity of eq. (4.109). Parameters: $NU_0 = -\omega_R$, $\kappa = 100\omega_R$, $\Delta_c = NU_0/2 - \kappa$ (i. e. $\delta = -\kappa$) and $\sqrt{N}\eta = 200\omega_R \equiv 2\sqrt{N}\eta_c$. As $\sqrt{N}\eta = \text{const.}$, the photon number scales only $\sim N$ and not $\sim N^2$ (superradiance effect). Furthermore, the equilibrium temperature is the same for both ensembles. The simulations were performed up to $\omega_R t = 40N$ and revealed a temperature $k_B T_{kin} \approx 0.57\kappa$, which agrees very well with the theoretical prediction (4.88). Ensemble average of 50 ($N = 250$) and 25 ($N = 1000$) initial conditions, respectively, and 10 realisations of the white noise process.

fluctuations.

Of course, a thorough investigation of the validity of eq. (4.68) would require a numerical integration thereof. However, in steady state, all results of numerical simulations of the SDE system (4.1) were found to be in excellent agreement with the predictions of the kinetic theory, both, below (e. g. fig. 4.2) and above (e. g. fig. 4.11) threshold.

4.11 Conclusion and Outlook

Collective light scattering from a dilute gas of cold particles into a high-Q resonator mode under suitable conditions leads to friction forces and cooling of particle motion even below the selforganization threshold. We have found that, as long as the collective light shift is small enough, arbitrarily large ensembles of polarizable particles can be cooled to very low energies without the need for a cyclic optical transition and direct interparticle interactions. Surprisingly, for a gas, which has crossed the

selforganization threshold, the cooling rate is predicted to be strongly diminished as compared to uncorrelated particles by collective suppression of motional sidebands.

One can easily envisage a combination of many species within the cavity to commonly interact with the same pump and cavity fields as a generalized form of sympathetic cooling without the need of direct interparticle interactions. This generalization will be studied in chapter 6.

4.12 Appendix

Here we will supply some details concerning the derivation of (4.87). First note that if the selfconsistent optical potential is strong, that is its potential depth is large in comparison to the energy per particle, we can assume

$$x(I,\theta) = x_0 + \sqrt{\frac{2I}{m\omega_0}}\sin(\theta), \tag{4.110}$$

where x_0 denotes position of the minimal potential energy, depending on the sign of the real part of the averaged mode amplitude. From this we obtain, for even n

$$|g_n(I)|^2 = \left| J_n\left(k\sqrt{\frac{2I}{m\omega_0}}\right)\right|^2 \tag{4.111}$$

and $|g_n(I)|^2 = 0$ for odd n. The assumption of strong trapping implies

$$k\sqrt{\frac{2I}{m\omega_0}} \ll 1 \tag{4.112}$$

and hence the only relevant "transition" amplitude is in fact $|g_2|^2$. Therefore, the sums in (4.85) and (4.85c) contain in effect only terms with $n = \pm 2$ and $m = \pm 2$. The first thing that follows is that the Balescu-Lenard term vanishes identically. Indeed, due to the positivity of $\omega(I)$, the only non-zero term in the double sum are those with $n = 2, m = 2$ and $n = -2, m = -2$. Using the expansion

$$\omega(I) \simeq \omega_0 + \omega_0' I \tag{4.113}$$

we have approximately

$$w_{22}(I,I') \approx 8\pi^2\hbar^2\Delta_c^2 N \,\frac{\eta^4|g_2(I)|^4}{|D(2i\omega(I))|^2}\,\frac{1}{|\omega_0'|}\,\delta\left(I - I'\right) \tag{4.114}$$

and $w_{-2-2}(I,I') = -w_{-2-2}(I,I')$. Hence,

$$C[f,f] \simeq 4\int w_{22}(I,I')\Big(\frac{\partial f}{\partial I}f(I') - \frac{\partial f}{\partial I'}f(I)\Big)\mathrm{d}I' = 0, \tag{4.115}$$

because the integrand vanishes for $I = I'$. Thus the steady state equation reduces to

$$\frac{\mathrm{d}}{\mathrm{d}I}\ln f = -\frac{A}{B} \simeq \frac{4\Delta_c\omega}{\hbar(\kappa^2 + \Delta_c^2 + 4\omega^2)}. \tag{4.116}$$

Approximating $\omega \simeq \omega_0$ and noticing that $H \simeq \omega_0 I$ the result (4.87) follows.

5 Kinetic Theory of Cavity Cooling and Selforganisation – Quantum

5.1 Introduction

The kinetic theory developed in the previous chapter rests on classical equations of motion. As such it should be a valid description of the system as long as the energy of the gas is not too low. Taking into account that the relevant energy scale for the interaction of the gas particles with the cavity photons is fixed by the so-called recoil energy

$$E_{\mathrm{R}} := \frac{\hbar^2 k^2}{2m} = \hbar\omega_{\mathrm{R}}, \tag{5.1}$$

we can expect that the criterion for the breakdown of classical theory will be

$$\langle H\rangle \lesssim E_{\mathrm{R}}, \tag{5.2}$$

where $\langle H\rangle := 2\pi \int H(I) f(I) \mathrm{d}I$ denotes the expected energy per particle in the mean optical potential. It is the purpose of this chapter to investigate, in how far the classical results obtained previously have to be modified, when quantum effects are taken into account. The quantum mechanical description rests on the Hamiltonian

$$\hat{H} = -\hbar\Delta_{\mathrm{c}}\hat{a}^\dagger\hat{a} + \int \hat{\Psi}^\dagger(x)\left(-\frac{\hbar^2}{2m}\frac{\partial^2}{\partial x^2} + \hat{\Phi}(x,\hat{a},\hat{a}^\dagger)\right)\hat{\Psi}(x)\mathrm{d}x, \tag{5.3}$$

where

$$\hat{\Phi}(x,\hat{a},\hat{a}^\dagger) \simeq \hbar\eta(\hat{a}^\dagger + \hat{a})\sin(kx) \tag{5.4}$$

is the quantized optical potential. Hence, we have from the beginning, for simplicity, assumed a weak collective shift as in (4.76), because our main aim is a comparison with the classical results of the previous chapter. Also, we have excluded direct interactions between the particles. If one wishes to retain them, a term

$$\hat{U} = \int \hat{\Psi}^\dagger(x)\hat{\Psi}^\dagger(x')u(x-x')\hat{\Psi}(x)\hat{\Psi}(x')\mathrm{d}x'\mathrm{d}x, \tag{5.5}$$

with a pair-interaction potential $u(x-x')$ must be added to the Hamiltonian. For the sake of definiteness, let's choose the particles to be bosons

$$[\hat{\Psi}(x),\hat{\Psi}^\dagger(x')] = \delta(x-x') \quad , \quad [\hat{\Psi}^\dagger(x),\hat{\Psi}^\dagger(x')] = [\hat{\Psi}(x),\hat{\Psi}(x')] = 0. \tag{5.6}$$

The case of fermionic particles can be treated without any major modification.

The following derivation is heavily inspired by the corresponding classical treatment and almost every single step can be traced back to its classical version as presented in the previous chapter. Nevertheless, the author of this thesis believes it to be an original piece of work.

To begin with, we need some dynamical variable to play the rôle of the Klimontovich distribution function. The field operator $\hat{\Psi}(x)$ is unsuited as it depends on only one variable and furthermore, as we know, a mean-field treatment involving $\langle\hat{\Psi}\rangle$ leads to Gross-Pitaievskii's equation, which is valid only at zero temperature. Fortunately, we don't have to search long for the desired object because quantum mechanics freely provides one, namely the (operator) density matrix

$$\hat{\rho}(x,x') = \hat{\Psi}^\dagger(x')\hat{\Psi}(x). \tag{5.7}$$

The quantum expectation value of this operator yields the position matrix elements of the reduced one-body density operator $\hat{\rho}_1$:

$$\langle\hat{\rho}(x,x')\rangle = \langle x|\hat{\rho}_1|x'\rangle. \tag{5.8}$$

With the help of the operator density matrix we can formulate the fundamental Heisenberg-Langevin equations of motion, which will constitute the starting point for the derivation of a quantum kinetic theory in the form

$$i\hbar\frac{\partial\hat{\rho}}{\partial t} = -\frac{\hbar^2}{2m}\left(\frac{\partial^2}{\partial x^2} - \frac{\partial^2}{\partial x'^2}\right)\hat{\rho} + \hat{\Phi}(x)\hat{\rho} - \hat{\rho}\hat{\Phi}(x'), \tag{5.9a}$$

$$\frac{\mathrm{d}\hat{a}}{\mathrm{d}t} = (-\kappa + i\Delta_\mathrm{c})\hat{a} - \frac{i}{\hbar}\int\frac{\partial\hat{\Phi}}{\partial\hat{a}^\dagger}\hat{\rho}(x,x)\mathrm{d}x + \hat{a}_{in}, \tag{5.9b}$$

where $\hat{a}$ denotes the cavity mode annihilation operator we have included cavity decay and vacuum fluctuations

$$\langle\hat{a}_{in}(t)\hat{a}^\dagger_{in}(t')\rangle = 2\kappa\delta(t-t'). \tag{5.10}$$

All other noise-correlations vanish. In what follows we will, as in the classical case, adopt periodic boundary conditions, such that the operator wave-function satisfies

$$\hat{\Psi}(x+L) = \hat{\Psi}(x) \tag{5.11}$$

for $L > 0$ some integer multiple of a wavelength. This implies, of course, that $\hat{\rho}(x,x')$ is L-periodic in both it's arguments.

5.2 Quantum Mean-Field Limit

We shall first investigate the so-called mean-field limit in order to erect the quantum kinetic theory as a super-structure upon it. To this end we take the expectation value of equations (5.9) and neglect all correlations to obtain

$$i\hbar\frac{\partial\rho}{\partial t} = -\frac{\hbar^2}{2m}\left(\frac{\partial^2}{\partial x^2} - \frac{\partial^2}{\partial x'^2}\right)\rho + \Phi(x)\rho - \rho\Phi(x') \tag{5.12a}$$

$$\frac{\mathrm{d}\alpha}{\mathrm{d}t} = (-\kappa + i\Delta_\mathrm{c})\alpha - i\eta \int \rho(x,x)\sin(kx)\mathrm{d}x, \tag{5.12b}$$

where

$$\Phi(x,\alpha,\alpha^*) = \langle\hat{\Phi}(x,\hat{a},\hat{a}^\dagger)\rangle = \hbar\eta(\alpha^* + \alpha)\sin(kx) \tag{5.13}$$

and, here and from hence onward,

$$\rho(x,x') := \langle\hat{\rho}(x,x')\rangle \tag{5.14}$$

as well as

$$\alpha := \langle\hat{a}\rangle. \tag{5.15}$$

It is easy to verify that every "pure state" $\rho(x,x') = \varphi_n^*(x')\varphi_n(x)$ in which φ_n solves the time-independent Schrödinger equation

$$-\frac{\hbar^2}{2m}\frac{\partial^2\varphi_n}{\partial x^2} + \Phi(x,\alpha,\alpha^*)\varphi_n = E_n\varphi_n \tag{5.16}$$

is a stationary solution to the first mean field equation. If α is non-vanishing, we know from Bloch's theorem that these solutions can be written as

$$\varphi_n(x) = e^{iqx}u_{q,s}(x), \tag{5.17}$$

where q is the quasi-wavenumber, restricted to the first Brillouin zone, and s denotes the so-called band index. $u_{s,q}$ is a $\lambda = 2\pi/k$-periodic function, $u_{s,q}(x+\lambda) = u_{s,q}(x)$. If there is no mean cavity field, $\alpha = 0$, and the gas is in the unordered phase, the wave-functions are simple momentum eigenstates, i.e.

$$\varphi_n(x) = \frac{1}{\sqrt{L}}e^{ip_nx/\hbar}, \tag{5.18}$$

where p_n denotes the momenta compatible with the periodic boundary conditions. Therefore, in what follows, $n = (s,q)$, if $a \neq 0$ and $n = p_n$ else. Hence, the most general stationary solution is a convex combination, or mixture, of "pure states"

$$\rho(x,x') = \sum_n f_n\varphi_n^*(x')\varphi_n(x) \tag{5.19}$$

with $\sum_n f_n = N$, the total number of particles. The coefficients $f_n \geq 0$ are called the occupancies of the states φ_n. In operator notation we can thus write a mean-field stationary reduced one-body density operator as

$$\hat{\rho}_1 = \sum_n f_n|n\rangle\langle n| \tag{5.20}$$

i.e. the states $|n\rangle$, defined via $\varphi_n(x) = \langle x|n\rangle$, are eigenvectors of $\hat{\rho}_1$. Therefore, every stationary mean-field density matrix is necessarily diagonal, when represented in terms of the eigenstates of the single particle Hamiltionian that corresponds to the average optical potential. This represents a strong resemblance to the classical case, where every distribution function depending on the action variable alone was a mean-field steady state. Remembering the Bohr-Sommerfeld correspondence principle of the old quantum theory, which (somewhat loosely) states that every action that is an integer multiple of the elementary quantum of action $\hbar$ corresponds to a quantum energy eigenstate, the analogy is near perfect.

5.3 Fundamental Suppositions

In analogy to the classical case, we assume that the long-term dynamics, driven by field-particle correlations, is such that the one-body density matrix is always close to some mean-field steady state and hence diagonal in the eigenbasis of the single particle Hamiltonian that corresponds to the *momentary* average optical potential:

$$\rho(x,x',t) \simeq \sum_n f_n(t)\varphi_n^*(x',t)\varphi_n(x,t), \tag{5.21a}$$

where

$$H(t)\varphi_n(x,t) = E_n(t)\varphi_n(x,t). \tag{5.21b}$$

Here we have introduced the one-body averaged Hamiltonian

$$H(t) := -\frac{\hbar^2}{2m}\frac{\partial^2}{\partial x^2} + \Phi(x,\alpha(t),\alpha^*(t)). \tag{5.22}$$

This assumption is the quantum mechanical analog of (4.15). For the sake of clarity, we have explicitly written down the time dependence of the wave-functions and the mean values of the creation and annihilation operators. We shall mostly suppress this dependence hereafter. In summary, this means we assume that after a "short" mean-field stage of the time evolution, the one-body density matrix has assumed the form (5.21a) and preserves it during the "slow" approach to equilibrium. This ansatz, which can be viewed as a form of "variation of the constant", is the key to the development of a quantum kinetic theory as it was the key to the development of the classical theory. In addition, we assert that the fluctuations around the mean values are, in some sense, small and fast-varying in comparison with the mean values.

Let us now explore the consequences of these suppositions in some detail. To this end we expand the density matrix according to

$$\hat\rho(x,x') = \sum_{mn} \hat b_m^\dagger \hat b_n\, \varphi_m^*(x')\varphi_n(x) =: \sum_{mn} \hat\rho_{mn}\varphi_m^*(x')\varphi_n(x). \tag{5.23}$$

Here, the operator $\hat b_n^\dagger$ creates a particle in the state φ_n. Let it be pointed out that this step exactly corresponds to the introduction of action-angle variables in the classical treatment. Let us also decompose the operator density matrix elements and the cavity mode annihilation operator in the usual manner

$$\hat\rho_{mn} = \rho_{mn} + \delta\hat\rho_{mn}, \tag{5.24a}$$

$$\hat a = \alpha + \delta\hat a \tag{5.24b}$$

into mean values and fluctuations.

As a side note let us remark that the restriction to a motion of the gas particles along the resonator axis is, for the derivation of a kinetic theory valid in the

quantum mechanical regime, a mere matter of convenience. The situation is different in the classical regime, where we found the existence of action-angle variables to be indispensable and which is guaranteed only in a one-dimensional setting.

Inserting these decompositions into (5.9) we find

$$i\hbar\frac{\partial\hat{\rho}_{nl}}{\partial t}+i\hbar\sum_m\left(\hat{\rho}_{ml}c_{mn}+\hat{\rho}_{nm}c^*_{ml}\right)= \\ =(E_l-E_n)\hat{\rho}_{nl}-\sum_m\left(\hat{\rho}_{ml}\delta\hat{\Phi}_{mn}-\delta\hat{\Phi}_{lm}\hat{\rho}_{nm}\right), \quad (5.25)$$

wherein the fluctuating optical potential is defined as $\delta\hat{\Phi}:=\hat{\Phi}-\langle\hat{\Phi}\rangle$ and the matrix elements are given by

$$\delta\hat{\Phi}_{nm}:=\int\varphi^*_n(x)\delta\hat{\Phi}(x)\varphi_m(x)dx \quad (5.26)$$

and

$$c_{mn}:=\int\frac{\partial\varphi^*_m(x)}{\partial t}\varphi_n(x)dx. \quad (5.27)$$

Taking the average of equation (5.25), we obtain the following equation of motion for the occupancies $f_n=\langle\hat{\rho}_{nn}\rangle=\rho_{nn}$

$$i\hbar\frac{\partial f_n}{\partial t}+i\hbar\sum_m\left(\rho_{mn}c_{mn}+\rho_{nm}c^*_{mn}\right)=-\sum_m\left[\left\langle\delta\hat{\rho}_{mn}\delta\hat{\Phi}_{mn}\right\rangle-\left\langle\delta\hat{\Phi}_{nm}\delta\hat{\rho}_{nm}\right\rangle\right]. \quad (5.28)$$

Now, if we exploit our assumption about the form of ρ, namely that $\rho_{nm}\simeq f_n\delta_{nm}$, we finally find

$$\frac{\partial f_n}{\partial t}=\frac{1}{i\hbar}\sum_m\left[\left\langle\delta\hat{\Phi}_{nm}\delta\hat{\rho}_{nm}\right\rangle-\left\langle\delta\hat{\rho}_{mn}\delta\hat{\Phi}_{mn}\right\rangle\right], \quad (5.29a)$$

where we have used the conservation of norm to conclude that $c_{nn}=0$. In keeping with the assumption of a slow evolution of the occupancies, the averaged mode amplitude is to be calculated from the quasi-stationarity equation

$$\alpha(t)=\frac{i\eta}{-\kappa+i\Delta_{\mathrm{c}}}\sum_n g_{nn}(t)f_n(t), \quad (5.29b)$$

which finds its classical counterpart in (4.83b). Here we had occasion to introduce the transition matrix elements

$$g_{mn}:=\int\varphi^*_m(x)\sin(kx)\varphi_n(x)\mathrm{d}x, \quad (5.30)$$

which correspond to (4.84). Concerning the fluctuations we assume once more that, because of their "smallness", we can linearize their equations of motion to the effect that

$$i\hbar\frac{\mathrm{d}\delta\hat{\rho}_{mn}}{\mathrm{d}t}+(E_m-E_n)\delta\hat{\rho}_{mn}=(f_m-f_n)\delta\hat{\Phi}_{nm} \quad (5.31a)$$

$$\frac{\mathrm{d}\delta\hat{a}}{\mathrm{d}t} = (-\kappa + i\Delta_\mathrm{c})\delta\hat{a} - i\eta\sum_{nm} g_{mn}\delta\hat{\rho}_{mn} + \hat{a}_{in}, \tag{5.31b}$$

where, in addition, we have neglected terms proportional to $c_{lk}\delta\hat{\rho}_{mn}$, because they are products of the time derivatives of the slowly evolving wave-functions with fluctuating density matrix elements and thus of higher order.

From (5.29) we see that the number of particles is conserved if and only if $[\delta\hat{\Phi}_{mn}, \delta\hat{\rho}_{mn}] = 0$. The approximations that we introduced concerning the fluctuations will violate these commutation relations in the course of time. Therefore, we shall use a symmetric form of equation (5.29), such that number conservation is guaranteed:

$$\frac{\partial f_n}{\partial t} = -\frac{1}{\hbar}\sum_m \mathrm{Im}\left\langle\left\{\delta\hat{\Phi}_{mn}, \delta\hat{\rho}_{mn}\right\}\right\rangle, \tag{5.32}$$

where $\{,\}$ denotes the anticommutator and use has been made of the fact that

$$\langle\delta\hat{\Phi}_{nm}\delta\hat{\rho}_{nm}\rangle = \langle(\delta\hat{\rho}_{mn}\delta\hat{\phi}_{mn})^\dagger\rangle = \langle\delta\hat{\rho}_{mn}\delta\hat{\Phi}_{mn}\rangle^*. \tag{5.33}$$

5.4 Conditions for a Quantum Kinetic Theory

Our goal is once again to find, starting from the above equations, some functional $\mathcal{J}_n$, such that in place of the first equation in (5.32) we can approximately write

$$\frac{\partial f_n}{\partial t} = \mathcal{J}_n[\{f_m(t)\}] \tag{5.34}$$

This means, we want to find a Markovian master equation approximation to the dynamics of the occupancies, where the latter assume the rôle of the classical distribution function $f(I)$. In complete analogy to the classical theory, one can show that such an approximation indeed exists, provided that

I. The limit $L/\lambda \to \infty$ is assumed, where L denotes the quantization length.

II. The one-body density matrix is mean-field stable, i.e. the analytic continuation of the response function $D(\Omega)$ (see (5.44) below) has no zeros with positive real part and all its zeros have a sufficiently negative real part.

III. It is assumed that the correlations of the fluctuating density matrix can be written as

$$\langle\delta\hat{\rho}_{ab}(t)\delta\hat{\rho}_{cd}(t)\rangle = f_a(t)[f_c(t)+1]\delta_{ad}\delta_{cb}(1-\delta_{ab}) + C_{a,b,c,d}(t), \tag{5.35}$$

such that

$$C_{a,b,c,d}(t) \equiv C_{s_a,\ldots,s_d}(q_a,\ldots,q_d;t) \tag{5.36}$$

is a *smooth* function of the quasi-momenta $q_a,\ldots,q_d$ (or momenta, if $\alpha \equiv 0$).

Condition I, namely the limit of many potential wells $L/\lambda \to \infty$, ensures that we have a continuous manifold of states within each band, which is necessary that certain expressions akin to Fermi's Golden Rule make sense. To clarify condition II we denote by $\gamma(t) < 0$ the largest real part of all zeros of the analytically continued dispersion relation D. Then, condition II means that we require that

$$|\gamma(t)| \gg \max_n |\dot{f}_n(t)/f_n(t)|. \tag{5.37}$$

It implies that there is no Markovian Master equation approximation in the vicinity of the selforganization threshold (because there $\gamma \to 0$) and guarantees a separation of timescales of evolution between the f_n's and the correlations everywhere else. It may be called the Markovian condition proper. Condition III is sufficient for the correlations to depend on the $f_n(t)$'s alone and it is at this point that the quantum statistics of the particles enters. It has been written down for bosons, but the fermionic case can easily be covered by replacing the assumption III by

$$\langle \delta\hat{\rho}_{ab}(t)\delta\hat{\rho}_{cd}(t)\rangle = f_a(t)[1 - f_c(t)]\delta_{ad}\delta_{cb}(1 - \delta_{ab}) + C_{a,b,c,d}(t). \tag{5.38}$$

Here, $C_{a,b,c,d}$ includes all correlations, which are not due to the bosonic (or fermionic) exchange symmetry (exchange-correlations). It presents a straightforward generalization of the classical (4.42). Note that only Condition I has no classical analog, because classically there is already a continuum of states.

Given these conditions we can, as in the classical case, introduce the new fast time τ, solve (5.31) neglecting the dependence of f_n, E_n, g_{nm} on the fast time scale and evaluate the correlations on the r.h.s of (5.32) in the limit $\tau \to \infty$ to obtain them as the sought for functional $\mathcal{J}_n[\{f_m(t)\}]$.

5.5 Quantum Master Equation

We do not report the lengthy calculations necessary to follow the procedure outlined above, because they are not essentially different from those performed in the classical case. Instead, we will state only the end result for the nonlinear master equation, which approximates (5.32). For Bosons it can be cast in the form

$$\frac{\partial f_n}{\partial t} = \sum_m \left(T_{m\to n} f_m - T_{n\to m} f_n + C(f_m, f_n) \right) \tag{5.39a}$$

wherein appears the quantum analog of the classical Balescu-Lenard operator

$$C(f_m, f_n) = \sum_{n'm'} w(n, n'; m, m') \times \\ \times \left[f_m f_{m'} (f_n + 1)(f_{n'} + 1) - f_n f_{n'} (f_m + 1)(f_{m'} + 1) \right], \tag{5.40}$$

with a cross section given by

$$w = \Delta_c^2 \eta^4 \frac{2\pi}{\hbar} \frac{|g_{mn}|^2}{|D(i\omega_{mn})|} \frac{|g_{m'n'}|^2}{|D(i\omega_{m'n'})|} \delta(E_n - E_m + E_{n'} - E_{m'}) \tag{5.41}$$

and the transition probabilities per unit time $T_{m\to n}[f_n] := B_{nm}(1 + f_n)$, where

$$B_{nm} := 2\kappa\eta^2 \frac{|g_{mn}|^2}{|D(i\omega_{mn})|^2} [\kappa^2 + (\Delta_c + \omega_{mn})^2]. \tag{5.42}$$

Here, the transition frequencies are defined as

$$\omega_{mn} := \frac{1}{\hbar}(E_n - E_m) = \omega_n - \omega_m \tag{5.43}$$

and the quantum linear response function is given by

$$D(\Omega) = (\Omega + \kappa)^2 + \Delta_c^2 + 2i\eta^2 \Delta_c \sum_{nm} |g_{nm}|^2 \frac{f_n - f_m}{\Omega + i\omega_{nm}}. \tag{5.44}$$

To summarize: we have found a nonlinear Markovian master equation for the populations f_n of the states $\varphi_n(x)$, which are eigenstates corresponding to the momentary expected optical potential. The latter is determined by the value of the expected cavity mode amplitude, which in turn depends on the instantaneous spatial distribution of the gas.

5.6 Discussion and Physical Interpretation

As we shall see presently, all the terms appearing in this quantum kinetic equation lend themselves easily to a fairly transparent physical meaning, somewhat in contrast to the classical case.

Let us start with the expression for $T_{m\to n}[f_n] = B_{nm}(1 + f_n)$, that is the transition probability per unit time from some state $|m\rangle$ to some other state $|n\rangle$. The most obvious observation is that this probability depends on the occupancy of the final state f_n and finds its explanation in the bosonic statistics of the gas particles, which favors the occupation of some state already occupied. This bunching effect is, of course, responsible for the existence of a Bose-Einstein condensate. For Fermions, the corresponding transition probability is given by $T_{m\to n}[f_n] = B_{nm}(1-f_n)$, clearly reflecting Pauli's principle. $T_{m\to n}[f_n]$ does, however, also depend on all the occupancies collectively through the linear response function $D(i\omega_{mn})$ evaluated at the corresponding transition frequency, a feature it shares with the classical drift and diffusion coefficients as can be seen from (4.85). To clarify the meaning of the prefactor B_{nm}, let us for the moment forget about the dependence of the linear response function on the state of the gas and take $D = D_{\text{bare}}$ in the defining equation (5.42), with

$$D_{\text{bare}}(\Omega) := (\Omega + \kappa)^2 + \Delta_c^2. \tag{5.45}$$

Then, simple algebra reveals that the bare prefactor may be written in the form

$$B_{nm}^{\text{bare}} = \frac{2\pi}{\hbar^2}|V_{nm}|^2\rho_0(\omega_L - \omega_{mn}). \tag{5.46}$$

Here we have defined the bare cavity density of modes

$$\rho_0(\omega) := \frac{1}{\pi}\frac{\kappa}{\kappa^2 + (\omega - \omega_c)^2}, \tag{5.47}$$

where ω_L and ω_c denote the driving laser- and cavity resonance frequency, respectively and we have introduced also the transition matrix element $V_{nm} := \hbar\eta g_{nm} = \hbar\eta\langle n|\sin(k\hat{x})|m\rangle$. The alert reader will have already recognized that the bare prefactor expresses nothing else but Fermi's Golden Rule for the process of a particle scattering a pump laser photon into the cavity while undergoing a transition $m \to n$, the probability per unit time of which is proportional to the density of states for the scattered photon at its frequency ω and the latter is given by $\omega = \omega_L - \omega_{mn}$ due to the conservation of pre- and post-scattering energy:

$$E_m + \hbar\omega_L = E_n + \hbar\omega. \tag{5.48}$$

Returning to the full expression (5.42) we may thus rewrite it in the form of Fermi's Golden Rule

$$B_{nm} = \frac{2\pi}{\hbar^2}|V_{nm}|^2\rho_0(\omega_L - \omega_{mn})\chi(\omega_{mn}), \tag{5.49}$$

where the dimensionless correction factor

$$\chi(\omega) := \frac{|D_{\text{bare}}(i\omega)|^2}{|D(i\omega)|^2} \tag{5.50}$$

has been introduced.

The expression (5.46) allows a very useful visualization of the cavity-cooling phenomenon as shown in figure 5.1. There one can see the (bare) cavity density of modes and the two frequencies at which photons corresponding to some particular transition $n \leftrightarrow m$ are scattered. The photon with higher frequency comes along with a downward, i. e. energy-decreasing transition, the one having a frequency below the laser frequency stems from an energy-increasing or upward transition. In optomechanics, these two frequencies $\omega = \omega_L \pm \omega_{mn}$ are called sidebands. One notes that for a laser frequency lower than the cavity resonance frequency (or red detuning, $\Delta_\mathrm{c} < 0$) the direction of transition corresponding to a removal of energy from the particles always dominates. It becomes also evident that if the transition frequency is smaller than the cavity linewith κ (unresolved sideband regime), the optimal detuning is given by $\Delta_c = -\kappa$. In the reverse case (resolved sideband regime), optimal cooling of that particular transition requires a detuning $\Delta_\mathrm{c} = -|\omega_{mn}|$. Hence the importance of correctly choosing the detuning to optimize cooling efficiency becomes easily understandable. Furthermore, the bosonic enhancement factor $1 + f_n$ shows that if low energy states are already populated by some particles, the rate of cooling increases even more. This is a genuine quantum statistical effect and has no classical counterpart.

Let us now proceed to the discussion of the quantum Balescu-Lenard operator as given by equation (5.40). It has the standard form for a two-body process with cross section defined in (5.41) and evidently describes a process that takes two particles, initially in the states $|m\rangle$, $|m'\rangle$, into the final states $|n\rangle$, $|n'\rangle$ (or vice versa), while conserving the total energy as seen by the appearance of the delta function. This is completely analogous to the resonance condition found in the classical treatment. Using the definition of the bare cavity density of modes, we can rewrite the cross section in the form

$$w = \frac{2\pi^3}{\hbar^4}\frac{\Delta_\mathrm{c}^2}{\kappa^2}|V_{nm}|^2|V_{n'm'}|^2\rho_0(\omega_L - \omega_{mn})\rho_0(\omega_L - \omega_{m'n'})\times \\ \times\, \chi(\omega_{mn})\delta(\omega_{mn} + \omega_{m'n'}). \quad (5.51)$$

From this expression we see that the cross section is proportional to a product of mode densities, which leads us to conclude that there are two scatterings involved in the given process. We have not succeeded in giving a fully satisfactory interpretation thereof but we will call the process *resonant* (due to the transition frequency resonance condition) *pair-scattering* (because it is a pair of particles, which scatters coordinately).

It is worth remarking that the Bose distribution

$$f_n = \frac{1}{e^{(\hbar\omega_n - \mu)/k_\mathrm{B}T} - 1} \quad (5.52)$$

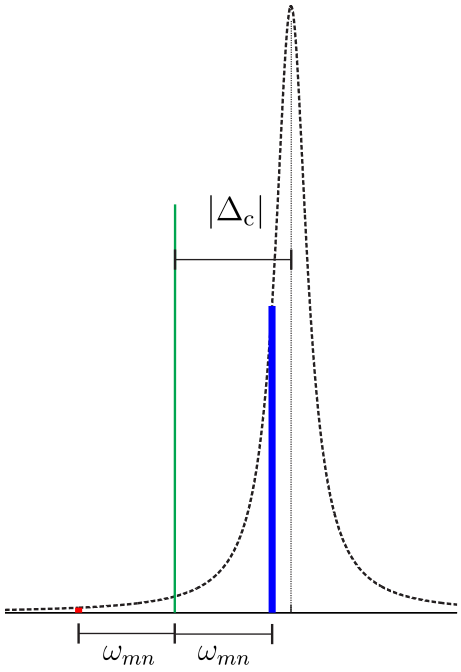

Figure 5.1 Bare cavity density of modes (black dotted line), driving laser frequency (green vertical line) and the two photon sidebands (red and blue vertical lines) from some transition $n \leftrightarrow m$. The right hand sideband corresponds to a cooling- the left hand sideband to a heating scattering process. For red detuning as depicted the heating sideband is suppressed due to the lack of available modes. For blue detuning the situation is reversed.

is invariant under such pair-scattering events. To prove this well-known fact we use the simple identity

$$e^{-x}\left(1+\frac{1}{e^x-1}\right)=\frac{1}{e^x-1} \tag{5.53}$$

to find

$$f_m f_{m'}(f_n+1)(f_{n'}+1)=f_n f_{n'}(f_m+1)(f_{m'}+1)\,e^{\hbar(\omega_{n'}-\omega_{m'}+\omega_n-\omega_m)/k_BT} \tag{5.54}$$

Because of the conservation of energy during resonant pair-scattering, the exponential equals unity and thus $C(f_m, f_n) = 0$. Therefore, these events can plausibly be expected to favor the establishment of a thermal distribution of particles among the levels of the average potential.

In concluding this section we wish to point out that the linear response function given by (5.44) represents the quantum mechanical generalization of the classical one. As such, its zeros determine, whether or not a given state of the gas f_n is stable.

5.7 Unordered Phase

Let us now have a closer look at the master equation, which rules the time evolution of the gas in the unordered phase, where there is no average field inside the cavity. As previously stated, the eigenstates of the one-body Hamiltonian (5.22) are momentum eigenstates

$$\phi_n(x) = \frac{1}{\sqrt{L}} e^{ip_n x/\hbar}. \tag{5.55}$$

The transition matrix elements g_{mn} are easily evaluated

$$g_{mn} = \frac{1}{2i} \left[\delta\left(p_n - p_m + \hbar k\right) - \delta\left(p_n - p_m - \hbar k\right)\right] \tag{5.56}$$

and express the conservation of overall momentum during the scattering of a cavity photon. Hence, only states with momenta p, p' that satisfy $p' = p \pm \hbar k$ are coupled. Consequently, in any stationary solution, the occupancies $f(p)$ with $0 \leq p < \hbar k$ remain undetermined. This is in striking contrast to the classical situation, where we found that below selforganization threshold the equilibrium state is uniquely determined, i.e. independent of the history of the system's evolution.

We observe that the dispersion relation of free particles

$$\hbar\omega(p) = \frac{p^2}{2m} \tag{5.57}$$

leads to the transition frequencies

$$\omega(p) - \omega(p \pm \hbar k) = \mp \frac{k}{2m}(2p \pm \hbar k) = \mp(kv \pm \omega_{\mathrm{R}}). \tag{5.58}$$

Let's introduce the semi-classical drift and diffusion coefficients

$$a(p) := -2\hbar k\, \kappa\eta^2 \Delta_{\mathrm{c}} \frac{kp/m}{|D(ikp/m)|^2} \tag{5.59}$$

$$b(p) := \frac{\hbar^2 k^2 \kappa\eta^2}{2} \frac{\kappa^2 + \Delta_{\mathrm{c}}^2 + (kp/m)^2}{|D(ikp/m)|^2}, \tag{5.60}$$

the current

$$J(p) = \frac{a(p + \hbar k/2)}{2\hbar k}[2f(p)f(p + \hbar k)) + f(p) + f(p + \hbar k)] + \\ + \frac{b(p + \hbar k/2)}{\hbar^2 k^2}[f(p + \hbar k) - f(p)] \tag{5.61}$$

and focus, as in the classical treatment, on symmetric momentum distributions $f(-p, t) = f(p, t)$. In this case, the quantum Balescu-Lenard operator vanishes identically and the Master equation (5.39) assumes the simple form

$$\frac{\partial f}{\partial t} = J(p) - J(p - \hbar k). \tag{5.62}$$

Let us check, whether this equation reduces to its classical counterpart (4.68) if $f(p)$ is slowly varying over an interval of length $\hbar k$. We shall call this case the *unresolved recoil regime* (or bad cavity limit). Its opposite we term *resolved recoil regime*(or good cavity limit). Under this assumption, a Taylor series expansion is justified and we obtain

$$J(p) - J(p - \hbar k) = \hbar k \frac{\partial}{\partial p} J(p) - \frac{\hbar^2 k^2}{2} \frac{\partial^2}{\partial p^2} J(p) + O(\hbar^3 k^3) \tag{5.63}$$

and

$$J(p) = \frac{a(p)}{\hbar k} f(p)(1 + f(p)) + \frac{1}{2} \frac{\partial}{\partial p}(af(1 + f)) + \frac{1}{2\hbar k} b(p) \frac{\partial f}{\partial p} + O(\hbar^2 k^2), \tag{5.64}$$

such that equation (5.62) becomes

$$\frac{\partial f}{\partial t} = \frac{\partial}{\partial p} \left(a(p) f(p)[1 + f(p)] + b(p) \frac{\partial f}{\partial p} \right) + O(\hbar^3 k^3). \tag{5.65}$$

The quantum dispersion relation may be easily shown to reduce to its classical counterpart in the said limit and hence, to order $O(\hbar^3 k^3)$, we indeed recover the classical equation provided we additionally require the occupancies to be small, $f(p) \ll 1$, and remember that $p = mv$ as well as the relation between the velocity distribution and the occupancies in the continuum limit $L/\lambda \to \infty$, namely

$$F(v) = \frac{mL}{2\pi\hbar N} f(p). \tag{5.66}$$

It is interesting to retain the bosonic correction factor $1+f(p)$ in the kinetic equation (5.65) and investigate, how the steady state solution (which is again unique) looks like. This corresponds to the situation that the momentum distribution is extended over many intervals of length $\hbar k$ but there are still sufficiently many particles to render the quantum statistical correction non-negligible. With the help of the q-deformed exponential defined in the previous chapter in (4.70), we find

$$f_{\mathrm{B}}(p) = \frac{1}{z^{-1} \exp_q \left(\frac{p^2}{2mk_{\mathrm{B}}T} \right) - 1}, \tag{5.67}$$

where, exactly as in the classical solution,

$$q = 1 + \frac{\omega_{\mathrm{R}}}{|\Delta_{\mathrm{c}}|} \tag{5.68}$$

and

$$k_{\mathrm{B}}T = \hbar \frac{\kappa^2 + \Delta_{\mathrm{c}}^2}{4|\Delta_{\mathrm{c}}|}. \tag{5.69}$$

The equilibrium solution (5.67) may be termed a q-deformed Bose distribution and generalizes the classical q-Gaussian found in the last chapter. The parameter z is

determined by the number of particles and can, due to the suggestive form of (5.67), be called the fugacity. The case of Fermions leads instead, in the aforementioned unresolved recoil regime, to a $q-$deformed Fermi-distribution

$$f_{\mathrm{F}}(p) = \frac{1}{z^{-1}\exp_q\left(\frac{p^2}{2mk_{\mathrm{B}}T}\right)+1}, \tag{5.70}$$

as could have been guessed. Needless to say, both (5.67) and (5.70) reduce to the ordinary Bose- and Fermi distributions for large detuning, i. e. if $|\Delta_{\mathrm{c}}| \gg \omega_{\mathrm{R}}$.

The normalization condition $\sum_n f(p_n) = N$ becomes, in the continuum limit,

$$\int_{-\infty}^{\infty} f(p)\mathrm{d}p = \frac{2\pi\hbar N}{L} \tag{5.71}$$

and is thus seen to involve the density N/L. This constitutes a major difference as compared to the classical case, where the actual density of the gas played no rôle, only the absolute number of particles. From (5.66) we can also learn, that the quantum statistical corrections featuring in (5.65) become noticeable only for sufficiently high densities, more precisely if

$$\frac{N\lambda}{L} \gtrsim 1, \tag{5.72}$$

that is, if there is more than a single particle per wavelength.

We have not performed a dynamical stability analysis of either (5.67) or (5.70), but it can be done making use of the semi-classical criterion given in (4.65), because, in the continuum limit, the quantum linear response function reduces to its classical form in the recoil unresolved regime. Such an endeavor, which would yield the generalized phase boundaries for both Bosons and Fermions, has to await some more opportune time.

5.8 Selfordered Phase

In the case of a non-vanishing averaged optical potential, that is in the case of a gas in the ordered phase, the eigenstates of (5.22) can, as mentioned before, be written down in terms of Bloch wave-functions

$$\varphi_n(x) = e^{iqx}u_{q,s}(x), \tag{5.73}$$

where q is the quasi-wavenumber, restricted to the first Brillouin zone, s denotes the so-called band index and $u_{s,q}(x)$ is a λ-periodic function. Like in the classical regime, the solution of the master equation becomes tractable only for a gas deep within the selfordered phase, i. e. for particles strongly trapped in the self-consistent

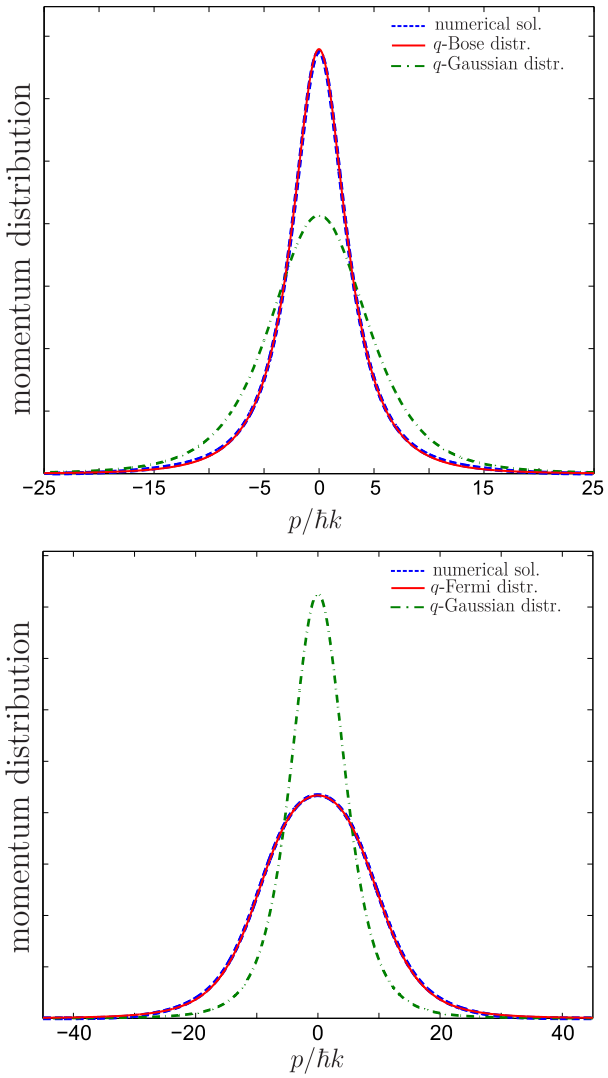

Figure 5.2 Examples of quantum equilibrium momentum distributions in the recoil unresolved regime and unordered phase for Bosons (upper plot) and Fermions (lower plot). The blue dotted curves depict the numerical solution of the master equation (5.62) and can hardly be distinguished from the theoretical predictions (5.67) and (5.70) (red curves). For the chosen $q = 1.4$ and 20 particles per wavelength there exists both a marked deviation from thermal equilibrium and from the semi-classical prediction (green dashed-dotted curve). The parameters are $N = 5000$, $\kappa = 6\omega_{\mathrm{R}}$ and $\Delta_{\mathrm{c}} = -2.5\omega_{\mathrm{R}}$ in both cases.

optical potential. In this regime, we can assume that the Bloch wave-functions are approximately given by

$$\varphi_n(x) \propto \frac{1}{\sqrt{n_L}} \sum_{x_j} e^{iqx_j} \psi_s(x - x_j), \tag{5.74}$$

where $n_L = L/\lambda$ denotes the number of potential wells and $x_j = x_0 + j\lambda = x_0 + R_j$ the position of the jth site. The wave-functions designated by $\psi_s(x)$ are taken to be the oscillator eigenfunctions, an approximation commonly referred to as tight-binding approximation. If we ignore the weak dependence of the transition matrix elements on the quasi wave number, we get, omitting terms proportional to $\delta_{q,q'}\delta_{s,s'}$ (because they drop from the master equation anyway)

$$|g_{nn'}|^2 = |\langle n|\sin(k\hat{x})|n'\rangle|^2 = \delta_{q,q'}T_{s,s'}, \tag{5.75}$$

where we have defined

$$T_{s,s'} := \left(\int_{-\infty}^{\infty}\psi_s(x)\frac{k^2x^2}{2}\psi_{s'}(x)\mathrm{d}x\right)^2. \tag{5.76}$$

This overlap integral is non-zero only if $s' = s + 2n$ for some integer number n and can, in fact be taken as coupling only $s, s-2$ and $s, s+2$, i. e. nearest levels with equal parity.

We will now show that the under these conditions stationary solution of the master equation is given by the thermal distribution. To this end, we first ignore the quantum Balescu-Lenard operator and look for the steady state without it. Introducing the inverse temperature β via

$$e^{-2\beta\hbar\omega_0} := \frac{\kappa^2 + (\Delta_c + 2\omega_0)^2}{\kappa^2 + (\Delta_c - 2\omega_0)^2}, \tag{5.77}$$

where ω_0 denotes the trap frequency defined in equation (4.90), the reduced steady-state master equation is equivalent to

$$f_{s+2}(q) - e^{-2\beta\hbar\omega_0}f_s(q) + (1 - e^{-2\beta\hbar\omega_0})f_s(q)f_{s+2}(q) = 0. \tag{5.78}$$

The solution to this equation is easily found to be the Bose-distribution for flat bands

$$f_s(q) = \frac{1}{e^{\beta(\hbar\omega_0 s - \mu)} - 1}. \tag{5.79}$$

On the other hand we know from (5.54), that the Balescu-Lenard term vanishes if the distribution is of the form $h_s(q, \tilde{\beta}) := [e^{\tilde{\beta}(E_s(q)-\mu)} - 1]^{-1}$, regardless of the value of $\tilde{\beta}$. Hence, in the limit of very deep potentials, where $E_s(q) \to \hbar\omega_0 s$ we have $f_s(q)/h_s(q,\beta) \to 1$ and thus (5.79) represents the equilibrium solution of the complete master equation as well. If the whole argument seems a little strange to the reader, let him consider that for strictly flat bands the cross section (5.41) becomes ill-defined and hence the above detour was necessary.

Therefore, as in the semi-classical theory, the equilibrium distribution for the strongly

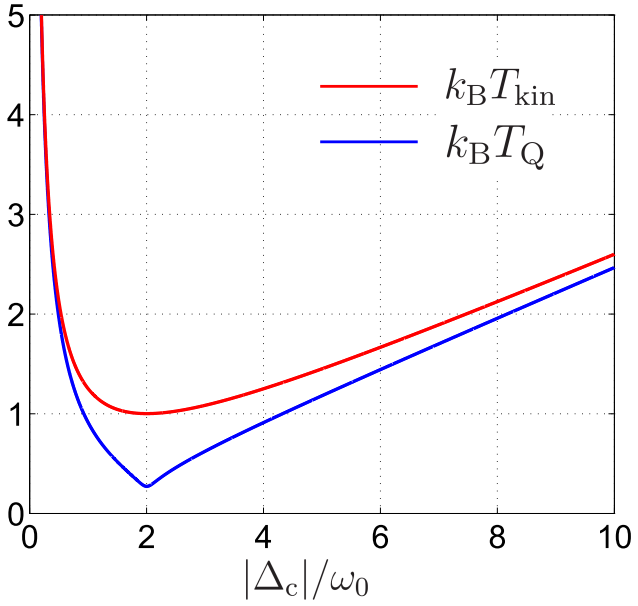

Figure 5.3 Thermal energy (in units of $\hbar\omega_0$) versus detuning in the selfordered phase according to classical- and quantum theory. The trap frequency was chosen to be $\omega_0 = 10\kappa$.

selforganized phase is thermal. However, quantum theory predicts a thermal energy β^{-1}, which is given by

$$k_{\mathrm{B}}T_{\mathrm{Q}} = 2\hbar\omega_0 \left[\ln\left(\frac{\kappa^2 + (\Delta_c - 2\omega_0)^2}{\kappa^2 + (\Delta_c + 2\omega_0)^2}\right)\right]^{-1} \neq k_{\mathrm{B}}T_{\mathrm{kin}}, \tag{5.80}$$

where $k_{\mathrm{B}}T_{\mathrm{kin}}$ is the classical result. This alone shows that the terms "temperature" and "thermal" should not be taken too seriously in the context of this open and dissipative system and bear their names only for reasons of similarity. Figure 5.3 depicts both the classical and the quantum thermal energies as functions of the detuning, assuming a fixed trap frequency.

A remark is in order. As the interaction couples only even states or odd states, we find that the equilibrium is actually given by a mixture of two thermal distributions for the odd and even states respectively, having the same temperature but possibly different chemical potentials.

Even though the classical temperature deviates from the quantum-mechanical temperature, it is important to recall that there exists no equipartition in the latter theory and hence the quantum energy is not equal to $k_{\mathrm{B}}T_{\mathrm{Q}}$. It is therefore interest-

ing to look at the equilibrium energy per particle

$$U_{\mathrm{Q}} := \frac{1}{N}\sum_{q,s}\hbar\omega_0\left(s+\frac{1}{2}\right)f_s(q) \tag{5.81}$$

for low densities and compare it to the classical value determined by

$$U_{\mathrm{C}} := 2\pi\int\omega_0 I f(I)\mathrm{d}I \tag{5.82}$$

with $f(I)$ given by (4.87). As remarked in the previous chapter, $U_{\mathrm{C}} = k_{\mathrm{B}}T_{\mathrm{kin}}$ due to equipartition. The result is shown in figure 5.4. Curiously, the classical prediction deviates from the corresponding quantum prediction most strongly for detunings, where the energy attains its minimum value in both cases, i. e. at $\Delta_{\mathrm{c}} = -2\omega_0$. The reason for the factor of two is that a photon must bridge an energy gap of $2\hbar\omega_0$, because only states thus far apart couple due to the parity- and overlap constraint. Contrary to the classical theory, quantum theory predicts (close to) ground state cooling.
This discrepancy is, at first sight, fairly disconcerting, because for deep potentials, where the harmonic approximation is valid, semi-classical- and quantum theories should, for low densities, be equivalent. The resolution of this conundrum lies in the degeneracy of the quantum-mechanical equilibrium pointed out above. Again, the number of particles occupying odd states N_{odd} and the number of particles occupying even states N_{even} are not fixed individually, only the total number of particles $N = N_{\mathrm{odd}} + N_{\mathrm{even}}$. In the above comparison, we have chosen them such that the chemical potentials of the two populations are equal. If, instead, we choose the equilibrium to be the one where $N_{\mathrm{odd}} = N_{\mathrm{even}} = N/2$, we find, for low densities, where Bose statistics can be replaced by Boltzmann statistics

$$U_{\mathrm{Q}} = \hbar\omega_0\frac{1+e^{-2\beta\hbar\omega_0}}{1-e^{-2\beta\hbar\omega_0}} = \hbar\frac{\kappa^2+\Delta_{\mathrm{c}}^2}{4|\Delta_{\mathrm{c}}|} + \hbar\frac{\omega_0^2}{|\Delta_{\mathrm{c}}|} = U_{\mathrm{C}}, \tag{5.83}$$

wherein we have made use of (5.77). Thus the discrepancy evaporates and we realize that the semi-classical kinetic theory singles out this particular case from among the infinitely many quantum equilibria. However, if there exist also direct interactions between the particles, we may plausibly expect an equalization of chemical potentials and thus ground state cooling as in figure 5.4.

5.9 Conclusions and Outlook

We have generalized the semi-classical kinetic theory of polarizable particles interacting with a mode of a high-Q resonator presented in the previous chapter to the fully quantum-mechanical regime. This has resulted in a very lucid interpretation of the cavity cooling effect and has revealed important corrections to the semi-classical predictions both for Bosons and Fermions, even though the discussion presented in

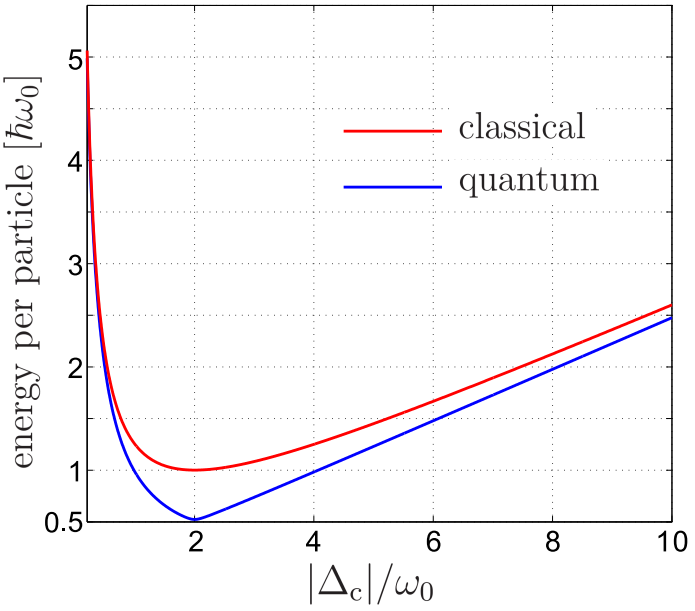

Figure 5.4 Energy per particle versus detuning in the selfordered phase according to classical and quantum theory (for Bosons) for a density of one particle every ten wavelengths. The classical curve approximates the quantum curve asymptotically but differs from it close to the minimal energy, attained at $\Delta_c = -2\omega_0$, where quantum theory predicts ground state cooling. The trap frequency was chosen to be $\omega_0 = 10\kappa$.

this chapter can by no means claim to be exhaustive. We have found that quantum kinetic theory agrees with its semi-classical counterpart in the appropriate limiting cases, thereby raising confidence in both theories.

If the computational cost of a numerical solution of the semi-classical SDEs is a hindrance to effectively study this many-body problem numerically, the situation is much worse for the corresponding quantum model. Indeed it seems fair to say that for a reasonable number of particles a direct numerical simulation is forever out of reach. Hence, the value of effective descriptions as the one developed in this chapter should be self-evident. In this respect we wish to point out that the way to arrive at a quantum kinetic theory chosen in this work is particularly suited to many-body systems with collective interactions and can easily be adapted to be applicable to other models of this type.

6 Cooperative Selfordering and Sympathetic Cooling of a Multispecies Gas in a Cavity

6.1 Introduction

Laser light induced forces are routinely used to manipulate polarizable particles from atoms and molecules [44] to larger objects such as nanoparticles, micro beads or even protozoae [45]. Laser trapping and cooling, however, is limited to a finite class of atomic species, very few kinds of molecules [46] or isolated vibration modes of nanomechanical objects [47]. Cooling requires specific setups with specifically chosen laser frequencies and configurations for any species, so that their number only slowly increases with time [48].

In principle, selforganization and cooling by coherent light-scattering in cavities gives a general alternative to trap and cool any kind of polarizable particles within an optical resonator [29, 30, 49]. In practice, however, the required phase-space densities and laser intensities have so far only been achieved for atomic ensembles [50, 51, 52], where theoretical expectations of fast sub-Doppler cooling were even surpassed [5], but the required phase-space density to achieve selfordering and trapping has not been reached for molecules or nanoparticles [30, 53].

As solution we propose to put ensembles of different species simultaneously into the same optical resonator. We predict that under suitable conditions all species are simultaneously trapped and cooled using only a single laser frequency and optical resonator. Our central claim is that the simultaneous presence of any additional species always increases the collective light scattering and improves trapping and cooling. As a particularly interesting case we study a mixture of a dense atomic ensemble with a smaller ensemble of heavier molecules or nanoparticles. Even when it is impossible to reach the selforganization threshold for the latter alone, combined trapping and sympathetic cooling can be readily achieved in cooperation with the atoms. Due to the nonlocal interaction the different particles might even be located at different regions within the cavity. This setup opens a novel possibility to simultaneous multispecies trapping and cooling without the need of a tailored laser configuration for each species. This can be improved further, using several cavity modes simultaneously [30].

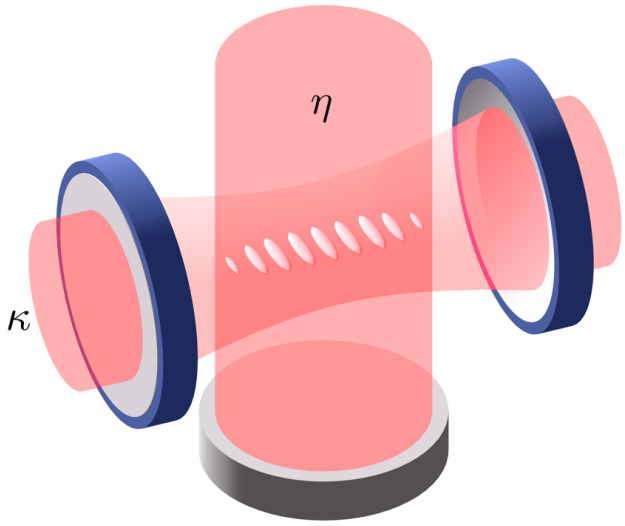

Figure 6.1 (Colour online) Ensembles of particles within a cavity illuminated transversely by a standing wave laser resonant with the cavity mode. Above threshold the particles order in regular tubes optimizing Bragg scattering into the mode.

6.2 Model

Consider a dilute gas consisting of S kinds of N_s polarizable point-particles of mass m_s within the overlap region of a high-Q optical resonator mode and a standing-wave pump laser tuned close to resonance with a cavity mode (figure 1). In this chapter we return to a semi-classical description. According to this view, the particles scatter light into and out of the cavity mode and the resulting interference pattern creates dynamical optical potentials guiding the particle motion. For simplicity we approximate pump and cavity field in the interaction region by plane standing waves and consider motion along the cavity axis only. This suffices to describe the essential physics of selforganization and cooling [28, 50, 31]. A practical experimental implementation can be envisaged by confining the particles by two crossed standing-wave pump lasers into a lattice of 1D tubes along the cavity axis [54, 49]. Extension to 3D motion and field geometries are straightforward and are expected to induce only minor quantitative changes [31]. The model used in this chapter is, of course, a straight-forward extension of the one used in chapter 4. In terms of the effective pump amplitudes η_s, the light shifts per photon $U_{0,s}$, and the semi-classical cavity mode amplitude a, the optical potentials along the cavity axis are given by [28]

$$\Phi_s(x, a, a^*) = \hbar\eta_s\,(a + a^*)\sin(kx) + \hbar U_{0,s}|a|^2\sin^2(kx), \tag{6.1}$$

which lead to the one-body Hamiltonian functions $h_s(x, p, a, a^*) = \frac{p^2}{2m_s} + \Phi_s(x, a, a^*)$, determining the dynamics of an individual particle belonging to the sth species through the canonical equations of motion [13]. h_s depends parametrically on the

cavity field amplitude a, which in turn is driven by the light scattered collectively by all the particles and by white noise ξ, modeling vacuum fluctuations. As detailed in refs. [7, 16], for a statistical treatment of the dynamics it is convenient to redefine the state of the particles of the sth species $\{x_{j_s}(t), p_{j_s}(t)\}$ in terms of the Klimontovich distribution [55]

$$f_{\mathrm{K}}^{s}(x,p,t) := \frac{1}{N_s}\sum_{j_s=1}^{N_s}\delta(x-x_{j_s}(t))\delta(p-p_{j_s}(t)). \tag{6.2}$$

Then the mode amplitude evolves according to

$$\dot{a} = (i\Delta_{\mathrm{c}} - \kappa)a - \frac{i}{\hbar}\sum_{s=1}^{S} N_s \int \frac{\partial h_s}{\partial a^*}\, f_{\mathrm{K}}^{s}(x,p,t)\,\mathrm{d}x\mathrm{d}p + \sqrt{\kappa}\;\xi, \tag{6.3}$$

where κ denotes the cavity decay rate and $\Delta_{\mathrm{c}} = \omega_{\mathrm{p}} - \omega_{\mathrm{c}}$ the detuning between pump- and cavity frequency. We decompose the Klimontovich distribution according to $f_{\mathrm{K}}^{s}(x,p,t) = f_s(x,p,t) + \delta f_s(x,p,t)$, where $f_s(x,p,t) := \langle f_{\mathrm{K}}^{s}(x,p,t)\rangle$, averaged over an ensemble of suitable initial conditions and the realizations of the white noise, is called one-body distribution function. Note that $f_s(x,p,t)\mathrm{d}x\mathrm{d}p$ is equal to the expected fraction of particles of the sth species in a phase space volume $\mathrm{d}x\mathrm{d}p$ around the point (x,p) at time t and the average over its fluctuations vanishes, $\langle \delta f_s(x,p,t)\rangle \equiv 0$. Likewise we decompose the mode amplitude into $a = \alpha + \delta a$, where $\alpha = \langle a\rangle$. The one-body distribution functions exactly satisfy

$$\frac{\partial f_s}{\partial t} + \frac{p}{m_s}\frac{\partial f_s}{\partial x} - \frac{\partial \langle \Phi_s\rangle}{\partial x}\frac{\partial f_s}{\partial p} = \left\langle \frac{\partial \delta\Phi_s}{\partial x}\frac{\partial \delta f_s}{\partial p}\right\rangle, \tag{6.4}$$

in which predominantly the r.h.s. describes statistical correlations. For $N_s \to \infty$ these tend to zero and we recover the Vlasov (or mean-field) kinetic theory. There, $\langle \Phi_s(x,a,a^*)\rangle$ is replaced by $\Phi_s(x,\alpha,\alpha^*)$ and the r.h.s. of (6.4) is set to zero, such that spatially homogeneous particle distributions scatter no light into the mode and constitute an equilibrium state at zero cavity field [16], exactly as in chapter 4.

6.3 Multispecies Selforganization Threshold

Following [16], the multispecies selforganization threshold is obtained as the boundary of dynamical stability of spatially uniform distributions in case of negative effective detuning $\delta := \Delta_{\mathrm{c}} - \frac{1}{2}\sum_s N_s U_{0,s} < 0$, by an analysis of the linearized Vlasov equation [56]. For convenience we rescale the uniform equilibrium distributions as $f_{0,s}(p) = (Lm_s v_s)^{-1} G_s(\frac{p}{m_s v_s})$ in terms of a typical velocity v_s and the cavity length L. Assuming a strictly monotonous decrease in $|p|$, as fulfilled by all relevant distributions (e.g. Gaussian, Bose-Einstein, q-Gaussian, etc.), a given set of spatially homogeneous distributions is unstable if and only if

$$\sum_{s=1}^{S}\frac{N_s\eta_s^2}{k_{\mathrm{B}}T_s}\left(\mathrm{P}\int_{-\infty}^{\infty}\frac{-1}{2u}\frac{\mathrm{d}G_s}{\mathrm{d}u}\mathrm{d}u\right) > \frac{\kappa^2+\delta^2}{\hbar|\delta|}, \tag{6.5}$$

with $k_{\mathrm{B}}T_s = m_s v_s^2/2$ and P the Cauchy principal value. For thermal (i.e. Gaussian) momentum distributions the integral in (6.5) is unity and the threshold condition assumes the simple form

$$\sum_{s=1}^{S} \frac{N_s \eta_s^2}{k_{\mathrm{B}} T_s} > \frac{\kappa^2 + \delta^2}{\hbar |\delta|}. \tag{6.6}$$

This threshold formula is one of the central results of the present work. Above threshold, density perturbations and the electric field amplitude grow exponentially and evolve, if the light shift is not too large, towards an ordered quasi-stationary state (figure 6.2) with growth exponent $\gamma > 0$ fulfilling

$$(\gamma + \kappa)^2 + \delta^2 = \sum_{s=1}^{S} \frac{N_s \eta_s^2 \hbar \delta}{2 k_{\mathrm{B}} T_s} \int_{-\infty}^{\infty} \frac{u \, \mathrm{d}G_s/\mathrm{d}u}{(\gamma/k v_s)^2 + u^2} \mathrm{d}u. \tag{6.7}$$

Note that, while the r.h.s. of equations (6.5) and (6.6) only depends on cavity parameters, all terms in the sum on the l.h.s. are manifestly positive and proportional to the pump intensity. This has the important consequence that inserting any extra particle species into the cavity will lower the power needed to start the selforganization process, regardless of temperature or polarizability of the added particles. Note that we neglect absorbtion of the pump beam, consistent with our assumption of a dilute and optically thin gas. At higher temperatures, where $(kv_s)^2 \gg \kappa^2 + \delta^2$, the field amplitude's growth rate is, from (6.7), given by

$$\gamma = -\kappa + \left(\sum_{s=1}^{S} \frac{\hbar |\delta|}{k_{\mathrm{B}} T_s} N_s \eta_s^2 - \delta^2 \right)^{1/2}. \tag{6.8}$$

We thus find strong sympathetic enhancement, i.e. the field grows faster the more species contribute such that the required power and time needed for selforganization is lowered by combining several species.

6.4 Long-Term Dynamics and Equilibrium

For a large but finite number of particles, the Vlasov kinetic theory, which neglects all dynamical correlations, provides an accurate description on a time scale essentially fixed by the solution of equation (6.7). The long-term evolution of the system and in particular its statistical equilibrium state are, on the other hand, governed by precisely these correlations [7] as shown in the previous two chapters for the case of a single species. In this section we shall deal with this stage of the time evolution in the limit of weak coupling, i.e.

$$\sum N_s |U_{0,s}| \ll |\Delta_{\mathrm{c}}|, \tag{6.9}$$

where we can neglect the terms $\hbar U_{0,s} |\alpha|^2 \sin^2(kx)$ in the averaged optical potentials (6.1), rendering them linear functions of the mode amplitude.

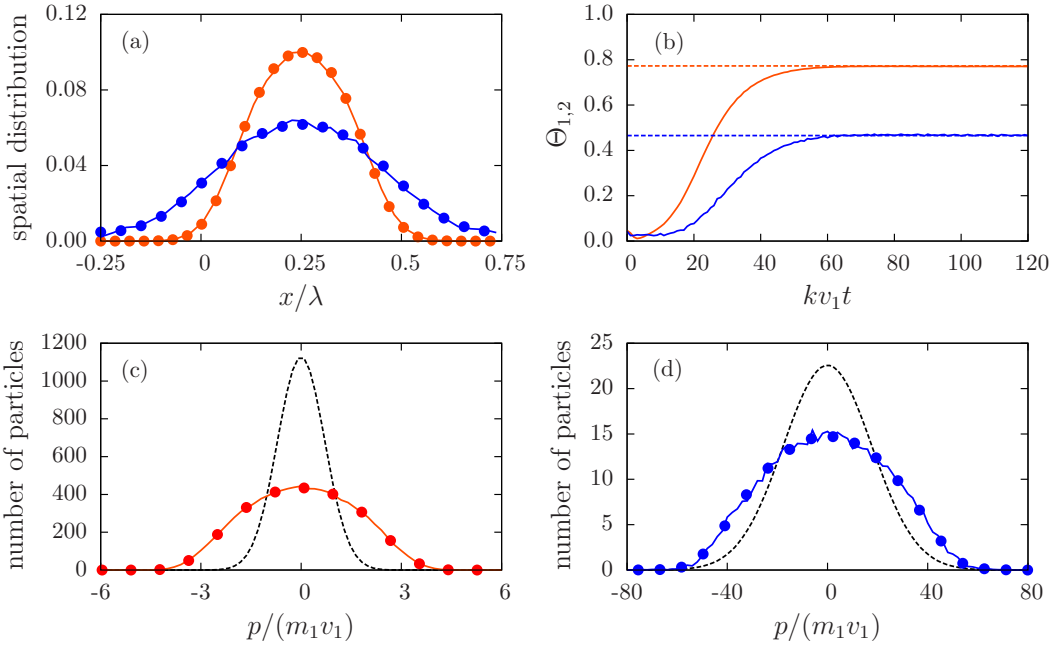

Figure 6.2 Concurrent selforganization of two species, initialized above the combined threshold. Species one (orange) is initialized well above, species two (blue) far below its proper threshold. (a) Final position distributions (periodic boundary conditions). (c,d) Initial (dashed) and selforganized (solid) momentum distributions obtained from numerical stochastic particle simulations (SDEs) [7]. Circles: theoretical predictions obtained from Vlasov kinetic theory assuming the adiabatic invariance of the action variables (6.13) as in [57]. (b) Growth of the order parameters $\Theta_s = |\int f_s \sin(kx)\mathrm{d}x\mathrm{d}p|$ to predicted values. Parameters: $N_1 = 10^4$, $N_2 = 500$, $m_2 = 10m_1$, $k_\mathrm{B}T_1 = 10^4\hbar\kappa$, $k_\mathrm{B}T_2 = 2.5 \times 10^5\hbar\kappa$, $\eta_1 = 2.4\kappa$, $\eta_2 = 27.4\kappa$ and recoil frequency $\omega_{\mathrm{R},1} = 10^{-2}\kappa$.

This is seen as follows: The mode amplitude α can, from its equation of motion be estimated as

$$\alpha \sim \frac{i\sum_s N_s\eta_s}{-\kappa + i\delta}. \tag{6.10}$$

with the help of this estimate we find for the potential

$$\langle \Phi_s \rangle \sim \frac{\hbar\eta_s \sum_r N_r\eta_r}{\kappa^2+\delta^2}\left(2\delta\sin(kx) + U_0^s\sum_r N_r\frac{\eta_r}{\eta_s}\sin^2(kx)\right). \tag{6.11}$$

If we use that

$$\frac{\eta_r}{\eta_s} = \frac{|U_0^r|}{|U_0^s|}, \tag{6.12}$$

we see that the second term in the brackets is much smaller than the first if $1/2\sum_r N_r|U_0^r| \ll |\delta|$, which yields (6.9). Using the same estimate for α, we see that $|\alpha||U_0^s| \ll \eta_s$ if $\sum_r N_r|U_0^r| \ll \sqrt{\kappa^2+\delta^2}$, which is also satisfied if (6.9) is.

As in the case of a single species we perform, for each species separately, a canonical transformation of variables $(x,p) \to (I_s, \theta_s)$. Here, I_s denotes the one-body action based on the ensemble-averaged Hamiltonian function, which satisfies $H_s(x,p,\alpha,\alpha^*) := \langle h_s(x,p,a,a^*)\rangle \equiv h_s(x,p,\alpha,\alpha^*)$ in the weak coupling limit.

$$I_s = \pm\frac{1}{2\pi}\oint\sqrt{2m_s\left[H_s - \langle\Phi_s(x')\rangle\right]}\,\mathrm{d}x' \tag{6.13}$$

and θ_s its canonically conjugate angle variable

$$\theta_s = \frac{\partial S_s}{\partial I_s}, \tag{6.14}$$

obtained from the generating function $S_s = \pm\int^x\sqrt{2m_s\left[H_s - \langle\Phi_s(x')\rangle\right]}\,\mathrm{d}x'$. The reason, to repeat what has been said in previous chapters, for doing this is that at the end of the initial, mean-field governed dynamics, the one-particle distributions depend on (x,p) solely through the ensemble-averaged one-body Hamiltonian functions and thus on the actions alone. This assumption is strongly supported by numerical results, see for example figure 6.2. From that point onwards, they are slowly modified by the dynamical correlations in such a way that the system evolves towards statistical equilibrium in a sequence of mean-field steady states [40]

$$f_s(x,p,t) \simeq f_s(I_s,t). \tag{6.15}$$

A straight-forward generalization of (4.55) and in particular (4.83a) of chapter 4, yields the set of *coupled* nonlinear Fokker-Planck equations describing the system's long-term evolution as

$$\frac{\partial f_s}{\partial t} = \frac{\partial}{\partial I_s}\Big(A_s f_s + B_s\frac{\partial f_s}{\partial I_s} + \sum_{r=1}^{S} C[f_s, f_r]\Big) \tag{6.16}$$

The slow evolution of the ensemble-averaged mode amplitude is again taken into account by the implicit equation

$$\alpha = \frac{2\pi}{\Delta_\mathrm{c} + i\kappa} \sum_{s=1}^{S} N_s \eta_s \int f_s(I_s)\, g_{0,s}(I_s, \alpha)\, \mathrm{d}I_s, \tag{6.17}$$

wherein

$$g_{n,s}(I_s, \alpha) := \frac{1}{2\pi} \int_0^{2\pi} \sin(kx)\, e^{-in\theta_s}\, \mathrm{d}\theta_s. \tag{6.18}$$

The r.h.s. of equation (6.16), describing the redistribution of particles among the orbits, consists of drift and diffusion terms originating from fluctuations and decay of the mode amplitude

$$A_s[f_s] = -4\hbar\Delta_\mathrm{c}\kappa\omega_s \sum_{n=-\infty}^{\infty} \frac{n^2\eta_s^2 |g_{n,s}|^2}{|D(in\omega_s)|^2} \tag{6.19}$$

$$B_s[f_s] = \hbar^2\kappa \sum_{n=-\infty}^{\infty} \frac{n^2\eta_s^2 |g_{n,s}|^2}{|D(in\omega_s)|^2} \left(\kappa^2 + \Delta_\mathrm{c}^2 + n^2\omega_s^2\right) \tag{6.20}$$

and a generalized Balescu-Lenard operator [41, 42, 39]

$$C[f_s, f_r] = \sum_{n,m=-\infty}^{\infty} \int w_{nm}(I_s, I_r') \Big(n \frac{\partial f_s}{\partial I_s} f_r' - m \frac{\partial f_r}{\partial I_r'} f_s \Big) \mathrm{d}I_r', \tag{6.21}$$

where the cross section is given by

$$w_{nm}(I_s, I_r') := 8\pi^2\hbar^2\Delta_\mathrm{c}^2 N_r \, \frac{\eta_s^2 |g_{n,s}|^2 \eta_r^2 |g_{m,r}'|^2}{|D(in\omega_s)||D(im\omega_r')|} \, n\, \delta\left(n\omega_s - m\omega_r'\right). \tag{6.22}$$

Here, $\omega_s(I_s) = \partial H_s / \partial I_s$ is the nonlinear orbital frequency and a prime denotes the function at $I_r = I_r'$. For spatially uniform ensembles $I_s \to p/k$ and the expressions for A_s and B_s given in [7] are recovered. The linear response function $D(i\omega)$ is given by

$$D(i\omega) = (i\omega + \kappa)^2 + \Delta_\mathrm{c}^2 - 4\pi\hbar\Delta_\mathrm{c} \sum_{s=1}^{S} \sum_{n=-\infty}^{\infty} N_s \eta_s^2 \int \frac{\partial f_s}{\partial I_s} \frac{n |g_{n,s}|^2}{\omega + n\omega_s - i0}\, \mathrm{d}I_s\,. \tag{6.23}$$

and characterizes the system's collective response. We do not deny that all the above is just a simple extension of what has been derived in chapter 4. Nevertheless, the present situation of multiple species does give rise to interesting consequences going beyond the previously treated case. Let us recall that the particle distribution functions $f_s(I_s, t)$ always have to be strongly Vlasov stable in order for (6.16) to be valid. This assumption breaks down close to the selforganization threshold and thus (6.16) is valid only away from the transition point.

As we have pointed out above, the evolution equations for the different species are

coupled. This coupling is two-fold. First, through the value of the mode amplitude α and the linear response function, both of which are determined jointly by the states of all the species. Secondly, through the interaction contained in the Balescu-Lenard operators (6.21), which quantify the energy and momentum exchange between particles of like and different species and involve resonant orbits I_r, I_s with $n\omega_r = m\omega_s$. In chapter 5 we have baptized the process giving rise to these terms *resonant pair-scattering*. It is, in effect, akin to a pair-collision albeit entirely nonlocal. The appearance of the linear response function function also reveals that the remaining particles participate collectively as a medium in that process. These quasi-collisions can be used for efficient sympathetic cooling as demonstrated below. The source of the remaining terms in (6.16) involves only single scattering events and subsequent loss through the cavity mirrors. It is worth remarking that the quasi-collision operator (6.21) vanishes for thermal distributions with equal temperatures, and thus the quasi-collisions can be expected to favor the establishment of global thermal equilibrium.

As for a single species, stable equilibria of (6.16) exist only for $\Delta_\mathrm{c} < 0$. Below threshold, that is in the unordered phase, they are homogeneous with vanishing field and, independent of the number of species, q-Gaussian momentum distributions:

$$f_{s,\mathrm{eq}}(p) \propto \exp_{q_s}\Big(\frac{-p^2}{2m_s k_\mathrm{B} T}\Big), \tag{6.24}$$

where

$$k_\mathrm{B} T := \hbar\,\frac{\kappa^2 + \Delta_\mathrm{c}^2}{4|\Delta_\mathrm{c}|} \tag{6.25}$$

and

$$\exp_q(u) = \Big[1 + (1-q)u\Big]^{\frac{1}{1-q}} \tag{6.26}$$

is the q-exponential with parameter $q_s = 1 + \omega_{\mathrm{R},s}/|\Delta_\mathrm{c}|$. For $q_s \to 1$ the distribution becomes an ordinary Gaussian. The recoil frequencies are given by $\omega_{\mathrm{R},s} := \hbar k^2/2m_s$ and $k_\mathrm{B} T$ denotes a "thermal" energy with a minimum of $\hbar\kappa/2$ for $\Delta_\mathrm{c} = -\kappa$.

This is seen as follows: First note that due to the coupling of the individual Fokker-Planck equations the determination of the joint equilibrium is not as trivial as for a single species. However, using the artifice of the following "free energy" functional

$$\mathcal{F} := \sum_s N_s \left(\int_{-\infty}^{\infty} U_s\, F_s\, \mathrm{d}v + \int_{-\infty}^{\infty} F_s\, \ln(F_s)\, \mathrm{d}v\right) = \sum_s N_s \mathcal{F}_s \tag{6.27}$$

where $F_s(v)$ denotes the velocity distribution of the s-th species and

$$U_s(v) := \int^v \frac{A_s(v')}{B_s(v')}\mathrm{d}v' \sim \ln\left(\kappa^2 + \Delta_\mathrm{c}^2 + k^2 v^2\right), \tag{6.28}$$

the equations of motion (6.16) in case of a vanishing mode amplitude $\alpha = 0$ can be cast into the form

$$\frac{\partial F_s}{\partial t} = \sum_s \frac{\partial}{\partial v} \frac{1}{|D|^2} \left[B_s F_s \frac{\partial}{\partial v} \left(\frac{\delta \mathcal{F}_s}{\delta F_s} \right) + \sum_r c_{sr} \left(\frac{F_r}{m_s} \frac{\partial F_s}{\partial v} - \frac{F_s}{m_r} \frac{\partial F_r}{\partial v} \right) \right], \tag{6.29}$$

where $c_{sr} := \lambda \hbar \omega_{\mathrm{R}s} \Delta_{\mathrm{c}}^2 N_r \eta_r^2 \eta_s^2$. Making use of the simple identities

$$\frac{1}{m_r} \frac{A_r}{B_r} = \frac{1}{m_s} \frac{A_s}{B_s} \tag{6.30}$$

and

$$N_s c_{sr} \frac{A_s}{B_s} = N_r c_{rs} \frac{A_r}{B_r}, \tag{6.31}$$

we find

$$\begin{aligned}
\frac{d\mathcal{F}}{dt} &= \sum_s N_s \int_{-\infty}^{\infty} \frac{\delta \mathcal{F}_s}{\delta F_s} \frac{\partial F_s}{\partial t} \mathrm{d}v \\
&= \sum_s \int_{-\infty}^{\infty} \frac{\delta \mathcal{F}_s}{\delta F_s} \frac{\partial}{\partial v} \frac{N_s}{|D|^2} \left[B_s F_s \frac{\partial}{\partial v} \left(\frac{\delta \mathcal{F}_s}{\delta F_s} \right) + \sum_r c_{sr} \left(\frac{F_r}{m_s} \frac{\partial F_s}{\partial v} - \frac{F_s}{m_r} \frac{\partial F_r}{\partial v} \right) \right] \mathrm{d}v \\
&= -\sum_s \int_{-\infty}^{\infty} \frac{N_s}{|D|^2} \Big[B_s F_s \left(\frac{\partial}{\partial v} \frac{\delta \mathcal{F}_s}{\delta F_s} \right)^2 + \\
&\qquad + \sum_r \frac{m_s c_{sr}}{2} \frac{1}{F_s F_r} \left(\frac{F_s}{m_r} \frac{\partial F_r}{\partial v} - \frac{F_r}{m_s} \frac{\partial F_s}{\partial v} \right)^2 \Big] \mathrm{d}v \\
&\leq 0.
\end{aligned} \tag{6.32}$$

The derivative vanishes only if for all species s, r there holds $\frac{\partial}{\partial v} \frac{\delta \mathcal{F}_s}{\delta F_s} = \partial_v U_s + F_s^{-1} \partial_v F_s = 0$ and simultaneously also $\frac{F_s}{m_r} \frac{\partial F_r}{\partial v} - \frac{F_r}{m_s} \frac{\partial F_s}{\partial v} = 0$. These two conditions fix the unique steady state and they are equivalent to

$$A_s F_s + B_s \frac{\partial F_s}{\partial v} = 0, \tag{6.33a}$$

$$\frac{F_s}{m_r} \frac{\partial F_r}{\partial v} - \frac{F_r}{m_s} \frac{\partial F_s}{\partial v} = 0. \tag{6.33b}$$

It is not immediately evident that these conditions are mutually compatible. However, solving the first equation (6.33a) we find $F_s = e^{-U_s}$ and substituting this solution into the second equation (6.33b), we find that it is indeed satisfied using again the equality (6.30).

Hence, the reason for the fact that in the unordered phase the equilibrium state of a given species is unaffected by the presence of others is the vanishing of resonant interspecies scattering $C[f_{s,\mathrm{eq}}, f_{r,\mathrm{eq}}] \equiv 0$.

Sufficiently deep within the ordered phase, the equilibrium distributions are, once more, well approximated by Maxwell-Boltzmann distributions

$$f_{s,\mathrm{eq}}(x,p) \propto \exp\Big(\frac{-H_s}{k_\mathrm{B}T^s_\mathrm{kin}}\Big), \tag{6.34}$$

with kinetic temperatures

$$k_\mathrm{B}T^s_\mathrm{kin} := \frac{\langle p^2\rangle}{m_s} = k_\mathrm{B}T + \frac{\hbar\omega^2_{0,s}}{|\Delta_\mathrm{c}|} \tag{6.35}$$

and trap frequencies $\omega^2_{0,s} = 4\eta_s\omega_{\mathrm{R},s}|\mathrm{Re}\,\alpha|$ proportional to the cavity field generated commonly by all species. Therefore, unlike below threshold, the equilibrium of a given species is by this fact affected by the presence of the others. However, as in the unordered phase, interactions due to resonant pair-scattering do not affect the equilibrium of a given species. The reason for this somewhat disappointing circumstance is as follows. If the kinetic temperatures (6.35) of two given species are very different, this implies that the trap frequencies experienced by these two species are also very different and there can be no resonant pair-scattering between the two, precisely because of the *lack of resonance* in this case. In the reverse case of similar trap frequencies on the other hand, the effect of pair-scattering on the distributions (6.34) can be shown to be negligibly small and vanishes identically for exactly equal trap frequencies as remarked before.
Figure 6.3 shows the formation and properties of a two-species selforganized steady state. The initial increase of the kinetic energy originates from the fast growth of the cavity intensity due to instability and is followed by cooling in the trapped state.

6.5 Sympathetic Cooling

Hence, as we have seen above, resonant pair-scattering between particles of different species has no effect on their steady states. This implies that from an observation of the equilibrium alone the existence of this process cannot be inferred. The approach to equilibrium, however, is indeed influenced by that very process, i. e. the energy exchange between different sorts of particles via resonant pair-scattering can in fact reduce the cooling time for any species in the presence of another via sympathetic cooling. At this point it is necessary to clarify the notion of *cooling*. The lessons learned in the previous chapters lead us to associate with cooling a reduction of the extension of the sth species in one-body phase space. As the quantity $\langle J_s\rangle := \int J_s f_s(I_s)\mathrm{d}I_s$, with $J_s = I_s$ for transient and $J_s = I_s/2$ for trapped orbits, provides a measure of this extension, cooling therefore corresponds to a decrease of $\langle J_s\rangle$.[1]

[1] Recall from chapter 5 that also the Bohr-Sommerfeld correspondence principle between integer multiples of $\hbar$ of the action variable and quantum mechanical energy eigenstates suggests this definition.

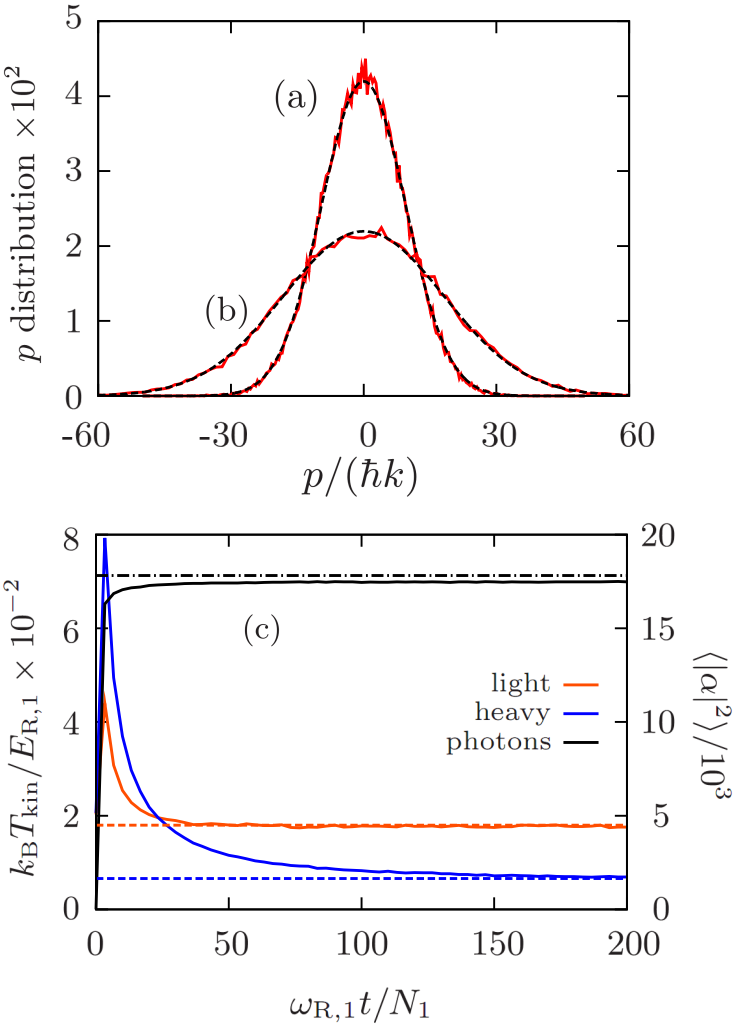

Figure 6.3 Selforganized steady-state momentum distributions of (a) species one and (b) species two with $m_2 = 10m_1$. (c) Kinetic temperatures and the photon number. Dashed lines: theoretical predictions. Dash-dotted line: maximally possible photon number. Parameters: $N_1 = 300$, $N_2 = 200$, $\sqrt{N_1}\eta_1 = \sqrt{N_2}\eta_2 = 600\omega_{R,1}$, $\kappa = 100\omega_{R,1}$, $\delta = -\kappa$ and $E_{R,1} = \hbar\omega_{R,1}$.

The case of interest here consists of a system of two species, a first one (species 1) acting as a coolant for a second species (species 2). Numerical simulations exhibit an invariance (as in figure 6.2) or even an increase of the occupied phase space volumes during selforganization triggered by an initial instability (i. e. if the system starts above threshold (6.5)) and there is only a small energy exchange between deeply trapped ensembles, if the resonance condition $\omega_{0,1} \sim \omega_{0,2}$ is not satisfied.

However, sympathetic cooling can be achieved by initializing the system below the joint threshold, such that resonant interspecies scattering can remove kinetic energy from the second species, which is then dumped by the first species by ordinary cavity cooling. The condition for this to happen efficiently is, by (6.22), that the two species possess not too dissimilar thermal velocities, i. e.

$$\frac{k_\mathrm{B} T_1}{m_1} \sim \frac{k_\mathrm{B} T_2}{m_2}. \tag{6.36}$$

Particles of a *heavier* species 2 at a *higher* temperature will therefore be able to resonantly scatter with those of a *lighter* species 1 at a *lower* temperature, which is quite fortunate, given that ordinary cavity cooling efficiency deteriorates with increasing mass.

Indeed, the energy flow per particle from species two to species one (the coolant), $\dot{Q}_{21}$, for two spatially homogeneous ensembles can, from equation (6.21), be estimated as

$$\dot{Q}_{21} \simeq \frac{2 N_1 \eta_2^2 \eta_1^2 \hbar \Delta_\mathrm{c}^2}{(\kappa^2 + \Delta_\mathrm{c}^2)^2} \sqrt{\frac{m_1}{m_2}} \sqrt{\frac{\pi \hbar \omega_{\mathrm{R},2}}{k_\mathrm{B} T_1}} \left[1 - \frac{T_2}{T_1}\right] \left[1 + \frac{m_1 T_2}{m_2 T_1}\right]^{-\frac{3}{2}}, \tag{6.37}$$

if we assume that the first species is already cold, i.e. $2 k_\mathrm{B} T_1 / \hbar\kappa \ll \kappa / \omega_{\mathrm{R},1}$, and the joint system is far from instability. Energy evidently flows from the warmer to the colder species at a rate which is maximal for a detuning $\Delta_\mathrm{c} = -\kappa$.

The process of sympathetic cooling continues until the point of joint selforganization is reached and the lighter particles are trapped. At this point, interspecies scattering is expected to cease because of the absence of mutually resonant particles. From here on, the lighter particles provide a continuously deepening potential for the the heavy species, which subsequently gets trapped as well.

This process is shown in figure 6.4 and provides a very satisfactory confirmation of the above scenario and hence the *existence* of resonant pair-scattering. Figure 6.5 depicts the result of a numerical simulation of the extreme case of a single, very heavy particle resonantly cooled by an ensemble of lightweight and cold particles.

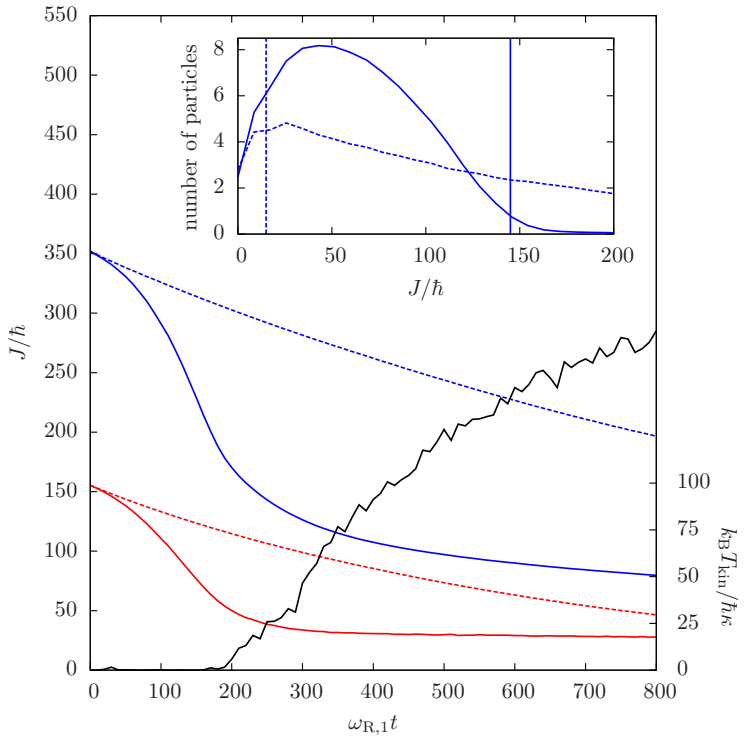

Figure 6.4 Time evolution of the kinetic energy per particle (lower red pair of curves) and phase space volume $\langle J \rangle$ (upper blue pair) of a heavy species alone (dashed lines) and in the presence of a lighter species (solid lines). The rising solid curve depicts the intracavity intensity (a.u.) for sympathetic cooling. The threshold and enhanced cooling due to resonant pair-scattering with particles of the second species is clearly visible. The inset depicts the distribution of the heavy particles at final time. The vertical lines are the action values separating trapped from untrapped particle orbits. In the case of the presence of the second species, almost all particles are finally trapped, whereas in the other case, almost no particle is trapped. Parameters: $N_1 = 1500$, $N_2 = 100$, $m_2 = 80m_1$, $\sqrt{N_1}\eta_1 = 400\omega_{\mathrm{R},1}$, $\sqrt{N_2}\eta_2 = 245\omega_{\mathrm{R},1}$, $\kappa = 100\omega_{\mathrm{R},1}$ and $\Delta_{\mathrm{c}} = -\kappa$.

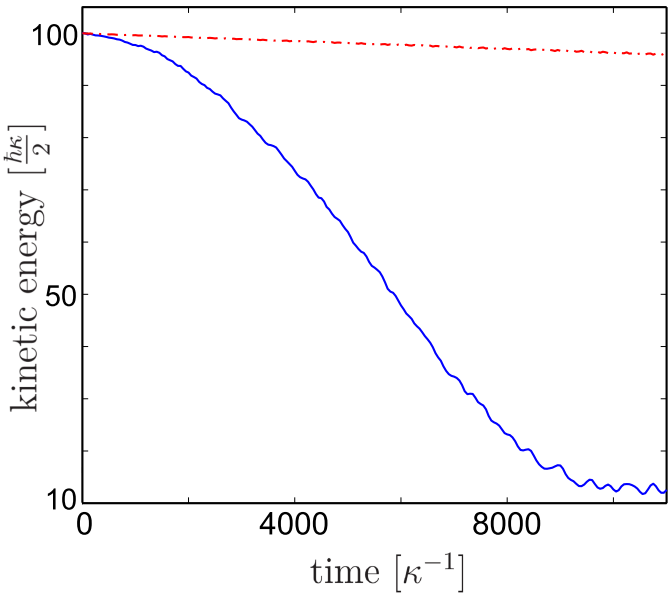

Figure 6.5 Cooling of a single heavy particle of mass $m_2 = 2000m_1$ (blue curve) by a small ensemble of one hundred lightweight and cold ($k_\mathrm{B}T^1_\mathrm{kin} \sim 5\hbar\kappa/2$) particles of mass m_1 without direct interactions. The red dashed-dotted curve shows the reduction of kinetic energy of the single heavy particle in the absence of the coolant species, i. e. ordinary cavity cooling, which is rather inefficient for the chosen parameters. The strongly enhanced cooling rate serves as an excellent proof for the reality of resonant pair-scattering. The flattening of the curve coincides with the onset of selforganization of the coolant species and the capturing of the heavy particle. The plot shows an average over 100 realizations yet without vacuum noise. Parameters: $N_1 = 100$, $N_2 = 1$, $\eta_2 = 5\eta_1 \approx 0.87\kappa$, $\kappa = 100\omega_{\mathrm{R},1}$ and $\Delta_\mathrm{c} = -\kappa$.

6.6 Conclusions

In summary we have shown that if the selforganization threshold can be reached with a certain species, any species can be added and will be trapped and cooled as well. The final temperatures are only limited by the resonator linewidth and, importantly, the cooling time of a given species can be reduced by means of resonant energy exchange with a second, already colder and lighter species. Because the general cooling and selforganization effects have successfully been demonstrated in single-species experiments [5, 10, 15], we are confident that the multispecies generalization proposed here is well within reach of current technology. New phases can also be expected in the case of a crystallization of a multispecies quantum gas close to absolute zero [58]. We expect that simultaneous additional cooling of one species will help to cool all others under the right conditions.

7 Light-Induced Crystallization of Cold Atoms in a 1D Optical Trap

7.1 Introduction

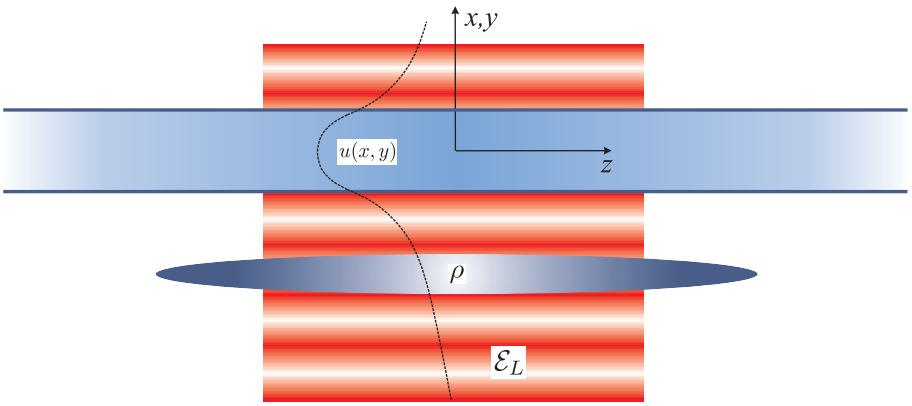

Figure 7.1 Cigar-shaped atomic gas alongside optical nanoguide

The astonishing experimental accomplishments in the optical control and manipulation of cold atomic gases in the past decade now allow to deterministically load them in precisely controlled optical traps of almost any shape down to effectively zero temperature. A particular fruitful example are periodic optical lattices in which many intriguing phenomena of solid state physics can be studied with unprecedented isolation and control[1].

In contrast to conventional solids, however, the spatial order and lattice geometry is fixed by the external lasers and does not appear from a self consistent atom-field dynamics, as the back-action of the atoms onto the confining light fields is generally negligible[59, 60]. Local lattice perturbations do not propagate and mediate long range interactions as phonons do in solids. This changes for spatially tightly confined fields as in small optical resonators or optical micro-structures[61], but experimentally it is very challenging to implement and load microtraps close to optical microstructures where atom field coupling is sufficiently enhanced[62, 63, 64].

In an important step Rauschenbeutel and coworkers, however, recently managed to trap atoms in an array of optical dipole traps generated by two color evanescent

light fields alongside a tapered optical fiber[65], where the backaction of even a single atom on the propagating fiber field is surprisingly strong[61, 66]. This setup was improved with higher control and coupling by other groups recently[67, 68]. With the atoms firmly trapped within the evanescent modes, field mediated atom-atom interaction and collective coupling to the light modes play a decisive role in this a setup[69].

Already a decade ago it was theoretically predicted[70] and experimentally confirmed[5, 52, 71] that light scattering within optical resonators induces self-ordering of atoms in regular patterns maximizing collective coupling to the cavity[72, 58]. This phase transition can be directly monitored from the super-radiant light scattering [5, 71] and appears also at zero temperature as quantum phase transition from a superfluid to a supersolid[52]. In an recent proposal Chang and coworkers predicted, that nanofiber-mediated infinite-range dipole-dipole coupling allows stable regular patterns of laser illuminated atoms trapped along the fiber[73]. The stable configurations, characterized by minimal dipole interaction energy, assume surprisingly complex configurations and exhibit characteristic collective light scattering.

Here we develop a generalized mean-field model to study the properties of light-scattering induced crystallization of a laser illuminated ultracold gas in an elongated 1D trap as depicted in Fig.7.1. The atoms, trapped parallel to the fiber, are illuminated at right angle by a laser of frequency ω_L, far detuned from any atomic resonance so that spontaneous emission only plays a minor role and the polarizability α has a negligibly small imaginary part.

7.2 Model Equations

The illuminating laser field

$$\mathbf{E}_L = (\mathcal{E}_L(\mathbf{x})e^{-i\omega_L t} + c.c.)\mathbf{e}_L \tag{7.1}$$

gives rise to the field $\mathbf{E}_s$ scattered by the atoms. Neglecting effects, which cause the polarization of the scattered field to be different from that of the the laser, $\mathbf{e}_L$, and retardation, it can be written as

$$\mathbf{E}_s = (\mathcal{E}_s(\mathbf{x},t)e^{-i\omega_L t} + c.c.)\mathbf{e}_L. \tag{7.2}$$

Its envelope $\mathcal{E}_s(\mathbf{x},t)$ satisfies Helmholtz's equation

$$\nabla^2\mathcal{E}_s + k_L^2(n_F^2 + \chi)\mathcal{E}_s = -k_L^2\chi\mathcal{E}_L. \tag{7.3a}$$

Here, $n_F(\mathbf{x})$ denotes the refractive index profile of the optical fiber and

$$\chi(\mathbf{x},t) := \alpha\frac{\rho(\mathbf{x},t)}{\epsilon_0} \tag{7.3b}$$

is the susceptibility of the particles. In describing the dynamics of the latter, we will employ mean-field theory. For a gas at finite temperature, we take the one-body distribution function $F(\mathbf{x}, \mathbf{p}, t)$ of the gas to satisfy Vlasov's equation

$$\frac{\partial F}{\partial t} + \frac{\mathbf{p}}{m} \cdot \frac{\partial F}{\partial \mathbf{x}} - \frac{\partial}{\partial \mathbf{x}} \left(\Phi_d + U_T\right) \cdot \frac{\partial F}{\partial \mathbf{p}} = 0, \tag{7.3c}$$

where U_T denotes the prescribed dipole trap potential and

$$\Phi_d = -\alpha \left|\mathcal{E}_s + \mathcal{E}_L\right|^2 \tag{7.4}$$

the optical potential due to pump laser and scattered field. The gas density ρ is obtained from the momentum integral $\rho(\mathbf{x}, t) = \int F(\mathbf{x}, \mathbf{p}, t) \mathrm{d}^3 p$ over the one-body distribution function.

As detailed in the appendix, for strong radial confinement the atomic one-body distribution approximately factorizes into a longitudinal and a transverse part,

$$F(\mathbf{x}, \mathbf{p}, t) \simeq f(z, p_z, t) F_\perp(\mathbf{x}_\perp, \mathbf{p}_\perp), \tag{7.5}$$

where $F_\perp$ is the Maxwell-Boltzmann distribution for the transverse degrees of freedom:

$$F_\perp := Z_\perp^{-1} \exp\left[-\beta \left(\frac{\mathbf{p}_\perp^2}{2m} + U_\perp(\mathbf{x}_\perp)\right)\right]. \tag{7.6}$$

β denotes the inverse thermal energy and $U_\perp$ the radial confining potential.

In the absence of atoms the fiber supports only a single relevant TE mode, which – within the framework of the present scalar theory – is supposed to possess a propagation constant $\beta_m \gtrsim k_L$ and a normalized transverse mode function $u(x, y)$ extending outside the fiber [65, 73]. The dominant forces on the particles along the $z-$direction are due to photon scattering into and out of the fiber. As long as the local atomic susceptibility stays small enough, the radial mode function of the fiber can be expected to be only weakly perturbed and we can set

$$\mathcal{E}_s(\mathbf{x}, t) \simeq \sqrt{A}\, E(z, t) u(x, y) \tag{7.7}$$

with the cross section defined by

$$A := \left(\int \mathrm{d}^2 x_\perp \mathrm{d}^2 p_\perp u^2 F_\perp\right)^{-1}. \tag{7.8}$$

Integrating over the transverse degrees of freedom we finally arrive at a onedimesional, effective description of the longitudinal dynamics

$$\frac{\partial^2 E}{\partial z^2} + \left(\beta_m^2 + k_L^2 \tilde{\chi}\right) E = -k_L^2 \tilde{\chi} E_L, \tag{7.9a}$$

$$\frac{\partial f}{\partial t} + \frac{p_z}{m}\frac{\partial f}{\partial z} - \frac{\partial}{\partial z}(U + \phi_d)\frac{\partial f}{\partial p_z} = 0, \tag{7.9b}$$

where E_r is the real part of E and

$$\phi_d := -\alpha\Big(|E|^2 + 2E_L E_r\Big) \tag{7.10}$$

denotes the effective dipole potential. The effective laser field is given by

$$E_L := \sqrt{A}\int \mathrm{d}^2x_\perp \mathrm{d}^2p_\perp \mathcal{E}_L u F_\perp \tag{7.11}$$

and the local atom-fiber coupling is governed by the effective susceptibility

$$\tilde{\chi} := \frac{\alpha}{\epsilon_0 A}\int_{-\infty}^{\infty} f(z, p_z, t)\mathrm{d}p_z \tag{7.12}$$

proportional to the atomic line density.

It is important to realize that we must supply (7.43a) with appropriate boundary conditions. As we assume no sources at infinity, the scattered electric field is purely outgoing there. Therefore we impose Sommerfeld's radiation conditions

$$\frac{\partial E(z,t)}{\partial z} = \pm i\beta_m E(z,t), \quad z \to \pm\infty \tag{7.13}$$

on the solutions to (7.9).

7.3 Equilibrium States

In analysing equilibrium solutions of the equations (7.9), we are confronted, like in the previous chapters, with the problem of infinitely many possible mean-field solutions. Indeed, every phase space distribution of the form

$$f(z, p_z) = F\left(\frac{p_z^2}{2m} + U + \phi_d\right) \tag{7.14}$$

is a stationary solution of (7.9b). We will restrict ourselves here to such stationary solutions, which correspond to a gas in thermal equilibrium[28], the particles being distributed according to a Maxwell-Boltzmann distribution

$$f_{\mathrm{MB}}(z, p_z) := Z^{-1} e^{-\beta(p_z^2/2m + U)}\, e^{\beta\alpha\left(|E|^2 + 2E_L E_r\right)}. \tag{7.15}$$

This is the form of distribution which is singled out in case of the gas being in contact with a thermal reservoir at temperature T. [1]

[1] Those readers, who fear that using Vlasov's equation and assuming of a thermal reservoir constitutes a bit of a contradiction, we refer to the comments at the end of section 7.9.1 of the appendix.

Substituting the effective susceptibility (7.12) obtained from a thermal distribution (7.15) into the effective Helmholtz equation (7.43a) leads to a highly nonlinear equation for the self-consistent electric field. For simplicity we take the external (i. e. non-selfconsistent) part of the potential to be given by

$$U(z) = \frac{1}{2} m\omega_z^2 z^2, \tag{7.16}$$

such that the gas has a (very large) thermal extension

$$l_z := \frac{2k_\mathrm{B}T}{m\omega_z^2} \gg \beta_m^{-1} =: \frac{\lambda_m}{2\pi} \tag{7.17}$$

and take the pump laser amplitude to be independent of position,
i.e. $E_L(z) = E_L$.

7.4 Normal Phase

With these assumptions one easily sees that the trivial, zero-field solution

$$E(z) \sim -\frac{\zeta_0}{\frac{l_z}{\lambda_m} + \zeta_0} E_L \to 0, \quad \text{as} \quad l_z/\lambda_m \to \infty \tag{7.18}$$

and the quasi-homogeneous density

$$f_\mathrm{np}(z, p_z) := Z^{-1} \exp[-\beta(p_z^2/2m + U(z))], \tag{7.19}$$

here called *normal phase*, always solves Helmholtz's equation.

Here, we had occasion to introduce the important dimensionless parameter

$$\zeta_0 := \frac{k_L}{\beta_m} \frac{N\alpha}{A\lambda_L \epsilon_0}, \tag{7.20}$$

which will be called *collective coupling parameter*. The ratio $k_L/\beta_m \lesssim 1$ is determined by the refractive index profile of the fiber. The second factor has the form of a susceptibility, albeit with a density N/V_eff, where the reference volume is given by $V_\mathrm{eff} = \lambda_L A$ rather than the real space volume occupied by the gas. This implies that even though we assume the gas to be dilute and hence the *local* gas-fiber coupling to be weak ($\tilde{\chi} \ll 1$), the *collective* coupling to the fiber can nevertheless be large.

As visible from (7.18), the limit $l_z/\lambda_m \gg 1$ is necessary to get a well defined non-scattering normal phase. It may be viewed as the thermodynamic limit appropriate for this system. Let us also point out that the exact form of the trapping potential $U(z)$ plays no rôle for the better part of the present theory, as long as a relation analogous to (7.17) holds. As will be seen presently, no parameter referring to the trapping potential will appear in any of the expressions given below.

At this point we would like to emphasize that the existence of *some* trapping potential, which confines the gas to an arbitrarily large but finite volume, is nevertheless essential. In commonly encountered many-body systems, where pairs of particles interact via some finite range potential, it is a useful idealization to consider the (thermodynamic) limit of infinitely many particles distributed over an infinite volume with a finite density, because in this limit surface effects become negligible without loosing any essential feature of the behavior of the bulk. In the present system, however, the coupling between gas particles is mediated by photons propagating arbitrarily far along the fiber and can therefore not be said to have some finite range. Consequently, the real space density does not determine the behavior of the gas (see also (7.20)). Furthermore, scattered light eventually leaves any sample, no matter how large, at some point and propagates to infinity. This, however, is a surface effect par excellence, which cannot be eliminated without loosing the ability to describe the actual system even in an idealized manner.

7.5 Stability of the Normal Phase

Before investigating the possibility of selfordered solutions, it is meet to first examine the dynamical stability of this normal phase, using the Helmholtz-Vlasov equations (7.9), linearized around the unordered state

$$\frac{\partial^2 E}{\partial z^2} + \beta_m^2 E = -E_L \frac{k_L^2 \alpha}{\epsilon_0 A} \int_{-\infty}^{\infty} f_1(z, p_z, t) \mathrm{d}p_z, \tag{7.21a}$$

$$\frac{\partial f_1}{\partial t} + \frac{p_z}{m}\frac{\partial f_1}{\partial z} - \frac{dU}{dz}\frac{\partial f_1}{\partial p_z} = -2\alpha \frac{\partial E_L E_r}{\partial z}\frac{\partial f_{\mathrm{np}}}{\partial p_z}. \tag{7.21b}$$

Here, $f_1(z, p_z, t)$ represents a small deviation from the normal phase, such that the complete distribution function is given by $f(z, p_z, t) = f_{\mathrm{np}}(z, p_z) + f_1(z, p_z, t)$. We seek solutions to (7.21), which are of the form

$$f_1(z, p_z, t) = \psi(z, p_z) e^{st} + \psi^*(z, p_z) e^{s^* t}, \tag{7.22a}$$

$$E(z, t) = a(z) e^{st} + b^*(z) e^{s^* t}. \tag{7.22b}$$

In this Ansatz, (ψ, a, b) will be referred to as normal mode and $s = \gamma + i\omega$ as the complex valued mode parameter. Whenever $\gamma > 0$, the deviation from equilibrium defined by the normal mode increases exponentially in time, causing the eventual destruction of the normal phase. The existence of such a mode implies dynamical instability.

As shown in the appendix, one finds that if (7.22) is to solve (7.21) and satisfy the radiation conditions (7.13), the mode parameter s must satisfy $D_n(s) = 0$ for some $n \in \mathbb{Z}$, where

$$D_n(s) = (2n+1)\pi + i \frac{k_L^2 \alpha^2}{\epsilon_0 A} \iint_{-\infty}^{\infty} \frac{E_L^2 \, \partial f_{\mathrm{np}}/\partial p_z}{s + i\beta_m v_z} \mathrm{d}p_z \mathrm{d}z. \tag{7.23}$$

This condition first demands $\omega = 0$, that is any normal mode is purely growing. Let us introduce the effective pump strength

$$\varepsilon := \frac{\alpha E_L^2}{k_\mathrm{B} T}, \tag{7.24}$$

which is the ratio of the two relevant energy scales of the system measuring kinetic- and potential energy respectively: the thermal energy of the gas $k_\mathrm{B}T$ and the dipole energy of a single induced dipole in the external laser field, $\alpha E_L^2 = dE_L$, where $d = \alpha E_L$ denotes the induced dipole moment. Then we then see that there exists at least one (family of) normal mode(s) with a positive growth rate $\gamma > 0$, if and only if

$$\varepsilon > \frac{1}{2\zeta_0} =: \varepsilon_c. \tag{7.25}$$

Hence the first important observation is that beyond this pump threshold (7.25), the normal phase ceases to be stable and no longer represents a physically realizable state of the system. Let us remark that the effective pump strength ε
An investigation of the equations $D_n(s) = 0$, however, reveals more. It is found that the normal phase supports exactly $n \geq 1$ (families of) growing modes with growthrates $\gamma_1 > \ldots > \gamma_n$, i. e. it is exactly n-fold unstable if

$$\varepsilon_c < \varepsilon < (1 + 2n)\varepsilon_c, \tag{7.26}$$

Let us now turn to the study of ordered thermal solutions of (7.9) for $\varepsilon > \varepsilon_c$.

7.6 Selfordered Thermal Equilibria

Due to the smallness of the local effective susceptibility $\tilde{\chi}$, the real and imaginary parts of the electric field envelope E_r, E_i

$$E_{r,i}(z) = a_{r,i}(z)\cos(\beta_m z + \phi_{r,i}(z))E_L, \tag{7.27}$$

can be assumed to behave almost harmonically with phases ϕ_r, ϕ_i and amplitudes a_r, a_i that vary slowly on a scale defined by β_m^{-1}. These amplitudes and phases are directly related to the complex amplitudes of the more familiar decomposition into left and right propagating waves,

$$E = (E_+(z)e^{i\beta_m z} + E_-(z)e^{-i\beta_m z})E_L \tag{7.28}$$

via

$$E_\pm = a_r e^{\pm i\phi_r} + i a_i e^{\pm i\phi_i}. \tag{7.29}$$

A perturbative analysis of the steady-state Helmholtz equation as indicated in the appendix reveals, that

$$\Theta := \frac{a_r^2 + a_i^2}{2} = \frac{1}{2}(|E_+|^2 + |E_-|^2), \tag{7.30}$$

proportional to the sum of locally right- and left propagating photons, is spatially constant, i. e. $\frac{\mathrm{d}\Theta}{\mathrm{d}z} = 0$, and will thus serve us as *order parameter*. Let it be remarked that this conservation law holds for every mean-field stationary gas distribution and is not restricted to thermal equilibrium.

Fortunately, it is possible to obtain explicit approximate solutions for the steady-state scattered field in the weak collective coupling regime, $\zeta_0 \ll 1$, as well as in the strong collective coupling regime $\zeta_0 \gg 1$.

Let us first consider the weak collective coupling regime, where scattering from the laser into the fiber and vice versa dominates over scattering within the fiber. The demand to satisfy the radiation conditions (7.13) leads to the equation(s) determining the order parameter(s)

$$2\zeta_0 I_1(2\varepsilon\sqrt{\Theta}) = (2m+1)\sqrt{\Theta} I_0(2\varepsilon\sqrt{\Theta}), \quad m \in \mathbb{N}_0, \tag{7.31}$$

where I_k denotes the kth modified Bessel function of the first kind.

As quite a surprise one observes that the solution is not unique. On the contrary, for

$$\varepsilon_c < \varepsilon < (1+2n)\varepsilon_c, \tag{7.32}$$

there exist n different solutions Θ_n. Thus, by comparison with (7.26) we see that each growing mode of the unstable normal phase corresponds to some selfordered thermal state.

As the phase of the outgoing scattered light is not determined, each solution of (7.31) corresponds to an infinite family of solutions of (7.9) with the periodic density modulation slightly displaced under a slow envelope. The appearance of this degeneracy of course corresponds to breaking of a continuous symmetry. It is important to note that the point of first appearance of an ordered family of solutions, $\varepsilon = \varepsilon_c$, exactly coincides with the point where the normal phase becomes unstable. All this is confirmed by a numerical solution of the underlying equations (7.9). Focusing on the region close to the first branching point, we find the behavior of the order parameter to be given by

$$\Theta_1 \sim \varepsilon - \varepsilon_c, \quad \varepsilon > \varepsilon_c. \tag{7.33}$$

This means that close to threshold the intensity of the light scattered off to infinity behaves on the principal branch in the same way as in the case of cavity-assisted selforganization[28].

Let us now turn to the strong collective coupling regime. Again, each possible value of the order parameter corresponds to an infinite family of stationary solutions and any nonzero value for Θ satisfies

$$\zeta_0\varepsilon = \frac{4(2m+1)}{\pi} P(\Theta) K[Q^2(\Theta)\Theta^2], \quad m \in \mathbb{N}_0, \tag{7.34}$$

where we have defined

$$P(\Theta) := \frac{1 + 2\varepsilon\Theta}{4 + 6\varepsilon\Theta}, \tag{7.35}$$

$$Q(\Theta) := \frac{1 + 2\varepsilon\Theta + 2\varepsilon}{4 + 6\varepsilon\Theta} \tag{7.36}$$

and K denotes the complete elliptic integral of the first kind. Once again, there are n families of ordered solutions whenever the generalized pump strength ε lies in the interval defined by (7.32). Furthermore, we find that according to perturbation theory, the order parameter is bounded by

$$\Theta < 4. \tag{7.37}$$

Numerical studies of this system indicate convincingly that the validity of this bound is not limited to the strong collective coupling limit and holds for the whole range of parameters.

The existence of this upper bound has an important implication. The reader will have noticed that the critical effective pump strength ε_c approaches zero if we let the number of particles and hence the collective coupling strength ζ_0 grow without bound. This seems to state that in that limit we can have an ordered state at infinitesimal laser power. The reason why this conclusion is erroneous lies in the observation that the intensity of the field scattered to infinity is proportional to ΘE_L^2 and hence approaches zero in the above limit due to (7.37). Thus, the "ordered" state assumed by the gas under such conditions is really but an *infinitesimal* modulation of the unperturbed density of the normal phase.

The order parameter corresponding to the principal branch behaves as

$$\Theta_1 \sim (\varepsilon - \varepsilon_c)^{\frac{1}{2}}, \quad \varepsilon > \varepsilon_c, \tag{7.38}$$

if $\zeta_0 \gg 1$, in stark contrast to the behavior seen in the weak collective coupling limit.

Even though the co-existence of multiple selfordered thermal solutions, i. e. a degeneracy of thermal equilibrium, has been explicitly shown only for the weak- and strong collective coupling regimes, we have good reason to expect the phasediagram to be as depicted in figure 7.2. This expectation rests, firstly, on numerical studies of the steady-state Helmholtz equation and, secondly, on the connection between growing modes and the number of selforganized stationary states given by (7.26). The latter seems to indicate that every unstable mode of the normal phase gives birth to some selfordered equilibrium. It should be noted, however, that while we have here shown the existence of multiple families of selfordered thermal solutions of the Vlasov-Helmholtz equations, nothing has been said about their dynamical stability properties, which remains an open and highly nontrivial problem.

The behavior of the order parameters as determined from the relations (7.31) and

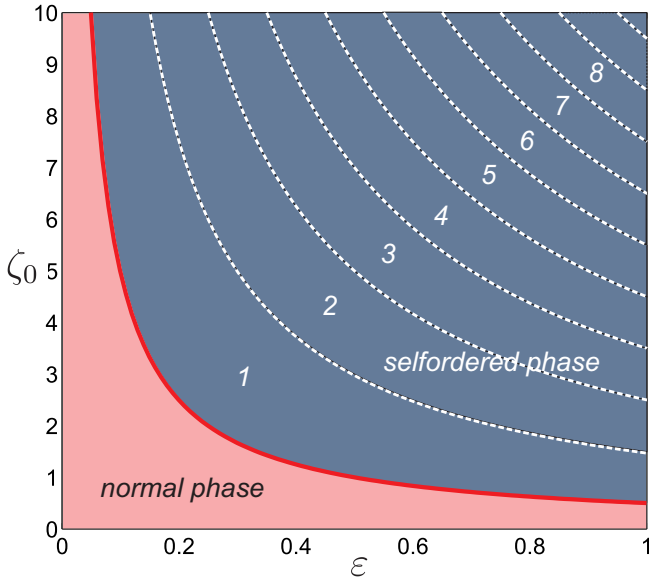

Figure 7.2 Phasediagram in terms of the principal parameters, the collective coupling strength ζ_0 and the effective pump strength ε. The red curve shows the phase boundary between the normal (unordered) and the selfordered phases. The numbers indicate the corresponding degeneracy of the thermal equilibrium solution which equals the number of growing modes supported by the (unstable) normal phase.

(7.34) is shown in figure 7.3. In the weak collective coupling limit we see that the order parameter belonging to the principal branch dominates and that increasingly higher branch numbers possess smaller and smaller orderparameters. Indeed, from (7.31) we deduce that as $\varepsilon \to \infty$ we have

$$\frac{\sqrt{\Theta_n}}{2\zeta_0} \to \frac{1}{2n-1}, \tag{7.39}$$

which explains why we have plotted $\sqrt{\Theta}/(2\zeta_0)$ for the weak collective coupling regime rather than Θ. This difference hence allows to distinguish the different thermal solutions by the light they scatter to infinity. In the strong collective coupling limit we note, however, that all branches of the order parameter converge to the limiting value $\Theta_n = 4$, implying that the intensity of light scattered off to infinity becomes equal. Figures 7.4 and 7.5 illustrate some properties of the first three of five co-existing thermal solutions in the strong collective coupling regime.

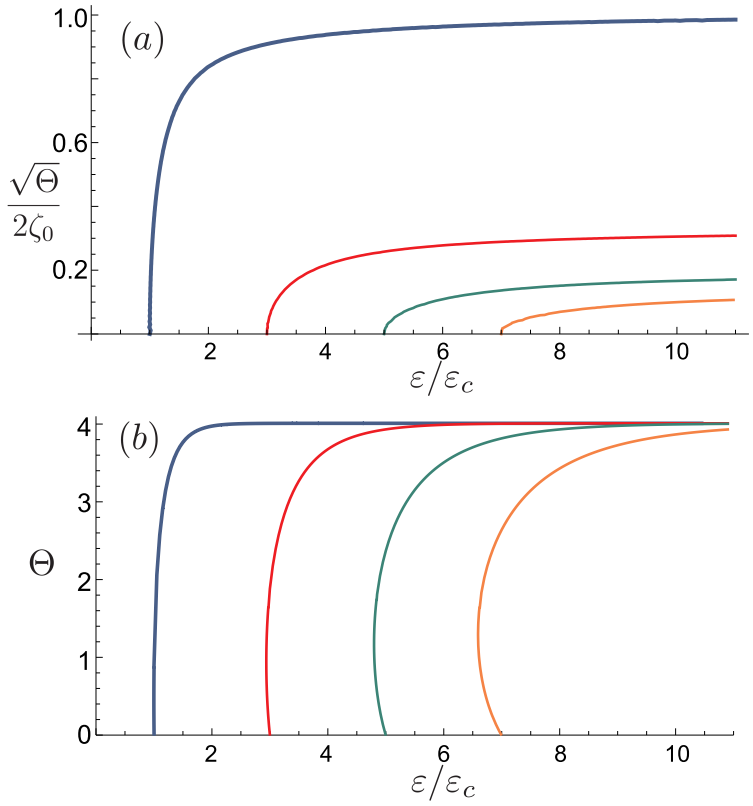

Figure 7.3 Branches of the order parameter vs energy ratio according to (7.31) and (7.34) for $m = 0, \ldots, 3$ in the weak collective coupling regime (a), with $\zeta_0 = 0.05$ and in the strong collective coupling regime (b), with $\zeta_0 = 75/\pi$. Note that in the latter regime all branches converge. The multi-valuedness seen for the higher order branches is most probably an artifact of the approximations used to derive (7.34).

7.7 Phase Boundary for a Quantum Gas

Before closing the main body of this chapter, we would like to throw a brief preliminary look on the system in the limit of zero temperature. Assuming the particles to be Bosons forming a condensate, it is simple (with the help of (7.113) of the appendix) to derive the zero temperature extension of equations (7.9):

$$\frac{\partial^2 E}{\partial z^2} + \left(\beta_m^2 + k_L^2 \tilde{\chi}\right) E = -k_L^2 \tilde{\chi} E_L, \tag{7.40a}$$

$$i\hbar \frac{\partial \psi}{\partial t} + \frac{\hbar^2}{2m} \frac{\partial^2 \psi}{\partial z^2} - \left(\bar{g}|\psi|^2 + U + \phi_d\right) \psi = 0, \tag{7.40b}$$

where now

$$\tilde{\chi} = \frac{\alpha}{\epsilon_0 A} |\psi|^2 . \tag{7.41}$$

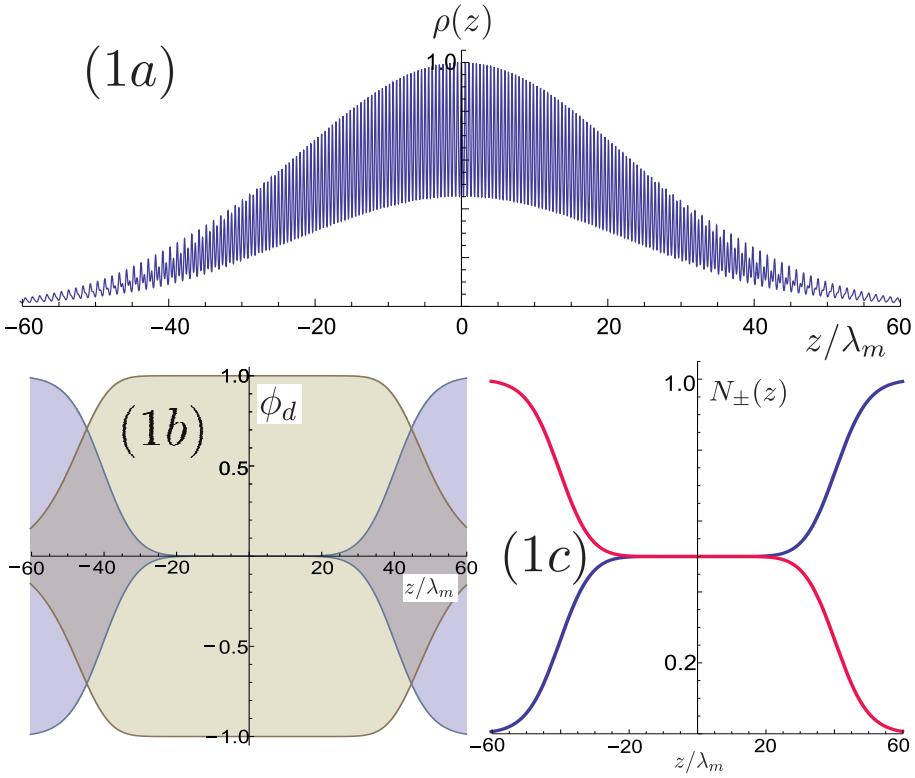

Figure 7.4 Properties of the principal ($n = 1$) of five coexisting thermal solution according to the analytical solution of (7.85) in the strong collective coupling regime with $\zeta_0 = 150/\pi$ and $\varepsilon = 9.5\varepsilon_c$. The upper plot (1a) shows the atomic density along the fiber, while the plot labeled (1c) depicts the local fraction of right N_+ (blue curve) and left N_- (red curve) traveling photons. The plot labeled (1b) depicts the magnitudes of two parts of the optical potential (7.10). The blue contribution arises from scattering between pump laser and fiber while the brown contribution area originates from photon redistribution within the fiber. The latter dominates core region causing a density modulation with a period of roughly one half of $\lambda_m = 2\pi/\beta_m$. In this region the fractions of right- and left propagating photons are seen to be equal. The reason why there is only a density modulation and not a proper lattice visible is found in the small value of the effective pump strength $\varepsilon \approx 0.1$, which however is required in order that the analytical solution be valid. Numerical studies show that all the features displayed by the analytical solutions are preserved for larger values of the effective pump strength, except that the modulation grows into a proper lattice.

The normal phase is, in analogy to the classical theory, defined as $E(z) \approx 0$ and $\psi(z,t) = \psi_{\rm np}(z,t) := \phi_0(z)e^{-i\Omega t}$, where $\phi_0(z)$ denotes the ground state in the potential $U(z)$ and $\hbar\Omega$ the corresponding ground state energy. In order to find the boundary which separates the unordered, normal phase from selforganized states, we have to determine the conditions under which the normal phase is dynamically

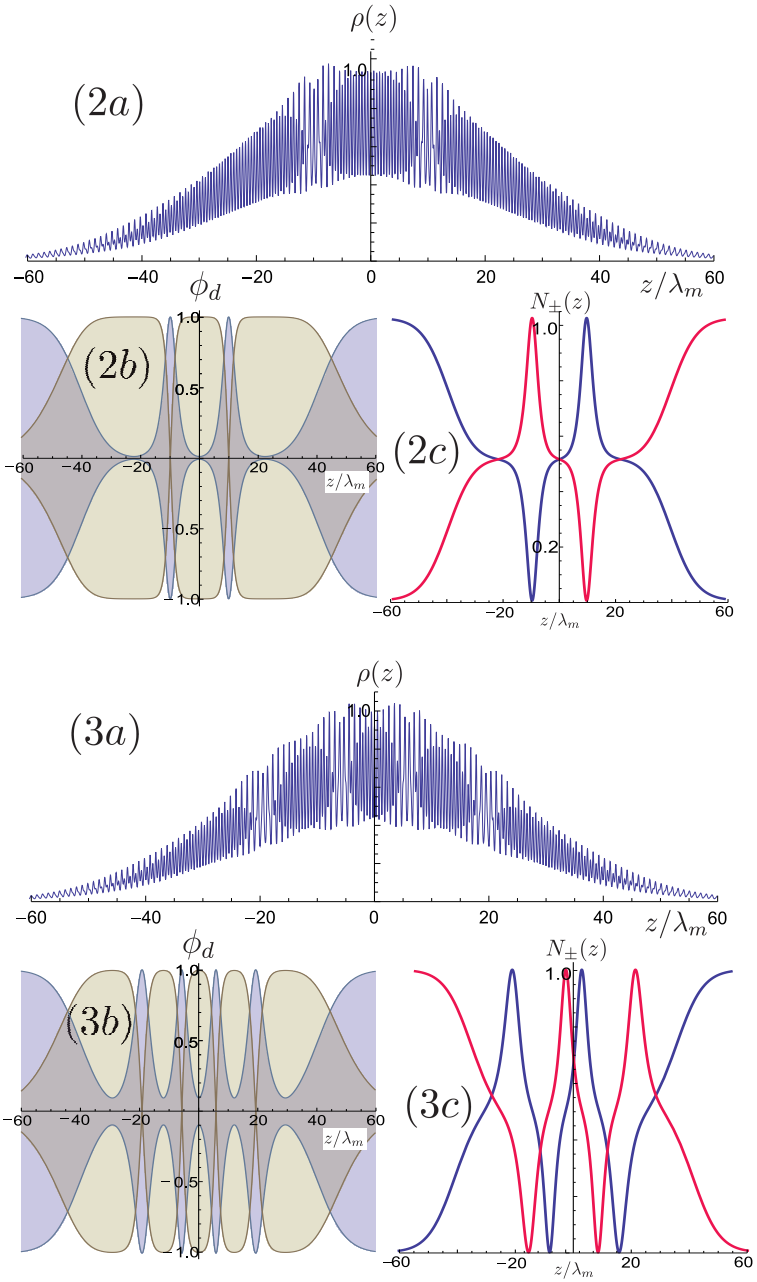

Figure 7.5 Properties of the next two thermal solutions ($n = 2, 3$) for the same parameters as in figure 7.5. Obviously, the number of regions, where the modulation has a periodicity of half a wavelength is equal to $2n-1$, which is a generally valid law outside the weak collective coupling regime ($\zeta_0 \gtrsim 1$)

unstable. Setting

$$\psi(z,t) = e^{-i\Omega t}\left(\phi_0(z) + \phi_1(z,t)\right) \tag{7.42}$$

and linearizing (7.44) around the normal phase, we obtain

$$\frac{\partial^2 E}{\partial z^2} + \beta_m^2 E = -\frac{k_L^2 \alpha \rho_1}{\varepsilon_0 A} E_L, \tag{7.43a}$$

$$i\hbar \frac{\partial \phi_1}{\partial t} + \frac{\hbar^2}{2m} \frac{\partial^2 \phi_1}{\partial z^2} - \bar{g} \rho_{\mathrm{np}} \phi_1 = [\bar{g} \rho_1 - 2\alpha E_L E_r] \phi_0, \tag{7.43b}$$

where $\rho_{\mathrm{np}} := |\psi_{\mathrm{np}}|^2 = |\phi_0|^2$, $\rho_1 := \phi_0^* \phi_1 + \phi_0 \phi_1^*$ and we have neglected the terms $U\phi_1$ and $\hbar\Omega\phi_1$ as being of higher order. We seek again normal mode solutions, i. e. solutions of the form

$$\phi(z,t) = \left(\phi_+(z) e^{i\beta_m z} + \phi_-^*(z) e^{-i\beta_m z} \right) e^{\gamma t}, \tag{7.44a}$$

$$E(z,t) = \left(E_+(z) e^{i\beta_m z} + E_-^*(z) e^{-i\beta_m z} \right) e^{\gamma t}, \tag{7.44b}$$

where $\phi_\pm$ and $E_\pm$ are slowly varying amplitudes and $\gamma > 0$.

It is not difficult to show, as in the classical case, that there exist exactly $n \geq 1$ (families of) growing normal modes if and only if

$$1 < 2\zeta_0 \varepsilon_{\mathrm{Q}} < 1 + 2n, \tag{7.45}$$

where the quantum effective pump strength

$$\varepsilon_{\mathrm{Q}} := \frac{\alpha E_L^2}{\hbar \omega_{\mathrm{R}}} \int_{-\infty}^{\infty} \frac{\rho_{\mathrm{np}}(z)}{N} \left(1 + \frac{\bar{g} \rho_{\mathrm{np}}(z)}{\hbar \omega_{\mathrm{R}}} \right)^{-1} \mathrm{d}z \tag{7.46}$$

and the recoil frequency

$$\omega_{\mathrm{R}} := \frac{\hbar \beta_m^2}{2m} \tag{7.47}$$

have been defined. We wish to point out that the criterion (7.45) is valid only as long as $\varepsilon_{\mathrm{Q}} > 0$. To treat also the case of a negative effective pump strength is not difficult, but will not be presented here. For repulsive two-body interactions we can immediately infer that

$$\varepsilon_{\mathrm{Q}} \leq \frac{\alpha E_L^2}{\hbar \omega_{\mathrm{R}}}, \quad \bar{g} \geq 0, \tag{7.48}$$

with equality only for $\bar{g} = 0$. Hence, the effect of such collisions is seen to strictly raise the threshold for instability, which could have been guessed. For attractive interactions on the other hand, we find

$$\varepsilon_{\mathrm{Q}} > \frac{\alpha E_L^2}{\hbar \omega_{\mathrm{R}}}, \quad \bar{g} < 0. \tag{7.49}$$

Thus, for a gas with attractive two-body interactions, the threshold is lower as compared to a noninteracting gas or a gas with repulsive interactions. This finding is entirely reasonable, as mutually attracting particles will by that fact comply more

readily in the selfordering process. If we estimate $\rho_{\rm np} \sim \frac{N}{l_T} =: n_0$, where $l_T \gg \lambda_m$ denotes the effective extension of the gas inside the trap, we obtain

$$\varepsilon_{\rm Q} \sim \frac{\alpha E_L^2}{\hbar\omega_{\rm R}} \frac{1}{1+\frac{\bar{g}n_0}{\hbar\omega_{\rm R}}}. \tag{7.50}$$

From this expression we see that, for attractive interactions, if the interaction energy approaches the recoil energy,

$$\bar{g}n_0 \to -\hbar\omega_{\rm R}, \tag{7.51}$$

we have $\varepsilon_{\rm Q} \to \infty$ and hence the threshold for instability becomes infinitesimally small. This circumstance may be attributed to the occurrence of resonance and could be tested experimentally. If we neglect the correction due to two-body interactions, (7.45) is equivalent to the classical result (7.26), if the thermal energy $k_{\rm B}T$ is replaced by the recoil energy $\hbar\omega_{\rm R}$.

In conclusion, the present analysis has shown that also at zero temperature, contradicting the classical theory, there is a finite pump threshold for the appearance of selfordered states, except at resonance $\bar{g}n_0 + \hbar\omega_{\rm R} = 0$, where the normal phase is unstable even at infinitesimal laser power, because the energetic cost to maintain a density modulation of λ_m-periodicity is compensated by a corresponding gain due to the attraction.[2]

7.8 Conclusions and Outlook

Similar phenomena, called optical binding, were observed with laser illuminated small beads in liquids[74] in 1D and 2D geometries. More interestingly, in analogy with cavity assisted self-ordering we expect a corresponding quantum phase transition at zero temperature, where the threshold is determined by the recoil- and interaction energy, replacing thermal energy as the relevant energy scale. This should have distinctly different properties as compared to a 1D prescribed optical lattice. Obviously, even without presence of the fiber, the interference of the scattered fields by two distant atoms can induced long range forces and ordering. As part of the scattered field is lost this leads to a higher threshold, but for a sufficiently dense gas the trapped atoms themselves form a fiber-like guide for the scattered light, thus enhancing long-range interactions. Preliminary calculations on the basis of a simple model system seem to confirm this conjecture. One could even speculate that the trapping field for the 1D confinement could be unnecessary and be provided by the light guided by the atoms. The predicted ordering phenomena might also be related to recent observations of collective scattering in dense atomic vapors[75, 76] where light induced selfordering mechanisms play an important rôle.

[2]The validity of this conclusion depends on the correctness of the neglect of the terms $U\phi_1$ and $\hbar\Omega\phi_1$ in (7.43b) and may well be erroneous.

7.9 Appendix

7.9.1 Linear Stability of the Normal Phase

In this part of the appendix, we will give the details of the linear stability analysis of the normal phase. We allow for a slow variation of the pump laser amplitude with position. Inserting the normal mode ansatz (7.22) into equations (7.21), we find that it must satisfy

$$v_z \frac{\partial \psi}{\partial z} - \frac{\mathrm{d}U}{\mathrm{d}z}\frac{\partial \psi}{\partial p_z} + s\psi = -\alpha \frac{\mathrm{d}E_L \mathcal{A}}{\mathrm{d}z}\frac{\partial f_{\mathrm{np}}}{\partial p_z}, \tag{7.52a}$$

$$\frac{\mathrm{d}^2\mathcal{A}}{\mathrm{d}z^2} + \beta_m^2 \mathcal{A} = -2E_L \frac{k_L^2 \alpha}{\epsilon_0 A}\int_{-\infty}^{\infty} \psi(z, p_z)\mathrm{d}p_z. \tag{7.52b}$$

Here, $v_z = p_z/m$ and $\mathcal{A}(z) := a(z) + b(z)$ and both a and b are solutions of the same equation

$$\frac{d^2 a}{dz^2} + \beta_m^2 a = -E_L \frac{k_L^2 \alpha}{\epsilon_0 A}\int_{-\infty}^{\infty} \psi(z, p_z)\mathrm{d}p_z. \tag{7.53}$$

and therefore differ only by a solution of the homogeneous equation. Defining $\mathcal{B}(z) = a(z) - b(z)$, we have

$$\mathcal{B}(z) = 2\mathcal{B}_+ e^{i\beta_m z} + 2\mathcal{B}_- e^{-i\beta_m z}. \tag{7.54}$$

Solving (7.52) exactly is neither possible nor necessary. First not that due to the assumed slow variation of the trapping potential, the term $\frac{dU}{dz}\frac{\partial \psi}{\partial p_z}$ is of higher order and can be neglected. Secondly, we can write

$$\mathcal{A}(z) = 2\mathcal{A}_+(z)e^{i\beta_m z} + 2\mathcal{A}_-(z)e^{-i\beta_m z}, \tag{7.55a}$$

$$\psi(z, \theta, p_z) = \psi_+(z, p_z)e^{i\beta_m z} + \psi_-(z, p_z)e^{-i\beta_m z}, \tag{7.55b}$$

where $\mathcal{A}_\pm$ and $\psi_\pm$ are slowly varying amplitudes. We immediately find

$$\psi_\pm(z, p_z) \simeq \mp 2i\beta_m \alpha E_L \mathcal{A}_\pm \frac{\partial f_{\mathrm{np}}/\partial p_z}{s \pm i v_z \beta_m}. \tag{7.56}$$

Substituting this approximate solution into equation (7.52b) we obtain

$$\frac{\mathrm{d}\mathcal{A}_\pm}{\mathrm{d}z} + i\beta_\pm(z)\mathcal{A}_\pm = 0, \tag{7.57}$$

where

$$\beta_\pm = i\alpha E_L^2 \frac{k_L^2 \alpha}{\epsilon_0 A}\int_{-\infty}^{\infty} \frac{\partial f_{\mathrm{np}}/\partial p_z}{s \pm i v_z \beta_m}\mathrm{d}p_z. \tag{7.58}$$

Hence, the solutions read

$$\mathcal{A}_\pm(z) = \mathcal{A}_\pm(0)\exp\left(-i\int_0^z \beta_\pm(z')\mathrm{d}z'\right). \tag{7.59}$$

We have $\beta_\pm(-z) = \beta_\pm(z)$ and also, due to the symmetry of the normal phase's distribution function, $\beta_-(z) = -\beta_+(z)$. Returning to $a(z)$ and $b(z)$ we have

$$a(z) = (\mathcal{A}_+(z) + \mathcal{B}_+)\, e^{i\beta_m z} + (\mathcal{A}_-(z) + \mathcal{B}_-)\, e^{-i\beta_m z}, \tag{7.60}$$

$$b(z) = (\mathcal{A}_+(z) - \mathcal{B}_+)\, e^{i\beta_m z} + (\mathcal{A}_-(z) - \mathcal{B}_-)\, e^{-i\beta_m z}. \tag{7.61}$$

To be a valid solution, the electric part of the normal mode must satisfy Sommerfeld's radiation conditions (7.13). They demand that

$$\lim_{z\to\pm\infty} (\mathcal{A}_\mp(z) + \mathcal{B}_\mp) = 0, \tag{7.62a}$$

$$\lim_{z\to\pm\infty} (\mathcal{A}_\pm(z) - \mathcal{B}_\pm) = 0, \tag{7.62b}$$

It is easy to show that these conditions lead to a condition for the mode parameter, given by $D_n(s) = 0$ for some integer n, where

$$D_n(s) = (2n+1)\pi - 2\int_0^\infty \beta_+(z)\mathrm{d}z, \tag{7.63}$$

which can also be written in the form

$$D_n(s) = (2n+1)\pi - i\frac{k_L^2\alpha^2}{\epsilon_0 A}\iint_{-\infty}^{\infty} \frac{E_L^2\, \partial f_{\mathrm{np}}/\partial p_z}{s + i\beta_m v_z}\mathrm{d}p_z\mathrm{d}z, \tag{7.64}$$

which is equation (7.23). Introducing the parameter

$$\xi := \frac{k_L^2\alpha^2}{\epsilon_0 A}\int_{-\infty}^{\infty} E_L^2(z)\rho_{\mathrm{np}}(z)\mathrm{d}z > 0, \tag{7.65}$$

we find

$$D_n(s) = (2n+1)\pi - i\xi\int_{-\infty}^{\infty} \frac{\mathrm{d}F_{\mathrm{np}}/\mathrm{d}p_z}{s + i\beta_m v_z}\mathrm{d}p_z, \tag{7.66}$$

where $f_{\mathrm{np}}(z, p_z) = \rho_{\mathrm{np}}(z)F_{\mathrm{np}}(p_z)$. Using the symmetry of the momentum distribution of the normal phase $F_{\mathrm{np}}(p_z) = F_{\mathrm{np}}(-p_z)$, the first of the radiation conditions, i. e. $\mathrm{Im}(D_n(\gamma + i\omega)) = 0$ can be cast in the form

$$\gamma\omega\int_0^\infty \frac{v_z\, \mathrm{d}F_{\mathrm{np}}/\mathrm{d}p_z}{[\gamma^2 + (\omega + \beta_m v_z)^2][\gamma^2 + (\omega - \beta_m v_z)^2]}\mathrm{d}p_z = 0, \tag{7.67}$$

which, for $\gamma \neq 0$, can only be satisfied if $\omega = 0$ as stated above. This leaves us with the following equation for the growth rate

$$(2n+1)\pi = \beta_m\xi\int_{-\infty}^{\infty} \frac{v_z\, \mathrm{d}F_{\mathrm{np}}/\mathrm{d}p_z}{\gamma^2 + \beta_m^2 v_z^2}\mathrm{d}p_z. \tag{7.68}$$

Realizing that the r.h.s. is a positive, monotonicly decreasing function of the growth rate, we conclude that this equation has exactly n solutions $\gamma_1 > \gamma_2 > \ldots > \gamma_n > 0$ if and only if

$$1 < \frac{\xi}{\beta_m\pi}\int_{-\infty}^{\infty} \frac{1}{v_z}\frac{\mathrm{d}F_{\mathrm{np}}}{\mathrm{d}p_z}\mathrm{d}p_z < 1 + 2n, \tag{7.69}$$

which yields (7.26) if we take $E_L(z) = E_L$ a constant.

For those readers who feel (understandably) a bit uneasy about the fact that the author has used Vlasov's equation to analyze states of the gas which actually require a thermal reservoir to maintain them, we will add a few remarks, which should disperse all worries. If we indeed assume a reservoir present, the equation of motion for the gas density $\rho(z,t)$ appropriate for this situation is, in the overdamped limit, given by Smoluchowski's equation

$$\frac{\partial \rho}{\partial t} - \frac{1}{\gamma_{\mathrm{B}}} \frac{\partial}{\partial z} \left(\rho \frac{\partial}{\partial z} [\phi_d + U] \right) = \frac{k_{\mathrm{B}} T}{\gamma_{\mathrm{B}}} \frac{\partial^2 \rho}{\partial z^2}, \tag{7.70}$$

where γ_{B} denotes the dynamical friction and T the temperature of the reservoir. This equation has the property, that the only steady states possible are the Maxwell-Boltzmann equilibria

$$\rho(z) = \frac{1}{Z} e^{-\beta(U+\phi_d)}, \tag{7.71}$$

where $\beta = (k_{\mathrm{B}} T)^{-1}$. This is exactly the type of equilibrium considered in this work and hence all the results concerning selfordered thermal solutions remains valid if we replace Vlasov's- by Smoluchowski's equation. It is also not at all difficult to perform a linear stability analysis of the normal phase using the linearized Smoluchowski equation and the result is again (7.26). The growth rates of the unstable normal modes depend, of course on the dynamical friction and thus differ from those determined by Vlasov's equation (see (7.68) above), but the main conclusion, that is their number, remains untouched. Alternatively, in the opposite limit one can justify the use of Vlasov's equation in the linear stability analysis performed above by arguing that it is valid for short enough times if the bath-induced friction and diffusion are weak. For a system in between these two regimes, we cannot exclude that the conclusions of this section may indeed have to be modified.

7.9.2 Perturbation Theory for Selforganized Equilibria

Here we indicate, how the results of the present work concerning selfordered equilibria can be obtained in a systematic manner by means of canonical perturbation theory. Helmholtz's equation with a stationary (not necessarily thermal) gas density ρ in the source term reads

$$\frac{\partial^2 E}{\partial z^2} + \beta_m^2 E = -\frac{k_L^2 \alpha}{\epsilon_0 A} (E + E_L) \rho. \tag{7.72}$$

It is important to note that for every stationary solution of Vlasov's equation (7.9b), which necessarily takes the form $f(z, p_z) = F(p_z^2/2m + \phi_d + U)$, we have for the corresponding density

$$\rho(z) = \int_{-\infty}^{\infty} F(p_z^2/2m + \phi_d + U) \mathrm{d}p_z =: g(\phi_d + U) \tag{7.73}$$

for some positive function g. Let G denote the antiderivative of g, i.e. $G' = g$, and let us define the canonical momenta

$$\Pi_{r,i} := \partial_z E_{r,i}. \tag{7.74}$$

Then, the above equations for the real and imaginary parts of the selfconsistent field are the canonical equations of the following Hamiltonian

$$H = \frac{1}{2}\left[\Pi_r^2 + \Pi_i^2 + \beta_m^2(E_r^2 + E_i^2) - \frac{k_L^2}{\epsilon_0 A} G[\phi_d + U]\right], \tag{7.75}$$

which has the physical interpretation of being proportional to the energy density of the scattered electric field. It can be written as the Hamiltonian of two uncoupled resonant oscillators, H_0, plus a coupling, $H = H_0 + H_1$, where

$$H_1 = -\frac{k_L^2}{2\epsilon_0 A} G[\phi_d + U], \tag{7.76}$$

which part we shall consider a perturbation due to the smallness of the effective susceptibility (7.12). Let us introduce action-angle variables $(J_r, J_i, \psi_r, \psi_i)$ for the unperturbed part H_0 via the prescription

$$E_{r,i} = \sqrt{\frac{2J_{r,i}}{\beta_m}} \sin(\psi_{r,i}) \tag{7.77a}$$

$$\Pi_{r,i} = \sqrt{2\beta_m J_{r,i}} \cos(\psi_{r,i}). \tag{7.77b}$$

Then we find the transformed Hamiltonian as $H = H_0(J) + \epsilon H_1(J, \psi, \epsilon z)$, where now $H_0(J) = \beta_m(J_r + J_i)$ and we have introduced a purely formal expansion parameter ϵ. The explicit dependence on z is due only to the external trap $U(z)$ and thus weak. Next we will seek a canonical transformation, effected by the mixed variables generating function $S = S(\bar{J}, \psi, z)$ to new variables $(\bar{J}, \bar{\psi}) \equiv (\bar{J}_r, \bar{J}_i, \bar{\psi}_r, \bar{\psi}_i)$ according to

$$J = \nabla_\psi S, \quad \bar{\psi} = \nabla_{\bar{J}} S \tag{7.78}$$

and leading to the new Hamiltonian

$$K = H + \frac{\partial S}{\partial z}, \tag{7.79}$$

which we wish to make as simple as possible. To exploit the assumed smallness of H_1, we express the generating function as

$$S = \bar{J} \cdot \psi + \epsilon S_1 + \epsilon^2 S_2 + \ldots, \tag{7.80}$$

appropriate for a near-identity transformation. Likewise expanding the transformed Hamiltonian $K = K_0 + \epsilon K_1 + \ldots$, we find

$$K_0(\bar{J}) = H_0(\bar{J}), \tag{7.81a}$$

$$K_1(\bar{J},\bar{\psi},\epsilon z) = \beta_m \sum_{k=r,i} \frac{\partial S_1}{\partial \bar{\psi}_k} + H_1(\bar{J},\bar{\psi},\epsilon z), \tag{7.81b}$$

and so forth. Setting $\epsilon = 1$ and introducing the unperturbed trajectories $\bar{\psi}_{r,i}(\zeta) := \bar{\psi}_{r,i} + \zeta$, we find

$$S_1(\bar{J},\bar{\psi}(\zeta),z) - S_1(\bar{J},\bar{\psi},z) = \\ = \frac{1}{\beta_m}\int_0^{\zeta} \Big[K_1(\bar{J},\bar{\psi}(\zeta'),z) - H_1(\bar{J},\bar{\psi}(\zeta'),z)\Big]\, d\zeta'. \tag{7.82}$$

Imposing the periodicity of the generating function in the angles leads to the solvability condition

$$\int_0^{2\pi} \Big[K_1(\bar{J},\bar{\psi}(\zeta),z) - H_1(\bar{J},\bar{\psi}(\zeta),z)\Big]\, d\zeta = 0, \tag{7.83}$$

which must be satisfied by any potential K_1. Now we use our freedom to choose K_1 to be a function of the phase difference only, $K_1 = \tilde{K}_1(\bar{J},\bar{\Delta},z)$, where $\bar{\Delta} := \bar{\psi}_r - \bar{\psi}_i$. Then it is easy to see, that (7.83) demands

$$\tilde{K}_1(\bar{J},\bar{\Delta},z) := \frac{1}{2\pi}\int_0^{2\pi} H_1(\bar{J},\zeta+\bar{\Delta},\zeta,z)d\zeta. \tag{7.84}$$

In this way we end up with the new and simplified Hamiltonian, to first order in the perturbation given by $K(\bar{J},\bar{\psi},z) = H_0(\bar{J}) + \tilde{K}_1(\bar{J},\bar{\Delta},z)$. As this new Hamiltonian depends, by construction, only on the phase difference $\bar{\Delta}$, we immediately obtain an integral of motion, $\bar{\Theta} := \bar{J}_r + \bar{J}_i$, proportional to the order parameter, which is the total number of quanta of excitation in the left and right propagating field components. Therefore, the number of degrees of freedom is reduced to just two, namely $\bar{\Delta}$ and $\bar{D} := \bar{J}_r - \bar{J}_i$, whose equations of motion are the canonical equations

$$\frac{\mathrm{d}\bar{\Delta}}{\mathrm{d}z} = \frac{\mathrm{d}\bar{H}}{\mathrm{d}\bar{D}}, \tag{7.85a}$$

$$\frac{\mathrm{d}\bar{D}}{\mathrm{d}z} = -\frac{\mathrm{d}\bar{H}}{\mathrm{d}\bar{\Delta}}, \tag{7.85b}$$

pertaining to the Hamiltonian

$$\bar{H}(\bar{D},\bar{\Delta},z) := 2\tilde{K}_1\left(\frac{\Theta+\bar{D}}{2}, \frac{\Theta-\bar{D}}{2}, \bar{\Delta}, z\right) \tag{7.86}$$

and can be solved in the weak and strong collective coupling limits respectively.

7.9.3 Strong-Trapping Approximation

In this part we will first show how the effective onedimensional Vlasov equation for the reduced atomic phase space distribution $f(z, p_z, t)$ can be obtained from perturbation theory. Afterwards we will give a corresponding reduced description of a bosonic gas a zero temperature.

As we have exclusively considered onedimensional situations in this thesis, the following derivations are relevant for the entire work and not just for this last chapter. It is mainly for this reason that we have decided to include them.

Classical Case

As stated in the main body of this chapter and depicted in figure 7.1, we assume that the trapping potential $U_T = U(z) + U_\perp(\mathbf{x}_\perp)$ be such that it provides strong trapping in the two spatial directions $(x, y) =: \mathbf{x}_\perp$ orthogonal to the fiber axis of symmetry and a far weaker in the latter's, the $z-$direction. In this case, equation (7.3c) can be considerably simplified. To this end, let us define $V := \Phi_d + U$ and keep in mind that to a good approximation $\partial U_\perp/\partial \mathbf{x}_\perp \gg \partial \Phi_d/\partial \mathbf{x}_\perp$, such that we can neglect the latter. Next, to signify the fact that the transverse trapping is strong, let us introduce a formal expansion parameter ϵ, which will be set equal to unity in the end. Then (7.3c) assumes the form

$$\frac{\partial F}{\partial t} + \frac{p_z}{m}\frac{\partial F}{\partial z} - \frac{\partial V}{\partial z}\frac{\partial F}{\partial p_z} + \frac{1}{\epsilon}\left(\frac{\mathbf{p}_\perp}{m}\cdot\frac{\partial F}{\partial \mathbf{x}_\perp} - \frac{\partial U_\perp}{\partial \mathbf{x}_\perp}\cdot\frac{\partial F}{\partial \mathbf{p}_\perp}\right) = 0. \tag{7.87}$$

Now, realizing that the transverse and longitudinal dynamics take place on very different time scales, we introduce an auxiliary fast time variable $\tau := t/\epsilon$ and expand the distribution function according to

$$F(\mathbf{x}, \mathbf{p}, t) = F^0(\mathbf{x}, \mathbf{p}, t, \tau) + \epsilon F^1(\mathbf{x}, \mathbf{p}, t, \tau) + \dots \tag{7.88}$$

Substituting this expansion into (7.87), we find that the lowest order equations are given by

$$\frac{\partial F^0}{\partial \tau} + \frac{\mathbf{p}_\perp}{m}\cdot\frac{\partial F^0}{\partial \mathbf{x}_\perp} - \frac{\partial U_\perp}{\partial \mathbf{x}_\perp}\cdot\frac{\partial F^0}{\partial \mathbf{p}_\perp} = 0, \tag{7.89a}$$

$$\frac{\partial F^1}{\partial \tau} + \frac{\mathbf{p}_\perp}{m}\cdot\frac{\partial F^1}{\partial \mathbf{x}_\perp} - \frac{\partial U_\perp}{\partial \mathbf{x}_\perp}\cdot\frac{\partial F^1}{\partial \mathbf{p}_\perp} = -\left(\frac{\partial F^0}{\partial t} + \frac{p_z}{m}\frac{\partial F^0}{\partial z} - \frac{\partial V}{\partial z}\frac{\partial F^0}{\partial p_z}\right). \tag{7.89b}$$

To solve the first, we introduce the radial orbits
$\mathbf{Z}_s[\mathbf{x}_\perp, \mathbf{p}_\perp] := (\mathbf{X}_s[\mathbf{x}_\perp, \mathbf{p}_\perp], \mathbf{P}_s[\mathbf{x}_\perp, \mathbf{p}_\perp])$ via

$$\frac{\partial \mathbf{X}_s}{\partial s} = \frac{1}{m}\mathbf{P}_s, \tag{7.90a}$$

$$\frac{\partial \mathbf{P}_s}{\partial s} = -\frac{\partial U_\perp}{\partial \mathbf{X}_s}, \tag{7.90b}$$

with the initial condition $\mathbf{Z}_0[\mathbf{x}_\perp, \mathbf{p}_\perp] = (\mathbf{x}_\perp, \mathbf{p}_\perp)$. The first equation (7.89a) then states that the zeroth order distribution function is invariant along the radial orbits on the fast time scale

$$\frac{\partial}{\partial \tau} F^0(\mathbf{Z}_\tau, z, p_z, t, \tau) = 0 \tag{7.91}$$

and the second

$$\frac{\partial}{\partial \tau} F^1(\mathbf{Z}_\tau, z, p_z, t, \tau) = -\left(\frac{\partial F^0}{\partial t} + \frac{p_z}{m}\frac{\partial F^0}{\partial z} - \frac{\partial V}{\partial z}\frac{\partial F^0}{\partial p_z} \right)_{\mathbf{Z}_\tau, \tau}. \tag{7.92}$$

As U_T is supposed to provide trapping, it is clear that for every $(\mathbf{x}_\perp, \mathbf{p}_\perp)$ there exists an orbital period T, such that $\mathbf{Z}_T = \mathbf{Z}_0$. If we therefore integrate the second equation over one orbital period and use that F^0 does not change according to the first equation, we find the integrability condition as

$$\frac{\partial F^0}{\partial t} + \frac{p_z}{m}\frac{\partial F^0}{\partial z} - \left(\frac{1}{T}\int_0^T \frac{\partial V}{\partial z}|_{\mathbf{Z}_\tau} \mathrm{d}\tau \right) \frac{\partial F^0}{\partial p_z} = 0. \tag{7.93}$$

Therefore, in the strong trapping approximation, $F \simeq F^0$ and (7.93) represents its equation of motion to lowest order, where the transverse coordinate and momentum enter only as parameters. The equation of motion may also be written in the form

$$\frac{\partial F}{\partial t} + \frac{p_z}{m}\frac{\partial F}{\partial z} - \frac{\partial}{\partial z}\left(U + \langle \Phi_d \rangle_\tau\right) \frac{\partial F}{\partial p_z} = 0, \tag{7.94}$$

where

$$\langle \Phi_d \rangle_\tau (\mathbf{x}, \mathbf{p}) := \frac{1}{T}\int_0^T \Phi_d(\mathbf{X}_\tau[\mathbf{x}_\perp, \mathbf{p}_\perp], z, t)\mathrm{d}\tau. \tag{7.95}$$

To simplify matters even more, we will assume that the radial confinement is so strong that we can safely replace the average

$$\langle \Phi_d \rangle_\tau \simeq \Phi_d(\mathbf{x}_{\perp 0}, z, t) \simeq \int \mathrm{d}^2 p_\perp \int \mathrm{d}^2 x_\perp \Phi_d(\mathbf{x}, t) F(\mathbf{x}, \mathbf{p}, t), \tag{7.96}$$

where $\mathbf{x}_{\perp 0}$ denote the transverse coordinates of the trap axis of symmetry. The reduced Vlasov equation (7.94) is then solved by the product $F = fF_\perp$, that is

$$F(\mathbf{x}, \mathbf{p}, t) = f(z, p_z, t) F_\perp(\mathbf{x}_\perp, \mathbf{p}_\perp), \tag{7.97}$$

where $F_\perp$ is a rather arbitrary function of the integrals of motion of the transverse Hamiltonian

$$H_\perp = \frac{\mathbf{p}_\perp^2}{2m} + U_\perp(\mathbf{x}_\perp) \tag{7.98}$$

and $f(z, p_z, t)$ satisfies the effective Vlasov equation

$$\frac{\partial f}{\partial t} + \frac{p_z}{m}\frac{\partial f}{\partial z} - \frac{\partial}{\partial z}\left(U + \langle \Phi_d \rangle\right) \frac{\partial f}{\partial p_z} = 0, \tag{7.99}$$

where

$$\langle \Phi_d \rangle (z,t) := \int d^2x_\perp \Phi_d(\mathbf{x},t) \int d^2p_\perp F_\perp(\mathbf{x}_\perp, \mathbf{p}_\perp). \tag{7.100}$$

In this work we have made the physically reasonable assumption that $F_\perp$ is given by the thermal distribution

$$F_\perp = Z_\perp^{-1} \exp\left[-\beta H_\perp\right]. \tag{7.101}$$

Quantum Case

The theory employed in the main body of this chapter is appropriate for a dilute gas at a sufficiently high temperature. As the temperature approaches zero, however, it has to be replaced by a quantum mechanical description. In this part of the appendix we consider an ultracold gas of Bosons, which we take to be describable by a macroscopic wave-function $\Psi(\mathbf{x},t)$ satisfying Gross-Pitaevskii's equation

$$i\hbar\frac{\partial\Psi}{\partial t} + \frac{\hbar^2}{2m}\nabla^2\Psi - \left(g|\Psi|^2 + U_T + \Phi_d\right)\Psi = 0, \tag{7.102}$$

where g measures the strength of two-body interactions. Here, the gas density is given by $\rho(\mathbf{x},t) = |\Psi(\mathbf{x},t)|^2$. As in the classical treatment, we introduce a formal expansion parameter to signify the strength of the transverse trapping to obtain

$$i\hbar\frac{\partial\Psi}{\partial t} = -\frac{\hbar^2}{2m}\frac{\partial^2\Psi}{\partial z^2} + \left(g|\Psi|^2 + V\right)\Psi - \frac{1}{\epsilon}\left[\frac{\hbar^2}{2m}\nabla_\perp^2\Psi - U_\perp\Psi\right] \tag{7.103}$$

as $\epsilon \to 0$. Likewise, we introduce again a two-scale ansatz

$$\Psi(\mathbf{x},t) = \Psi_0(\mathbf{x},t,t/\epsilon) + \epsilon\Psi_1(\mathbf{x},t,t/\epsilon) + \ldots \tag{7.104}$$

into the equation and equate order by order to get

$$i\hbar\frac{\partial\Psi_0}{\partial\tau} + \frac{\hbar^2}{2m}\nabla_\perp^2\Psi_0 - U_\perp\Psi_0 = 0 \tag{7.105}$$

$$i\hbar\frac{\partial\Psi_1}{\partial\tau} + \frac{\hbar^2}{2m}\nabla_\perp^2\Psi_1 - U_\perp\Psi_1 = -i\hbar\frac{\partial\Psi_0}{\partial t} - \frac{\hbar^2}{2m}\frac{\partial^2\Psi_0}{\partial z^2} + \left(g|\Psi_0|^2 + V\right)\Psi_0, \tag{7.106}$$

etc., where $\tau := t/\epsilon$ is considered an independent variable. We solve the first equation by

$$\Psi_0(\mathbf{x},t,\tau) = \psi(z,t)\Phi_0(\mathbf{x}_\perp)e^{-i\omega_0\tau}, \tag{7.107}$$

where Φ_0 is the groundstate corresponding to the energy $\hbar\omega_0$ of the lowest order transverse Hamiltonian

$$H_\perp = -\frac{\hbar^2}{2m}\nabla_\perp^2 + U_\perp \tag{7.108}$$

and which we assume to be non-degenerate. In the second equation we introduce the decomposition

$$\Psi_1 = \sum_\nu \psi_\nu(z,\tau)\Phi_\nu(\mathbf{x}_\perp)e^{-i\omega_\nu\tau}, \tag{7.109}$$

where $\Phi_\nu(\mathbf{x}_\perp)$ are eigenfunctions of (7.108) and $\psi_0 \equiv \psi$ to get

$$i\hbar\frac{\partial\psi_\nu}{\partial\tau} - \hbar\omega_\nu\psi_\nu = e^{-i\omega_0\tau}\int S[\psi]\Phi_0\Phi_\nu^*\mathrm{d}^2x_\perp, \tag{7.110}$$

wherein

$$S[\psi] := -i\hbar\frac{\partial\psi}{\partial t} - \frac{\hbar^2}{2m}\frac{\partial^2\psi}{\partial z^2} + \left(g|\psi|^2|\Phi_0|^2 + V\right)\psi. \tag{7.111}$$

In (7.110) only the $\nu = 0$ equation is problematic due to resonance. In order to have Ψ_1 non-secular and thus to have a meaningful expansion, we must demand that the driving term vanishes identically, i.e.

$$\int S[\psi]\Phi_0\Phi_0^*\mathrm{d}^2x_\perp \equiv 0. \tag{7.112}$$

This gives the effective Gross-Pitaevski equation for the longitudinal wave-function $\psi(z,t)$ as

$$i\hbar\frac{\partial\psi}{\partial t} + \frac{\hbar^2}{2m}\frac{\partial^2\psi}{\partial z^2} - \left(\bar{g}|\psi|^2 + U + \langle\Phi_d\rangle\right)\psi = 0, \tag{7.113}$$

where the effective collision parameter is given by

$$\bar{g} := g\int|\Phi_0|^4\mathrm{d}^2x_\perp \tag{7.114}$$

and the effective dipole potential reads

$$\langle\Phi_d\rangle := \int\Phi_d|\Phi_0(\mathbf{x}_\perp)|^2\mathrm{d}^2x_\perp. \tag{7.115}$$

Bibliography

[1] I. Bloch, J. Dalibard, and W. Zwerger. Many-body physics with ultracold gases. *Reviews of Modern Physics*, 80(3):885, 2008.

[2] Peter Horak, Gerald Hechenblaikner, Klaus M. Gheri, Herwig Stecher, and Helmut Ritsch. Cavity-induced atom cooling in the strong coupling regime. *Phys. Rev. Lett.*, 79(25):4974–4977, Dec 1997.

[3] P. Domokos and H. Ritsch. Mechanical effects of light in optical resonators. *J. Opt. Soc. Am. B*, 20(5):1098–1130, 2003.

[4] Peter Domokos and Helmut Ritsch. Collective cooling and self-organization of atoms in a cavity. *Phys. Rev. Lett.*, 89(25):253003, 12 2002.

[5] A.T. Black, H.W. Chan, and V. Vuletić. Observation of collective friction forces due to spatial self-organization of atoms: from rayleigh to bragg scattering. *Physical review letters*, 91(20):203001, 2003.

[6] Tobias Grießer and Helmut Ritsch. Nonlinear atom-field dynamics in high-q cavities: from a bec to a thermal gas. *Optics express*, 19(12):11242–11255, 2011.

[7] W. Niedenzu, T. Grießer, and H. Ritsch. Kinetic theory of cavity cooling and selforganisation of a cold gas. *EPL*, 96:43001, 2011.

[8] Tobias Grießer, Wolfgang Niedenzu, and Helmut Ritsch. Cooperative self-organization and sympathetic cooling of a multispecies gas in a cavity. *New Journal of Physics*, 14(5):053031, 2012.

[9] Tobias Grießer and Helmut Ritsch. Light-induced crystallization of cold atoms in a 1d optical trap. *Phys. Rev. Lett.*, 111:055702, Aug 2013.

[10] D. Kruse, M. Ruder, J. Benhelm, C. von Cube, C. Zimmermann, Ph. W. Courteille, Th. Elsässer, B. Nagorny, and A. Hemmerich. Cold atoms in a high-q ring cavity. *Phys. Rev. A*, 67(5):051802, May 2003.

[11] M. Khudaverdyan, W. Alt, I. Dotsenko, T. Kampschulte, K. Lenhard, A. Rauschenbeutel, S. Reick, K. Schörner, A. Widera, and D. Meschede. Controlled insertion and retrieval of atoms coupled to a high-finesse optical resonator. *New Journal of Physics*, 10:073023, 2008.

[12] P. Domokos and H. Ritsch. Mechanical effects of light in optical resonators. *Journal of the Optical Society of America B*, 20(5):1098–1130, 2003.

[13] P. Domokos, P. Horak, and H. Ritsch. Semiclassical theory of cavity-assisted atom cooling. *Journal of Physics B: Atomic, Molecular and Optical Physics*, 34:187, 2001.

[14] J. M. Zhang, F. C. Cui, D. L. Zhou, and W. M. Liu. Nonlinear dynamics of a cigar-shaped bose-einstein condensate in an optical cavity. *Phys. Rev. A*, 79(3):033401, Mar 2009.

[15] S. Ritter, F. Brennecke, K. Baumann, T. Donner, C. Guerlin, and T. Esslinger. Dynamical coupling between a Bose–Einstein condensate and a cavity optical lattice. *Applied Physics B: Lasers and Optics*, 95(2):213–218, 2009.

[16] T. Grießer, H. Ritsch, M. Hemmerling, and G. R. M. Robb. A Vlasov approach to bunching and selfordering of particles in optical resonators. *Eur. Phys. J. D*, 58(3):349–368, 2010.

[17] J. Javaloyes, M. Perrin, G. L. Lippi, and A. Politi. Self-generated cooperative light emission induced by atomic recoil. *Phys. Rev. A*, 70(2):023405, Aug 2004.

[18] R. Bach, K. Burnett, MB d'Arcy, and SA Gardiner. Quantum-mechanical cumulant dynamics near stable periodic orbits in phase space: Application to the classical-like dynamics of quantum accelerator modes. *Physical Review A*, 71(3):33417, 2005.

[19] Subhadeep Gupta, Kevin L. Moore, Kater W. Murch, and Dan M. Stamper-Kurn. Cavity nonlinear optics at low photon numbers from collective atomic motion. *Phys. Rev. Lett.*, 99(21):213601, Nov 2007.

[20] András Vukics, Wolfgang Niedenzu, and Helmut Ritsch. Cavity nonlinear optics with few photons and ultracold quantum particles. *Phys. Rev. A*, 79(1):013828, Jan 2009.

[21] F. Brennecke, S. Ritter, T. Donner, and T. Esslinger. Cavity optomechanics with a Bose-Einstein condensate. *Science*, 322(5899):235, 2008.

[22] D. Nagy, P. Domokos, A. Vukics, and H. Ritsch. Nonlinear quantum dynamics of two BEC modes dispersively coupled by an optical cavity. *The European Physical Journal D-Atomic, Molecular, Optical and Plasma Physics*, 55(3):659–668, 2009.

[23] F. Brennecke, T. Donner, S. Ritter, T. Bourdel, M. Köhl, and T. Esslinger. Cavity QED with a Bose–Einstein condensate. *Nature*, 450(7167):268–271, 2007.

[24] M. Cristiani and J. Eschner. private communication.

[25] T. Valenzuela, M. Cristiani, H. Gothe, and J. Eschner. Cold Ytterbium atoms in high-finesse optical cavities: cavity cooling and collective interactions. In *Lasers and Electro-Optics 2009 and the European Quantum Electronics Conference. CLEO Europe-EQEC 2009. European Conference on*, page 1. IEEE, 2009.

[26] R. Grimm, M. Weidemüller, and Y. B. Ovchinnikov. Optical dipole traps for neutral atoms. *Adv. At. Mol. Opt. Phys.*, 42:95–170, 2000.

[27] J. D. Miller, R. A. Cline, and D. J. Heinzen. Far-off-resonance optical trapping of atoms. *Phys. Rev. A*, 47(6):4567–4570, 1993.

[28] J. K. Asbóth, P. Domokos, H. Ritsch, and A. Vukics. Self-organization of atoms in a cavity field: Threshold, bistability, and scaling laws. *Phys. Rev. A*, 72(5):053417, 11 2005.

[29] Vladan Vuletić and Steven Chu. Laser cooling of atoms, ions, or molecules by coherent scattering. *Phys. Rev. Lett.*, 84(17):3787–3790, 4 2000.

[30] B. L. Lev, A. Vukics, E. R. Hudson, B. C. Sawyer, P. Domokos, H. Ritsch, and J. Ye. Prospects for the cavity-assisted laser cooling of molecules. *Phy. Rev. A*, 77(2):023402, 2008.

[31] T. Salzburger and H. Ritsch. Collective transverse cavity cooling of a dense molecular beam. *New J. Phys.*, 11:055025, 2009.

[32] Wolfgang P. Schleich. *Quantum Optics in Phase Space*. Wiley-VCH, Berlin, first edition, 2001.

[33] P. E. Kloeden and R. Pearson. The numerical solution of stochastic differential equations. *J. Austral. Math. Soc. Ser. B*, 20:8, 1977.

[34] W. Rümelin. Numerical treatment of stochastic differential equations. *SIAM J. Numer. Anal.*, 19(3):604–613, 1982.

[35] David C. Montgomery. *Theory of the unmagnetized plasma*. Gordon and Breach, 1971.

[36] André M. C. de Souza and Constantino Tsallis. Student's t-and r-distributions: Unified derivation from an entropic variational principle. *Physica A*, 236(1-2):52–57, 1997.

[37] Eric Lutz. Anomalous diffusion and tsallis statistics in an optical lattice. *Phys. Rev. A*, 67(5):051402, 5 2003.

[38] P. Douglas, S. Bergamini, and F. Renzoni. Tunable tsallis distributions in dissipative optical lattices. *Phys. Rev. Lett.*, 96(11):110601, 3 2006.

[39] J. F. Luciani and R. Pellat. Kinetic equation of finite Hamiltonian systems with integrable mean field. *J. Physique*, 48(4):591–599, 1987.

[40] Pierre-Henri Chavanis. Kinetic theory with angle-action variables. *Physica A*, 377:469–486, 2007.

[41] R. Balescu. Irreversible processes in ionized gases. *Phys. Fluids*, 3:52, 1960.

[42] A. Lenard. On bogoliubov's kinetic equation for a spatially homogeneous plasma. *Ann. Phys.*, 10(3):390–400, 1960.

[43] H. A. Posch and W. Thirring. Stellar stability by thermodynamic instability. *Phys. Rev. Lett.*, 95(25):251101, 2005.

[44] H. J. Metcalf and P. van der Straten. *Laser cooling and trapping.* Springer-Verlag, New York, 1999.

[45] G. Thalhammer, R. Steiger, S. Bernet, and M. Ritsch-Marte. Optical macro-tweezers: trapping of highly motile micro-organisms. *J. Opt.*, 13:044024, 2011.

[46] J. Doyle, B. Friedrich, R. V. Krems, and F. Masnou-Seeuws. Quo vadis, cold molecules? *Eur. Phys. J. D*, 31:149–164, 2004.

[47] T. J. Kippenberg and K. J. Vahala. Cavity optomechanics: back-action at the mesoscale. *Science*, 321(5893):1172, 2008.

[48] E. S. Shuman, J. F. Barry, and D. DeMille. Laser cooling of a diatomic molecule. *Nature*, 467(7317):820–823, 2010.

[49] S. Nimmrichter, K. Hammerer, P. Asenbaum, H. Ritsch, and M. Arndt. Master equation for the motion of a polarizable particle in a multimode cavity. *New J. Phys.*, 12:083003, 2010.

[50] V. Vuletić, H. W. Chan, and A. T. Black. Three-dimensional cavity doppler cooling and cavity sideband cooling by coherent scattering. *Phys. Rev. A*, 64(3):033405, 2001.

[51] S. Slama, S. Bux, G. Krenz, C. Zimmermann, and Ph. W. Courteille. Superradiant rayleigh scattering and collective atomic recoil lasing in a ring cavity. *Phys. Rev. Lett.*, 98(5):053603, 2007.

[52] K. Baumann, C. Guerlin, F. Brennecke, and T. Esslinger. Dicke quantum phase transition with a superfluid gas in an optical cavity. *Nature*, 464(7293):1301–1306, 2010.

[53] S. Deachapunya, P. J. Fagan, A. G. Major, E. Reiger, H. Ritsch, A. Stefanov, H. Ulbricht, and M. Arndt. Slow beams of massive molecules. *Eur. Phys. J. D*, 46(2):307–313, 2008.

[54] E. Haller, M. Gustavsson, M. J. Mark, J. G. Danzl, R. Hart, G. Pupillo, and H.-C. Nägerl. Realization of an excited, strongly correlated quantum gas phase. *Science*, 325(5945):1224, 2009.

[55] Y. L. Klimontovich. *Statistical theory of open systems.* Kluwer Academic Publishers, Dordrecht, first edition, 1995.

[56] L. D. Landau. On the vibrations of the electronic plasma. *J. Phys. USSR*, 10(25):574, 1946.

[57] V. B. Krapchev and A. K. Ram. Adiabatic theory for a single nonlinear wave in a vlasov plasma. *Phy. Rev. A*, 22(3):1229, 1980.

[58] S. Gopalakrishnan, B.L. Lev, and P.M. Goldbart. Emergent crystallinity and frustration with bose–einstein condensates in multimode cavities. *Nature Physics*, 5(11):845–850, 2009.

[59] JK Asbóth, H. Ritsch, and P. Domokos. Optomechanical coupling in a one-dimensional optical lattice. *Physical Review A*, 77(6):063424, 2008.

[60] JK Asbóth, H Ritsch, and P Domokos. Collective excitations and instability of an optical lattice due to unbalanced pumping. *Physical review letters*, 98(20):203008, 2007.

[61] P. Domokos, P. Horak, and H. Ritsch. Quantum description of light-pulse scattering on a single atom in waveguides. *Physical Review A*, 65(3):033832, 2002.

[62] Y. Colombe, T. Steinmetz, G. Dubois, F. Linke, D. Hunger, and J. Reichel. Strong atom–field coupling for bose–einstein condensates in an optical cavity on a chip. *Nature*, 450(7167):272–276, 2007.

[63] DJ Alton, NP Stern, T. Aoki, H. Lee, E. Ostby, KJ Vahala, and HJ Kimble. Strong interactions of single atoms and photons near a dielectric boundary. *Nature Physics*, 7(2):159–165, 2010.

[64] M.H. Schleier-Smith, I.D. Leroux, H. Zhang, M.A. Van Camp, and V. Vuletić. Optomechanical cavity cooling of an atomic ensemble. *Physical review letters*, 107(14):143005, 2011.

[65] E. Vetsch, D. Reitz, G. Sagué, R. Schmidt, ST Dawkins, and A. Rauschenbeutel. Optical interface created by laser-cooled atoms trapped in the evanescent field surrounding an optical nanofiber. *Physical review letters*, 104(20):203603, 2010.

[66] DE Chang, L. Jiang, AV Gorshkov, and HJ Kimble. Cavity qed with atomic mirrors. *New Journal of Physics*, 14(6):063003, 2012.

[67] A. Goban, KS Choi, DJ Alton, D. Ding, C. Lacroûte, M. Pototschnig, T. Thiele, NP Stern, and HJ Kimble. Demonstration of a state-insensitive, compensated nanofiber trap. *Physical Review Letters*, 109(3):33603, 2012.

[68] J Lee, DH Park, S Mittal, M Dagenais, and SL Rolston. Integrated optical dipole trap for cold neutral atoms with an optical waveguide coupler. *New Journal of Physics*, 15(4):043010, 2013.

[69] H. Zoubi and H. Ritsch. Hybrid quantum system of a nanofiber mode coupled to two chains of optically trapped atoms. *New Journal of Physics*, 12(10):103014, 2010.

[70] P. Domokos and H. Ritsch. Collective cooling and self-organization of atoms in a cavity. *Physical review letters*, 89(25):253003, 2002.

[71] KJ Arnold, MP Baden, and MD Barrett. Self-organization threshold scaling for thermal atoms coupled to a cavity. *Physical Review Letters*, 109(15):153002, 2012.

[72] Helmut Ritsch, Peter Domokos, Ferdinand Brennecke, and Tilman Esslinger. Cold atoms in cavity-generated dynamical optical potentials. *Reviews of Modern Physics*, 85(2):553, 2013.

[73] DE Chang, JI Cirac, and HJ Kimble. Self-organization of atoms along a nanophotonic waveguide. *Physical Review Letters*, 110(11):113606, 2013.

[74] M.M. Burns, J.M. Fournier, J.A. Golovchenko, et al. Optical matter: crystallization and binding in intense optical fields. *Science (New York, NY)*, 249(4970):749, 1990.

[75] J.A. Greenberg, B.L. Schmittberger, and D.J. Gauthier. Bunching-induced optical nonlinearity and instability in cold atoms [invited]. *Optics express*, 19(23):22535–22549, 2011.

[76] B.L. Schmittberger, J.A. Greenberg, and D.J. Gauthier. Free-space, multimode spatial self-organization of cold, thermal atoms. *Bulletin of the American Physical Society*, 57, 2012.